Dissertation

Hypoxia-induced vascular remodeling: identification of new molecular target

submitted by

Mag.

Valentina BIASIN

for the Academic Degree of

Doctor of Philosophy (PhD)

at the

Medical University of Graz

and

Ludwig Boltzmann Institute for Lung Vascular Research

under the Supervision of

Prof. Dr. Andrea OLSCHEWSKI

and

Dr. Grazyna KWAPISZEWSKA

2014

Statutory Declaration

I hereby declare that this dissertation is my own original work and that I have fully acknowledged by name all of those individuals and organisations that have contributed to the research for this dissertation. Due acknowledgement has been made in the text to all other material used. Throughout this dissertation and in all related publications I followed the guidelines of “Good Scientific Practice”.

Date 04.10.2014

Acknowledgements

This PhD thesis is the result of work and study at the Ludwig Boltzmann Institute for Lung Vascular Research and at the Center of Medical Research (ZMF) of the Medical University of Graz.

First of all I am very grateful to Prof. Andrea Olschewski and Dr. Grazyna Kwapiszewska to have given me the possibility to perform my PhD in this laboratory and for their help and support. Thanks to Leigh M. Marsh for his help with the animal experiments and Bakytbek Egemnazarov for his enthusiastic motivation. Thank you to all my colleagues in the lab for their everyday help and fruitful discussions. I would also like to thank Sabine Halsegger, Sabrina Reinisch, Julia Schittl, Lisa Oberreiter and Ida Niklasson for their excellent technical assistance and for their help.
A big thank you to all friends and also collegues, Chandran Nagaraj (and Kavitha), Foris Vasile, Zoltan Balint (and his family), Pritesh Jain and Michael Pienn for their entertainment and great time inside but especially outside work. A special thank goes to Diana Zabini and Bence M. Nagy for supporting and standing by me.

I would like to finally express my gratitude to my parents and my brother for helping me in this choice four years ago and for their constant support, love and patience with me despite the distance.

Table of Contents

1 Introduction 12

1.1 Pulmonary hypertension 12

1.1.1 Classification 12

1.1.2 Diagnosis and treatment 14

1.2 Pathobiology of PH 15

1.2.1 Endothelial cells 15

1.2.2 Smooth Muscle Cells 16

1.2.3 Adventitial fibroblasts 16

1.3 Molecular mechanisms 17

1.3.1 ECM and proteases 17

1.3.2 Growth factors 18

1.3.2.1 PDGF-BB 18

1.3.2.2 ET-1 20

1.3.2.3 TGF-β 21

1.3.3 Activator Protein 1 (AP-1) 23

1.3.3.1 c-jun and c-fos 24

1.3.3.2 Fra-2 25

1.4 Animal Models 26

1.4.1 Hypoxia model 26

1.4.2 Monocrotaline model 27

1.4.3 Other models 27

2 Rationale of the study 29

3 Material and methods 30

3.1 Animals 30

3.1.1 Fra-2 overexpressing transgenic (TG) mice 30

3.1.2 Hypoxia mouse model 30

3.1.3 Monocrotaline rat model 30
3.1.4 Hemodynamic measurements 30
3.1.5 Organ collection 32
3.1.6 Assessment of the right ventricular hypertrophy 32
3.2 Human material 32
3.2.1 Human lung samples 32
3.2.2 Isolation of human pulmonary artery smooth muscle cells (hPASMC) 33
3.3 Cell culture experiments 34
3.3.1 Cell culture 34
3.3.2 Immunofluorescence staining 34
3.3.3 Transfection of primary cells 35
3.3.4 Stimulation of primary cells 36
3.3.5 Proliferation assay 37
3.3.6 Apoptosis assay 37
3.4 Molecular biology techniques 38
3.4.1 Isolation of RNA and cDNA synthesis 38
3.4.2 Real-time PCR 38
3.4.3 Microarray 40
3.4.4 Protein isolation and western blot 40
3.4.5 Electrophoretic mobility shift assay (EMSA) 41
3.4.6 Hydroxyproline assay 42
3.4.7 Tissue staining and immunohistochemistry 42
3.5 Statistical analysis 45
3.5.1 Animal studies 46
3.5.2 Studies using human samples 46
3.5.3 *In vitro* experiments 46
4 Results 47

4.1 AP-1 regulation by hypoxia 47

4.2 Fra-2 in experimental pulmonary hypertension 50

4.2.1 Fra-2 is expressed in smooth muscle cells of human pulmonary vessels 50

4.2.2 Fra-2 TG mice show increase of the right ventricular systolic pressure 52

4.2.3 Fra-2 TG mice show pronounced pulmonary vascular remodeling 53

4.2.4 Pathways leading to pulmonary vascular remodeling in the fra-2 TG mice 57

4.2.5 Fra-2 signaling in human pulmonary artery smooth muscle cells, the role of PDGF-BB 59

4.3 Fra-2/Ap-1 target gene: Meprin β 65

4.3.1 Meprin β is the most up-regulated gene in fra-2 TG mice lung 65

4.3.2 Meprin β is expressed in the endothelial, smooth muscle and inflammatory cells in fra-2 TG mice lung 65

4.3.3 Regulation of meprin β by TGF-β in human pulmonary artery smooth muscle cells 67

4.3.4 The role of meprin β for the human disease 71

4.4 The role of the AP-1 members c-fos/c-jun in hypoxia induced vascular remodeling 74

4.4.1 Hypoxia regulates factors responsible for the development of PAH 74

4.4.2 The regulation of c-jun/c-fos by ET-1 76

4.4.3 The regulation of c-jun/c-fos by CTGF 81

4.4.4 c-jun/c-fos relevance in animal models and in the human 84

4.4.4.1 Animal models 84

5 Discussion 86

5.1 AP-1 regulation 86

5.2 AP-1 in cell proliferation 87

5.3 AP-1 and target genes 89

5.3.1 Meprins: structure 89

5.3.2 Meprins: functions 90

5.3.3 Meprins in the lung 91

5.3.4 Meprin β role in vascular remodeling and ECM 91

5.3.5 Meprin regulation in hPASMC 93

6 References 95

Abbreviations and Definitions

ADAM	A disintegrin and metalloproteinase
AKT/PKB	Protein kinase B
AP-1	Activator protein 1
BNP	Brain natriuretic peptide
BMP(R)	Bone morphogenetic protein (receptor)
COX	Cyclooxigenase
cGMP/cAMP	Cyclic guanosine/adenosine monophosphate
COPD	Chronic obstructive pulmonary disease
CREB	cAMP responsive element
CTEPH	Chronic thromboembolic pulmonary hypertension
DAG	Diacylglycerol
DBD	DNA binding domain
ECM	Extracellular matrix
ERA	Endothelin receptor antagonist
FGF	Fibroblast groWTh factor
hPAECs	Human pulmonary artery endothelial cells
hPASMCs	Human pulmonary artery smooth auscle cells
IP_3	Inositoltriphosphat
IPF	Idiopathic pulmonary fibrosis
JNK	c-Jun N-terminal kinase
LOX	Lysyl oxidase
LV+S	Left ventricle plus septum
LZD	Leucine zipper domain
MAPK	Mitogen activated protein kinase
MCT	Monocrotaline
MMP	Matrix metalloproteinase
mPAP	Mean pulmonary artery pressure

NO	Nitric oxide
PA	Pulmonary artery
PAH	Pulmonary arterial hypertension
PCNA	Proliferating cell nuclear antigen
PDE	Phospho diesterase enzyme
PDGF	Platelet derived groWTh factor
PH	Pulmonary hypertension
PI3K	Phosphoinositide 3-kinase
PKC	Protien kinase C
PLC	Phospho lipase C
RTK	Receptor tyrosine kinase
RT-PCR	Reverse transcriptase polymerase chain reaction
RV	Right ventricle
RVSP	Right ventricular systolic pressure
SAP	Systemic arterial pressure
sGC	Soluble guanosile
SIE	Sis-inducible enhancer
SRE	Serum response element
TAD	Transactivation domain
TF	Transcription factor
TGF	Transforming groWTh factor
TIMP	Tissue inhibitor of metalloproteinase
TNF-α	Tumor necrosis factor- α
TRE	TPA (12-0-tetradecanoylphorbol-13-acetate) resp. element
VEGF	Vascular endothelial groWTh factor
vWF	von willebrand factor
α-sma	Smooth muscle alpha-actin

Abstract in German

Ein Hauptmerkmal der pulmonalen Hypertonie (PH) ist Gefäßumbau, der durch vermehrte Proliferation von humanen Glattmuskelzellen (hPASMCs) gekennzeichnet ist. In unserer Studie wurde überprüft, ob Transkriptionsfaktoren eine entscheidende Rolle in diesem Gefäßumbauprozess spielen. Insbesondere beabsichtigten wir die Regulation und Rolle des AP-1 Transkriptionsfaktors bei der Entstehung des Gefäßumbaus zu identifizieren. Wir konnten zeigen, dass AP-1 eine entscheidende Rolle in der durch ET-1 und PDGF-BB induzierten Proliferation von hPASMCs spielt. Diese beiden bekannten Wachstumsfaktoren sind in der Entstehung von PH involviert. Außerdem induzierte die Überexpression von Fra-2, einem AP-1 Mitglied, die Erhöhung des RVSP (right ventricular systolic pressure) und Verdickung der Gefäßwand in der Lunge. Weiterführende Analysen zeigten die AP-1 abhängige Regulation einer neuartigen Protease, Meprin β, die zur Proliferation von hPASMCs beitrug. Die Expressionen von AP-1 und Meprin β wurden in Tiermodellen und in Humanlungen verifiziert. Unsere Ergebnisse geben Aufschluss über die molekularen Mechanismen, die den Gefäßumbauprozessen zugrunde liegen. Darüber hinaus hebt unsere Studie die Wichtigkeit der AP-1 Transkriptionsfamilie als zentralen Regulator von Proliferation und direkten Regulator von nachgelagerten Targetgenen, die möglicherweise in Gefäßumbauprozessen beteiligt sind, hervor.

Abstract in English

A hallmark of pulmonary hypertension (PH) is vascular remodeling characterized by enhanced human pulmonary artery smooth muscle cell (hPASMCs) proliferation. In this study we hypothesized that transcription factors play a crucial role in the remodeling process. Therefore, we aimed to identify the regulation and the role of the AP-1 transcription factors in the development of vascular remodeling. Here, we showed that AP-1 has a crucial role in proliferation of hPASMCs induced by ET-1 and PDGF-BB, well known growth factors involved in PH development. Moreover, overexpression in mice of an AP-1 member, fra-2, induced increased RVSP (right ventricular systolic pressure) together with thickening of the vessel wall in the lung. Further analysis revealed AP-1 dependent regulation of a novel protease, meprin β, which contributed to proliferation of hPASMCs. Expression of AP-1 and meprin β was confirmed in animal model and importantly in human samples. These findings shed light on the molecular mechanism underlying the remodeling process. Moreover, our study emphasizes the importance of AP-1 transcription family, as a central regulator of proliferation and as well as a direct regulator of downstream target genes, which might be involved in the vascular remodeling process.

1 Introduction

1.1 Pulmonary hypertension

1.1.1 Classification

Pulmonary hypertension (PH) is a rare but severe condition which is characterized by elevated intrapulmonary resistance and elevated pulmonary pressure (≥ 25 mmHg) which leads eventually to right heart hypertrophy and to right heart failure (1). According to the clinical classification PH can be divided in different groups depending on the etiology of the disease and on the histological manifestations ((1) and Table 1).

Table 1: Updated classification of Pulmonary Hypertension according to the last guidelines (Table from (1)).

Table 1 Updated Classification of Pulmonary Hypertension*

1. Pulmonary arterial hypertension
   - 1.1 Idiopathic PAH
   - 1.2 Heritable PAH
   - 1.2.1 BMPR2
   - 1.2.2 ALK-1, ENG, SMAD9, CAV1, KCNK3
   - 1.2.3 Unknown
   - 1.3 Drug and toxin induced
   - 1.4 Associated with:
   - 1.4.1 Connective tissue disease
   - 1.4.2 HIV infection
   - 1.4.3 Portal hypertension
   - 1.4.4 Congenital heart diseases
   - 1.4.5 Schistosomiasis

1′ Pulmonary veno-occlusive disease and/or pulmonary capillary hemangiomatosis

1″. Persistent pulmonary hypertension of the newborn (PPHN)

2. Pulmonary hypertension due to left heart disease
   - 2.1 Left ventricular systolic dysfunction
   - 2.2 Left ventricular diastolic dysfunction
   - 2.3 Valvular disease
   - 2.4 Congenital/acquired left heart inflow/outflow tract obstruction and congenital cardiomyopathies

3. Pulmonary hypertension due to lung diseases and/or hypoxia
   - 3.1 Chronic obstructive pulmonary disease
   - 3.2 Interstitial lung disease
   - 3.3 Other pulmonary diseases with mixed restrictive and obstructive pattern
   - 3.4 Sleep-disordered breathing
   - 3.5 Alveolar hypoventilation disorders
   - 3.6 Chronic exposure to high altitude
   - 3.7 Developmental lung diseases

4. Chronic thromboembolic pulmonary hypertension (CTEPH)

5. Pulmonary hypertension with unclear multifactorial mechanisms
   - 5.1 Hematologic disorders: chronic hemolytic anemia, myeloproliferative disorders, splenectomy
   - 5.2 Systemic disorders: sarcoidosis, pulmonary histiocytosis, lymphangioleiomyomatosis
   - 5.3 Metabolic disorders: glycogen storage disease, Gaucher disease, thyroid disorders
   - 5.4 Others: tumoral obstruction, fibrosing mediastinitis, chronic renal failure, segmental PH

*5th WSPH Nice 2013. Main modifications to the previous Dana Point classification are in bold.
BMPR = bone morphogenic protein receptor type II; CAV1 = caveolin-1; ENG = endoglin; HIV = human immunodeficiency virus; PAH = pulmonary arterial hypertension.

Group 1: Pulmonary arterial hypertension (PAH); including heritable PAH due to BMPR2 mutation, idiopathic PAH, toxin/drugs induced PAH and associated PAH (APAH). The APAH is usually a condition where other disease (systemic sclerosis, schistosomiasis, HIV infections, porto-pulmonary hypertension) are associated with similar histology and clinical parameters which are seen in PAH. Usually remodeling process and pathological changes are present in distal smaller vessels (~500 µm diameter). The hallmark of vascular remodeling is media and adventitial thickening, intima proliferation and intima lamina fibrosis (concentric or eccentric) (Figure 1). Moreover, more complex lesions, called plexiform lesion, are found in this group. Generally vein side is unaffected.

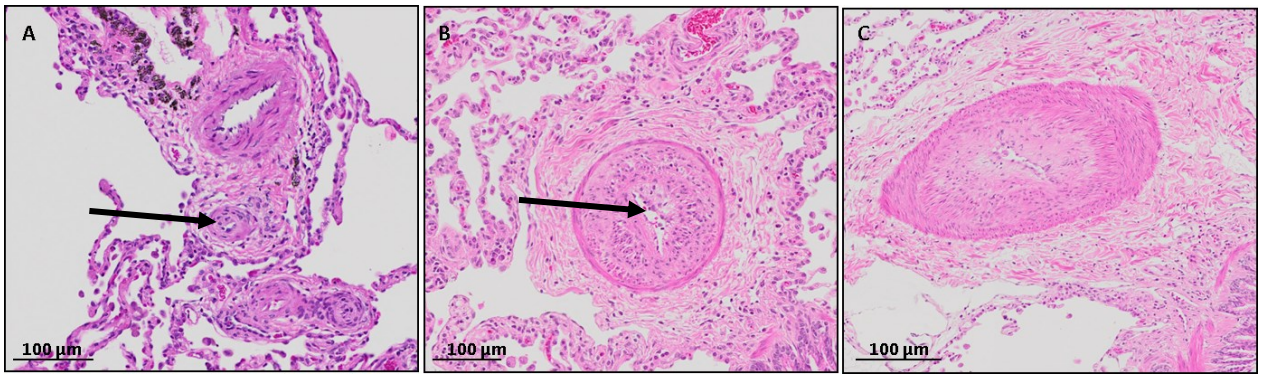

Figure 1: Remodeling of intimal and medial layer in PAH. A-C): Extensive remodeling of the pulmonary vessels in PAH lung with medial and intimal thickening and reduced lumen of the vessel.

Group 1: Pulmonary veno-occlusive disease and/or pulmonary capillary haemangiomatosis. In this group the most affected vessels are veins (occlusion because of fibrotic lesions, venous muscolarization, and alveolar hemorrhage) with medial hypertrophy and intima fibrosis of the distal vessels.

Group 1: Persistent pulmonary hypertension of newborn.

Group 2: PH due to left heart disease. In this group the pathological changes are characterized by enlargement and thickening of the veins, capillary dilation, edema formation while arterial bed may even not be affected.

Group 3: Pulmonary vascular disease due lo lung disease or hypoxia. Different lung disease such as chronic obstructive pulmonary disease (COPD), interstitial lung fibrosis (IPF) or chronic exposure to high altitude belong to this group, therefore different pathological changes can be observed depending on the disease. However, medial

hypertrophy, fibrotic deposition or intimal proliferation can be found together with some degree of disruption of the vasculature structure (Figure 2).

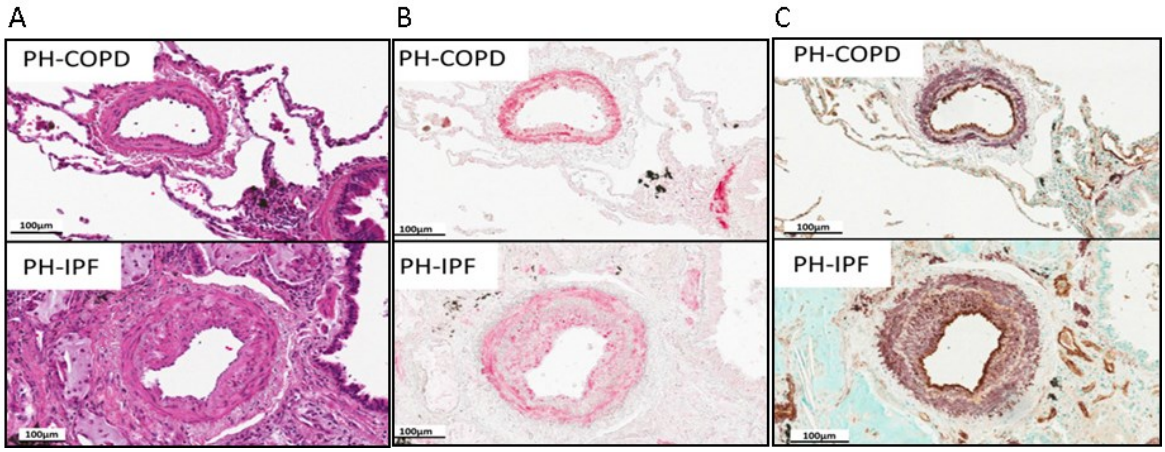

Figure 2: Vascular remodeling in COPD and fibrosis lungs associated with PH. Remodeling of the media layer with only minor affection of the intimal layer in A) H&E, B) α-sma and C) v-WF and α-sma staining (Figure modified from (2)).

Group 4: Chronic thromboembolic pulmonary hypertension (CTEPH). CTEPH is characterized by formation of organized thrombi inside the vascular bed which can attach to the intimal layer of the vascular wall and replace the normal intima.

Group 5: PH with unknown or multifactorial mechanisms. This group includes very heterogeneous conditions which for unknown reasons lead to development of PH.

1.1.2 Diagnosis and treatment

The diagnosis of PH is currently performed with the invasive right heart catheterization, which is the gold standard method in the clinic. In the right heart catheterization a catheter is inserted via the superior vena cava, from where it will reach the right side of the heart and pass into the pulmonary artery (3). During the last decade, however, radiological methods such as echocardiography, computer tomography (CT) and magnetic resonance tomography (MRI) have started to establish their role especially in the early detection and diagnostic follow-up of the disease (4),(5),(6).

All drugs available on the market are proved only for the therapy of PAH. Normally the reactivity towards some of these medications is tested during the right heart catheterization, in order to prove the sensitivity of the pulmonary circulation to the vasodilators (7). Currently used therapies include calcium channel blockers, prostanoids,

endothelin receptors (ER) antagonist or phosphodiesterase type 5 inhibitors (PDE inhibitors) (8), (9), (10). Calcium channel blockers are normally used in patients with systemic hypertension. However, a small percentage of PH patients respond to them (11), (9). Prostanoids, endothelin receptor antagonist and posphodiesterase enzyme inhibitors are widely used in PAH patients, and they act on molecular pathways which were shown to be deregulated in PAH patients (12). *Prostanoids* are prostacyclin analogues, which are normally produced by the endothelial cells. They act on the prostacyclin receptor leading to increase of cAMP, a potent vasodilator agent (13). *ER antagonist* (ERA) act on the endothelin-1 pathway. They bind to the endothelin receptors, inhibiting the contractive effect of endothelin-1(14). *PDE inhibitors* inhibit the cGMP-degrading enzyme, PDE, causing an increase of cGMP which in turns leads to vasodilation (15).

1.2 Pathobiology of PH

Vascular remodeling is the hallmark of PH and it can lead to a complete obliteration of the vessel. The remodeling process includes proliferation of the vascular cells, deposition of extracellular matrix and alteration of the cell phenotype within the vasculature (16).

1.2.1 Endothelial cells

The endothelium (intima layer) is important in maintaining the vascular tone, regulating the platelet aggregation, releasing chemo-attractant factors or growth factors which can influence angiogenesis or inflammatory cells infiltration (17). Endothelial cells proliferation and disorganization is considered to be the major cause for the formation of intimal lesions (18) Intimal lesions commonly found in PAH are plexiform lesions (19). Plexiform lesions usually occur at branching point as a result probably of shear stress or turbulent flow. The histology of plexiform lesions present single endothelial layer of cells in very small blood vessels and a core of cell aggregates which morphologically resemble myofibroblast or less differentiated cells (18). Often in proximity of plexiform lesion, concentric lesions are also present (20). These lesions are more structured, and present a so called “onion-skin” layers, where endothelial cells are still lined up on vascular channel which lumen is significantly decreased (21). To this date the etiology of the intimal lesions is not clear. It is believed that these lesions might results from an endothelium injury which in turn activates endothelial cell proliferation, extracellular matrix deposition, migration of different cells such as smooth muscle cells (22). It has been suggested that due to the

endothelium injury, apoptosis is occurring and apoptosis-resistant endothelial cells can be the source of the proliferating pool present in plexiform lesions (23).

1.2.2 Smooth Muscle Cells

Smooth muscle cells are components of the vessel wall (media layer), which surround the endothelial layer. The presence of smooth muscle cells allows the differentiation between muscularized, partially muscularized and not muscularized vessel (24). The function of smooth muscle cells is to regulate vasoconstriction and vasodilation of the vessels (25). However, it has been shown that different smooth muscle cell phenotypes exist in the vessel wall (26). Investigations in the systemic circulation after balloon dilation described two different phenotypes in the remodelled vessel walls as the reaction after the injury, the contractile and the synthetic phenotype (27). An early study on cattle kept at high altitude showed that the contractile smooth muscle cell expresses contractile protein (eg. smooth muscle-myosin heavy chain, α-smooth muscle actin) and has an elongated morphology, spindle shaped. The synthetic phenotype smooth muscle cell showed a rhomboid shape, so called cobblestone morphology and these cells are more prone to proliferation, migration and production of ECM (28), (27). These two phenotypes co-exist with balance in the physiological remodeling of the vessel. However in pathological condition, such as in pulmonary hypertension, this balance might be altered and synthetic phenotype cells secrete, proliferate and migrate more, while contractile phenotype cells maintain a persistent vasoconstriction status (29). Moreover a possible shift of cells from a contractile to a synthetic phenotype could be possible, due to the surrounding environment. It has been shown that smooth muscle cells stimulated with growth factors respond with high grade proliferation and migration and with decreased expression of contractile proteins (30).These mechanisms lead to the thickening of the media layer in pulmonary hypertension (29), (31).

1.2.3 Adventitial fibroblasts

Adventitial fibroblasts are present in the outer layer of the vessel wall (adventitial layer) which was, for long time, thought to be a structural component of the vessel involved in maintaining and supporting the vessel wall (32),(33). However, a growing number of evidence shows, instead, that the advential fibroblasts actively take part to the remodeling process. The thickening is mediated by different mechanisms including aberrant secretion of extracellular matrix (ECM) and myofibroblast proliferation and differentiation (34). The

thickening of the adventitial layer has been reported in experimental model of pulmonary hypertension, such as hypoxia and monocrotaline (35),(36). It has been shown that adventitial fibroblasts have the highest rate of proliferation in the hypoxic mouse model (37). Moreover trans-differentiation to myofibroblast occurs during the remodeling process, and presence of myofibroblasts has been assessed in the inner layers of the vessels (38). The trans-differentiation to myofibroblast has been associated with increased expression of contractile protein, such as α-sma (39). Consequently, the expression of contractile proteins can influence the response to vasoconstrictor or dilatory stimuli. Taken together, the change from adventitial fibroblast to a myofibroblast phenotype has an important impact in the remodeling process by enhancing proliferating rate, ECM secretion and the contractile status of the vessel.

1.3 Molecular mechanisms

The molecular mechanisms which have been delineated to play a role in the vascular remodeling process can be grouped in three main categories, which in the physiological and pathological conditions are dynamically interacting which each other. These three categories are extracellular matrix (ECM) and proteases, growth factors and transcription factors.

1.3.1 ECM and proteases

The ECM is the extracellular part which is surrounding the cells and building the vascular wall. The function of ECM is to give structural support to the vessel; however, the common knowledge that ECM is a passive structural component has changed in the last years (40). ECM is rather a dynamic structure, which can influence cell behavior and respond to cell stimuli (40). Moreover, ECM is in a continuous and dynamic balance between degradation and accumulation, and in this process proteases and proteases inhibitor play a crucial role (41). Some of the main components of the ECM are collagens, glycoproteins (e.g fibronectin, tenascin-C, elastin, integrins) and proteoglycans (42). These components are quite important in the vascular wall. For instance, elastin is a major component of the vessel wall and physiologically it gives an elastic component to the vessels, in order to distribute the stress throughout the vasculature (43). Fragmented elastin has been reported to be present in vessels from PAH patients (44). Degradation of elastin is a consequence of activated proteases such as MMPs or inactive protease inhibitors such as elafin (45) or tissue inhibitor of metalloproteinases (TIMPs)(46). Other ECM component

such as tenascin-C was shown to be highly present in vessel from PH patients and to stimulate hPASMC proliferation (47). Collagens impart tensile strength to the vessel, preventing the rupture in high pressure conditions (48). It has also been notice that in vascular remodeling there is increase collagen deposition around the adventitial layer. This is probably due to the constant increased pressure which then induces collagen deposition increasing in turn the stiffness of the vessel wall (49). Collagen amount is regulated by the deposition and the degradation rate. Whilst degradation of collagen is mainly controlled by MMPs (MMP-1, MMP-8, MMP-2, MMP-9) (50); the deposition can be regulated at different stages. Lysil oxidases are enzyme able to catalyze aldehydes group from lysine residues of collagen. These groups are highly reactive and they react with other aldehydes group of other collagen fibrils, resulting in a covalent cross-linking of collagen (51).

ECM, above the structural component, can also function as a growth factor reservoir for the neighboring cell. Growth factors, such as FGF, TGF-β and VEGFs, can bind to ECM components (heparin-heparan sulfate or ECM protein) and therefore degradation of ECM can enhance growth factor release, which in turn can influence cell behavior (40). The dynamics of the ECM are very complex and subjected to a very fine and balanced regulation. Any small change in this equilibrium will be counteracted by other mechanisms, however if the balance is not restorable this might result in a pathological condition.

1.3.2 Growth factors

Several growth factors have been associated with the development and progression of the vascular remodeling process in PH. Amongst other, platelet derived growth factor (PDGF-BB), transforming growth factor-β (TGF-β) and endothelin-1 (ET-1) have been extensively studied.

1.3.2.1 PDGF-BB

PDGF was identified as a platelet released factor which can induce growth of fibroblast, smooth muscle cells and glia cells (52).There are 4 different PDGF proteins PDGF-A, PDGF-B, PDGF-C and PDGF-D and they can assemble as homodimers and just very rarely as heterodimers (53). PDGFs are produced by several types of cells such as endothelial cells, smooth muscle cells and macrophages (54). They usually act in a paracrine way and they bind to two tyrosine kinase receptors (RTKs), PDGFR-α and PDGFR-β. The binding of the ligand stimulate the dimerization of the RTKs which hence,

undergo auto-phosphorylation. In this way the receptors are activated and the phosphorylation provides docking sites for downstream molecules (55). Important downstream molecules are ras-MAPK, PI3K and PLC-γ. As represented in figure 3A, activation of Ras and consequent activation of MAPK is mediated by the SH2 domain of Grb2 protein which binds to Sos1 complex and in turn activates Ras (56). PI3K can also be activated by phosphorylated RTKs and in turn activate AKT (57), JNK (58), and eventually PLC-γ which, with release of DAG and IP_3 leads to activation of PKC and mobilization of intracellular calcium (59). Moreover PDGFRs can also bind with integrins, and this interaction direct localization of the receptors in specific part of the membrane, favoring the beginning of the signaling pathway (60) (Figure 3B).

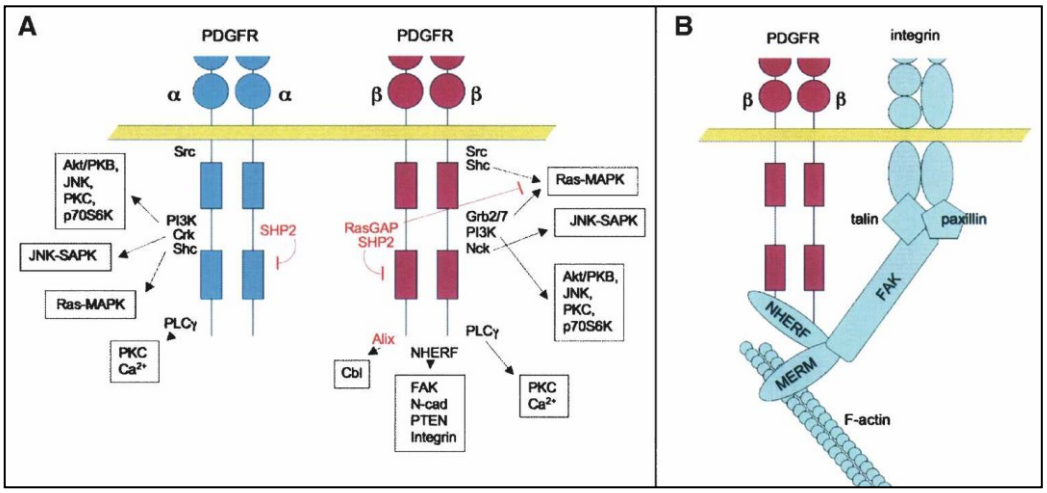

Figure 3: PDGFR signaling. (A) The cytosolic domains of PDGFRs are represented with their direct interactors. Arrows link to downstream signaling pathways. Negative feedback mechanism are marked by red (B) Representation of PDGFRs and integrin interaction (Figure from (52)).

Activation of these pathways induces cell response within seconds to minutes. Different cellular responses are mediated by the two different receptors. Both PDGFR-α and PDGFR-β stimulates actin rearrangement, affecting therefore mobility of cells, and PDGFR-β can inhibit gap junction protein connexin-43 and therefore intracellular communication (61). In addition to the fast changes, activation of PDGFRs induce also transcriptional activation of the so called *immediate early genes*, usually transcription factors (TFs) and target of TFs, which mediate the long term effect of PDGF, such as proliferation of cells or developmental processes (52). In pulmonary hypertension PDGF-BB was extensively studied in human and animal models as well. It has been proved that activated forms of the PDGFRs co-localize with PCNA and PDGF-BB in endothelial and smooth muscle cells of PAH patients (62). Moreover, it has been also shown that PDGF-

BB can induce proliferation and migration of hPASMCs and fibroblasts (54), which can be inhibited by Imatinib treatment, a PDGFR inhibitor (62). In animal model Imatinib treatment could reverse hypoxia and monocrotaline induce pulmonary hypertension, suggesting a key role of PDGF-BB in pulmonary hypertension (63).

1.3.2.2 ET-1

Endothelins are a family of peptides consisting of three isoform ET-1, ET-2 and ET-3 (64). The isoform ET-1 is the most abundant *in vivo* and it is synthetized as a pre-pro-form (PPET1) of 212 amino acids (aa). PPET1 is cleaved by furin-like proteases to big-ET-1 (38 aa) which will be further cleaved to active peptide (21 aa) by three endothelin converting enzymes (65). The big ET-1 has no biological function, and the active ET-1 in physiological conditions, has a low plasma concentration because after binding irreversibly to the receptors, the whole complex (receptor and ligand) is internalized and degraded (66). There are two receptors for ETs, the ET receptor A and B (ET_A and $ET_{B)}$ which are 7 trans-membranes G protein coupled receptor (67). Upon binding of the ligand on the receptor, G protein is activated and consequently PLC is stimulated. Activation of PLC leads to production of IP3 and DAG which will increase intracellular calcium. The increase of calcium is mediated by two mechanisms: 1) calcium is recruited from the reticulum by activation of IP3 receptors 2) from the extracellular environment through activation of Ca^{2+} channels on the cell membrane (68). ET-1 is mostly secreted by endothelial cells to the smooth muscle layer and bind to the receptors which are expressed in EC and SMC (ET_B) or just in SMC (ET_A). The binding to both ET_B and ET_A induces Ca^{2+} release and vasoconstriction (69); however binding to ET_B induces NO (nitric oxide) release and consequent vasodilation (70). In addition to control the vascular tone, ET-1 can also affect cell growth and inflammation (71) (Figure 4).

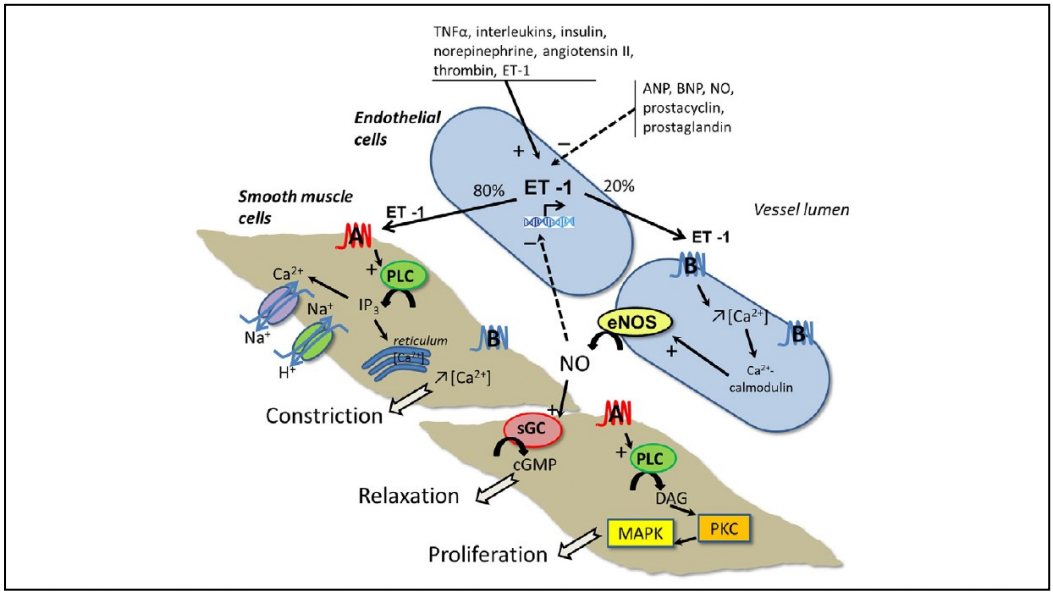

Figure 4: ET-1 pathway within the vessel wall. Different factors (TNF, ILs, insulin) lead to increase ET-1 production from endothelial cells. Binding to endothelin receptor B (ETrB), induces release of NO from endothelial cells. Binding to endothelin receptor A (ETrA) induces activation of PLC and increases of intracellular calcium. Moreover, via the ETrA, MAPK kinases are activated and proliferation of smooth muscle cells is induced (Figure from (72)).

ET-1 serum level has been reported to be elevated in PAH patients and locally on vascular EC, suggesting that EC might produce more ET-1 in PAH disease condition (22). Importantly serum level of ET-1 significantly correlates with important parameters such as pulmonary vascular resistance, oxygen saturation and right heart hypertrophy (73),(74). Selective and non-selective antagonist of ET-1 receptors reduces PH and vascular remodeling in animal models (75), (76), (77). Currently ET receptors antagonist is one of the therapies used with PAH patients in class III and IV of the NYHA classification.

1.3.2.3 TGF-β

TGF-β is the first discovered member of a big superfamily which currently consists of 40 members, including bone morphogenetic proteins (BMPs) (78). There are two receptors (type I and type II) for TGF-β and BMPs, which belong to the serine threonine kinase receptor family. Binding of the substrate induces association of the two receptors and unidirectional phosphorylation from receptor type II to receptor type I (79). Thus, the activated receptor I can phosphorylate SMAD protein. SMAD are downstream molecules to the TGF-β/BMPs signaling and they can be divided in three classes. The receptor regulated SMADs (R-SMAD: SMAD-2,-3,-5 and -8), are directly phosphorylated by the type I receptor and therefore they are released from the SMAD anchor receptor activation

(SARA) complex. The R-SMAD can then accumulate in the nucleus where they will interact with the Co-SMADS (SMAD-4), and regulate transcription of target genes together with other transcription factors. On the other hand the inhibitory SMAD counteracts the effect of R-SMAD, hence providing a sort of negative feedback loop to antagonize the TGF-β/BMPs signaling ((80) and Figure 5).

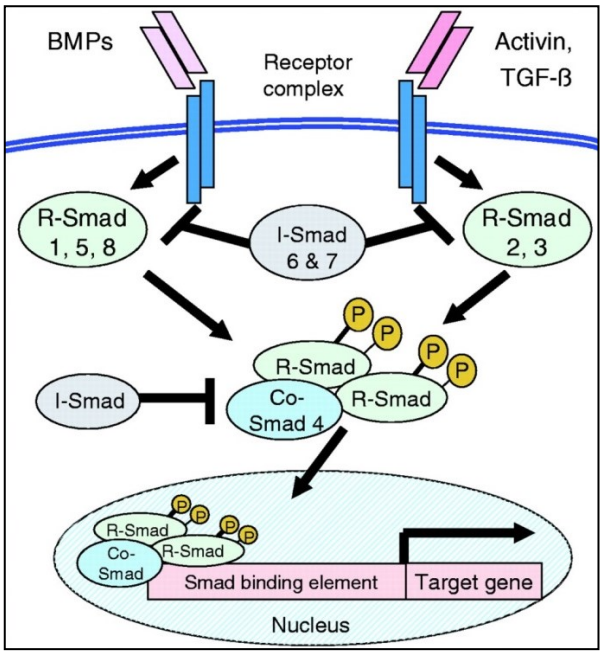

Figure 5: Representation of TGF-β superfamily signaling. Binding of the TGF-β superfamily leads to activation of the receptors**.** Subsequently, the receptors phosphorylate the downstream molecules Smad2 and Smad3 (upon TGF-β) or Smad1, Smad5 and Smad8 (upon BMPs). The phosphorylated SMADs interact with Co-Smad4. The complex then translocate into the nucleus where they regulate transcription of target genes. Smad6 and Smad7 are inhibitory and they antagonize the canonical TGF-β signaling (Figure from (81)).

The TGF-β superfamily regulates many different physiological processes, such as ECM production, migration, cell differentiation and many others (82). Mutation in the gene of BMP receptor type 2 (BMPRII) is associated with familiar idiopathic PAH. Many mutations have been identified in patients with hereditary PAH, and all of them resulted in a loss of function of the receptor (78). Moreover, BMPRII expression level is reduced in PAH cases where no mutations were identified (22). This suggests that the TGF-β superfamily might play an important role in the development of the disease. How this mutation can induce PAH is still not clear but there are some hypotheses. It is believed that BMPs and BMPRII signaling in some extend counteract and balance TGF-β and TGF-β receptors pathway (83). It is known that TGF-β/TGFβR-I, II signal via SMAD2 and 3,

while BMPs and BMPR-I and II via SMAD 1 and 5 (figure 5 and (84)). Moreover it has been proved that there is an antagonism between these two pathways, for instance BMP7 seems to inhibit TGF-β induced renal fibrosis in animal model. Hence, reduction of functional BMP receptor in PAH might result in an overactive TGF-β pathway.

1.3.3 Activator Protein 1 (AP-1)

Activation of different pathways by growth factors (PDGF-BB, ET-1 or TGF-β) or influence of the cell behavior via ECM turnover will induce activation of transcription factors in the cells which will allow them to respond consequently to the received stimulus. Transcription factors are the converging molecules from many different signaling pathways. AP-1 protein complex is a family of transcription factors, including JUN (c-jun, junB and junD), FOS (c-fos, fra-2, fra-1 and fosB), ATF and MAF components (85). These transcription factors are also called the *immediate early genes*, due to their capability to be activated transiently and rapidly upon many different stimuli (85). C-fos and c-jun were first identified as oncogenic genes activated by the FBJ murine osteosarcoma virus (86) and avian sarcoma virus (87) respectively. Specific AP-1 dimers can be regulated and expressed depending on the cell type. In this way, different cell type can have different responses to same stimuli depending on the AP-1 dimer induced (88). AP-1 can regulate many different biological processes and this is due mainly to their complex regulation and their structure. AP-1 is indeed not composed by a single protein but they are usually dimers, because of their basic region leucin-zipper (LZD, leucine zipper domain), which enable dimerization. Moreover, while the JUN family can form homodimers, FOS family cannot, therefore they need to combine with the JUN family. All component of AP-1 family have a DBD (DNA binding domain) and only some of them (JUN family, c-fos and fosB) have the transactivation domain (TAD). Consequently some members of the FOS family (fra-1, fra-2 and fosB) cannot activate transcription of any gene by themselves but they need a partner protein with a transactivation domain ((89) and Figure 6).

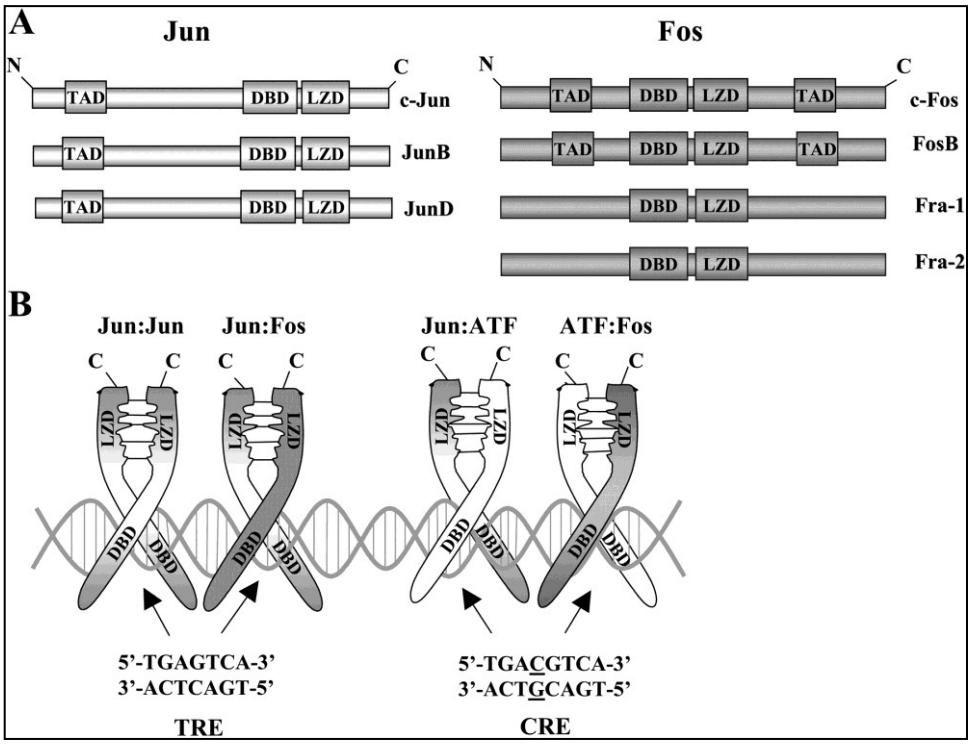

Figure 6: Schematic representation of AP-1 members. A) The structure of JUN and FOS proteins and B) the dimerization due to LZD domain which facilitates the binding of the dimer to the DNA binding sequence. (Figure from (90))

1.3.3.1 c-jun and c-fos

c-jun and c-fos are probably the most studied transcriptions factors in the AP-1 family. Stimulation of cells with different stimuli increases c-fos expression level rapidly and transiently (91). This is due to its regulatory element in the promoter region. There are three *cis* regulatory element in c-fos promoter, CRE (Calcium response element), SIE (Sis-inducible enhancer) and SRE (serum response element). CRE is usually recognized by CREB (CRE-binding protein) which induce c-fos expression via cAMP and Ca^{2+} dependent pathway. SIE is occupied by STAT (signal transducer and activator of transcription) proteins and SRE sequence is recognized by SRF (serum-response factor) and TCFs (ternary complex factors) (92), (93). One of the members of TCFs is Elk-1, which is phosphorylated by ERK (extracellular signal regulated kinase). ERK kinase is known to be activated by mitogens, therefore might be responsible for the mitogen induced c-fos (92). On the other side c-jun induction is mediated by the TRE (TPA (12-0-tetradecanoylphorbol-13-acetate) responsive element), which is recognized by c-jun and ATF factor, rather than the usual AP-1. The activity of c-jun and c-fos depend not just on the abundance of the protein but also on their phosphorylation status. Both c-jun and c-fos

are phosphorylated at specific sites which increase their transcriptional activity. Ser-63 and ser-73, which are positioned in the transactivation domain of c-jun, can be phosphorylated by JNK kinase potentiating the transcriptional activity (92). Similarly, the ser-232 has a similar effect on c-fos transcriptional activity (92). The phosphorylation of c-fos is mediated by a novel MAPK, called FRK. Recently it has been shown that c-fos resulted to be up-regulated in pulmonary arteries of mice overexpressing the serotonin transporter. These mice develop PH at basal condition and exaggerated PH under hypoxia. The clinical relevance was confirmed in hPASMC from donor and PAH patients, where c-fos level was increased (94). Another study showed that c-jun enhances proliferation of hPASMCs and depolarize the cells, which in turn respond with an increase in cytosolic Ca^{2+}, further stimulating c-jun/c-fos expression (95).

1.3.3.2 Fra-2

Fra-2 (Fos related antigen) is a component of the FOS family and it is regulated, similarly to c-fos, by CRE and SRE sequences and, similarly to c-jun, by TRE sequence (96). Also the protein sequence has a high homology to the FOS protein family and, similarly to c-fos, it can form heterodimer whit c-jun (97). It has been shown that fra-2 expression is regulated by c-fos/c-jun on the fra-2 promoter at the beginning, and this complex is later on exchanged for the fra-2/c-jun complex, which seems to have a lower transcriptional activity. This suggests that there might be a negative feedback mechanism regulating fra-2 expression (98). Indeed, it has been reported that fra-2/c-jun dimers have a suppressed transactivation activity while fra-2/jun-D possess higher transactivation activity (99). Beside the biochemical regulation and dimerization, fra-2 has been recently shown to be a crucial molecule controlling lung vessel and parenchymal architecture (100). Overexpression of fra-2 (Fra-2 transgenic (TG)) in mice induces development of pulmonary vascular remodeling and pulmonary fibrosis. Interestingly, in fra-2 transgenic mice the vascular remodeling preceded the onset of fibrosis (100) and it was reported that in the pulmonary vessel α-sma positive cells were stained for Ki67 (a proliferating marker) (Figure 7). Following study reported that fra-2 TG mice combine several clinical features of systemic sclerosis with pulmonary vascular remodeling (101) (102).

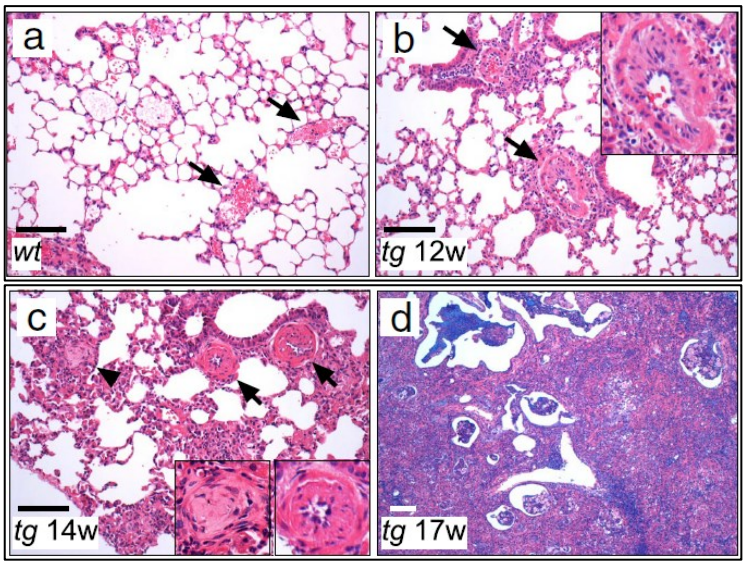

Figure 7: Obliteration of pulmonary arteries precedes pulmonary fibrosis in fra-2 TG mice. Histological analysis of different disease stages of A) wild-type controls in comparison to in 12-14 and 17 weeks old fra-2 TG identifying (B) remodeling and subsequent C) obliteration of pulmonary arteries as early event of pulmonary disease in transgenic mice accompanied by a strong inflammatory infiltrates. At later stage D) fibrotic phenotype was observed. In contrast, pulmonary arteries in wild-type controls appeared normal (arrows in a) (Figure modified from (100)).

1.4 Animal Models

Different animal models have been established to study and understand the molecular processes taking place in PH, such as the BMPR-2 mutation model (103), sugene 5416 and hypoxia model (104) or the overexpression of the calcium binding protein S100A4 in mice (105). The most widely used animal models for PH are the hypoxia model in mouse and the monocrotaline model in rat (106). Even though these two models greatly increased the knowledge on mechanism underlying PH, both models have limitations and do not resemble completely the complexity of the human disease (106).

1.4.1 Hypoxia model

The hypoxic model has been used for many years as a model of PH (group 3). Indeed in chronic lung diseases (such as COPD) and in people who live at high altitude, development of hypoxia is a common feature (107). The mechanism by which there is increase in pressure is mediated by two ways: the hypoxic pulmonary vasoconstriction and the pulmonary vascular remodeling (108, 109). The hypoxic vasoconstriction is a mechanism by which the pulmonary arteries respond with vasoconstriction to low oxygen

concentration in order to direct the blood flow to more oxygenated regions (110). In this way the intrapulmonary pressure increases together with the pulmonary resistance. Small pre capillaries mainly contribute to the increase resistance in the small arteries and they are the most affected vessels by the remodeling process induced by hypoxia (111). The smooth muscle cell layer becomes thicker due to hypertrophy and proliferation of vascular cells, affecting the structure of the vessel which further increase the pressure (111). Even though the hypoxic mouse model has some limitations (112), it recapitulates several important aspect of PH and it helped to understand the hypoxic induced vasoconstriction and to identify some molecular mechanism involved in PH (113).

1.4.2 Monocrotaline model

Monocrotaline (MCT) is a toxic pyrrolizidine alkaloid which is extracted from the plant, *Crotalia spectabilis*. It induces pulmonary vascular injury in rats only after being activated by the liver to monocrotaline pyrrole. One single administration of monocrotaline causes in 3 or 4 weeks PH with right ventricular hypertrophy (RVH). From the histological point of view the rats develop an early endothelial damage/apoptosis which probably initiates the progressive remodeling process (114). Other studies suggested that the vascular remodeling is mainly mediated by the important inflammatory infiltrate which accumulates in the adventitial layer of the vessels (115). A more severe phenotype is given by the association of monocrotaline with pneuomonectomy. Rats which underwent monocrotaline and pneumonectomy develop severe PH with plexiform like-lesion, which appears before onset of PH (116). MCT administration does not only affect pulmonary vessel but also lung parenchyma inducing alveolar edema, alveolar septa hyperplasia and injury in the vein bed (117), therefore MCT is considered to be an acute lung injury model as well. For this reason it should be taken into account that some of the features developed by the MCT are not PAH characteristic.

1.4.3 Other models

The BMPRII mutation model is based on the human evidence that BMPRII is affected by loss of function mutation (118). It has been shown that mutation of BMPRII in smooth muscle positive cells increased the right ventricular systolic pressure, induced slight remodeling and inflammation in mice (119). Sugen 5416 and hypoxia was developed to understand the severe pulmonary hypertension. As VEGF is important for the endothelium integrity and maintenance, this model combined hypoxia exposure with VEGF receptor

blockage, leading to apoptosis of endothelial cell followed by hyper-proliferation (104). The pulmonary hypertension developed by this model is severe and irreversible with pre capillary arterial remodeling and neo-intimal lesions (104). Another investigated model is the overexpression of S100A4 in mice (120). It was noticed that mice overexpressing S100A4, which were used as a tumor model, exhibited changes in the arterial wall of the lung vasculature arteries (105). When S100A4 overexpressing mice were exposed to hypoxia, they developed higher increase of pulmonary arterial pressure and RV hypertrophy. Regarding the remodeling process, it was not greater than wild type hypoxic mice; however it did not regress when moved to normoxic conditions(121).

2 Rationale of the study

The rationale of this study is to identify new molecular mechanisms and possibly new players in the remodeling process of pulmonary hypertension. A special attention is given in this study to the AP-1 transcription factors due to their central and crucial role in regulating molecular pathways in the cell biology. In order to delineate how AP-1 transcription factors can be regulated and can play a role in remodeling underlying PH we studied two different animal models:

1 Fra-2 overexpressing mouse was characterized and the role of fra-2 in the remodeling process was investigated.

2 Short hypoxic exposure in mice was applied to identify factors triggering the remodeling process and to investigate the role of AP-1 in this molecular mechanism.

3 Material and methods

3.1 Animals

3.1.1 Fra-2 overexpressing transgenic (TG) mice

Fra-2 overexpressing (TG) mice were a kind gift from Prof. E. Wagner and have been already described (100).The Research Institute of Molecular Pathology (IMP, Vienna, Austria) has provided the breeding pairs for the current study. The line was housed at the Medical University of Graz, in specific pathogen free (SPF) conditions and to maintain the line, fra-2 TG positive mice were crossed with C57BL/6 background mice. The animals were fed with normal chow-fed diet. The generated fra-2 TG mice and the correspondingly age and sex matched wild-type (WT) littermates were used for experiments. All animal experiments were approved by the local authorities (Austrian Ministry of Education, Science and Culture, BMWF-66.010/0086-II/3b/2012).

3.1.2 Hypoxia mouse model

C57BL/6 mice were used for the short and long-term hypoxia exposure. Mice were exposed to normobaric hypoxic conditions (10% O_2) for 12 and 24 hours (short time) and for 21 days (long time). The concentration of oxygen was continuously monitored and maintained by the OxyCycler system (BioSpherix, NY, USA). Control mice were kept in normobaric normoxia conditions (21% O2). The hypoxic mice and the corresponding age and sex matched normoxic mice were used for experiments. The animals were fed with normal chow-fed diet. All animal experiments were approved by the local authorities (Austrian Ministry of Education, Science and Culture BMWF-66.010/0076-II/3b/2011, BMWF-66.010/0105-II/3b/2013).

3.1.3 Monocrotaline rat model

The monocrotaline rat model was performed in University of Giessen, Germany. Paraffin blocks were kindly provided to us for immunohistochemical staining.

3.1.4 Hemodynamic measurements

The hemodynamic measurements were performed on fra-2 TG mice under anesthetized condition, using 2-5% isofluorane. The mice were continuously monitored for several parameters (electrocardiogram, temperature, and heart-beat) during the whole procedure.

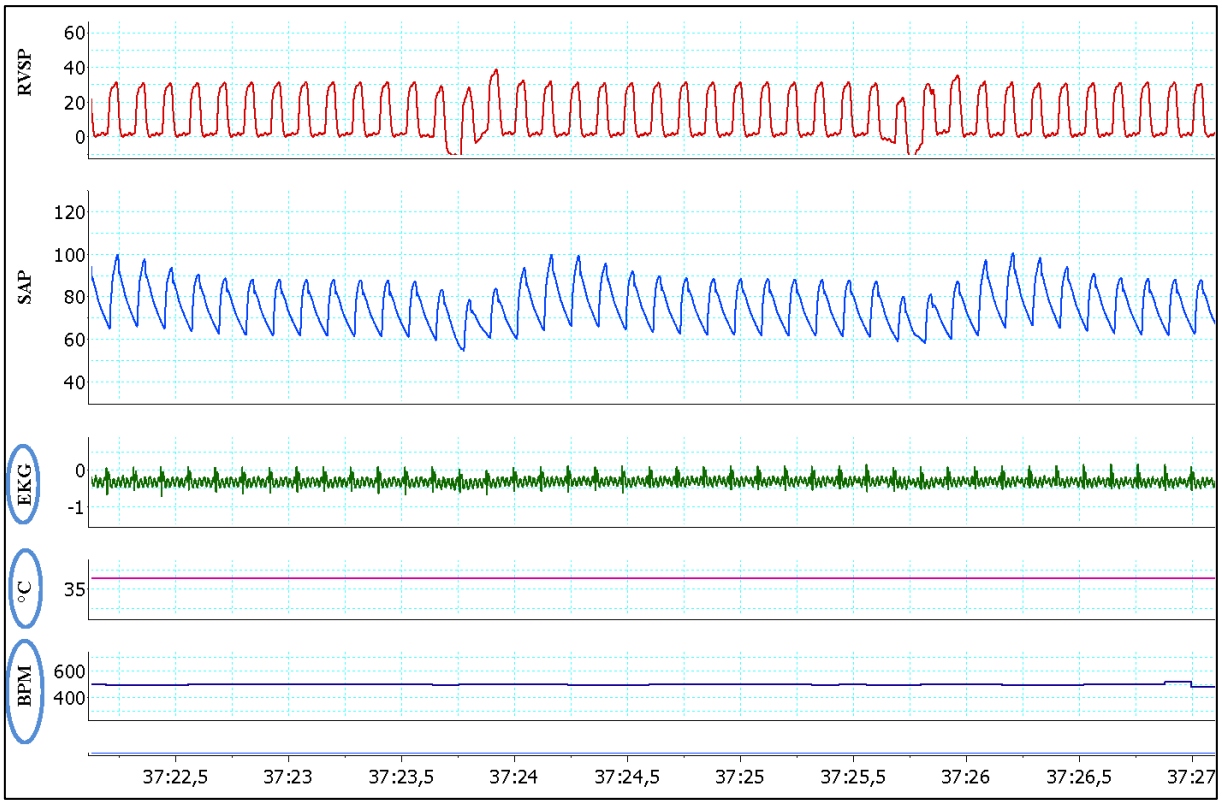

Figure 8: Snapshot from a hemodynamic recording.

Parameters monitored during the hemodynamic procedure are indicated by the circles. Beat per minutes (BPM), °C (Temperature) and EKG (Electrocardiogram). SAP (systemic arterial pressure and RVSP (right ventricular systolic pressure) are also shown in the two upper lanes of the graph.

Right ventricular systolic pressure (RVSP) was measured by inserting a 1.4 mm catheter (Millar Instruments, Houston, TX, USA) into the jugular vein, which was then guided to the right ventricle. Subsequently, the systemic arterial pressure (SAP) was measured by inserting the same catheter in the left carotid artery which was afterwards guided to the left ventricle for the measurement of the left ventricular systolic pressure (LVSP). Pressure measurements were recorded for at least 2 minutes and analysed with Powerlab Pro software (AD Instruments Spechbach, Germany). Part of the recording was selected and the average max value of the selected region was provided by the software and considered for analysis. The size of the selected region was kept constant among different mice and groups. (This technique was performed by Sabrina Reinisch and Sabine Halsegger, LBI LVR, Graz, Austria). An example of the recording and the monitored parameters is shown in Figure 8.

3.1.5 Organ collection

After hemodynamic measurements the animals were rapidly euthanized according to the Austrian regulations. The chest was opened and blood was collected. To perfuse the lung, the left atrium was incised and PBS injected via the right ventricle until the lungs became free from blood. After perfusion the right lobes were ligated and dissected from the rest of the lung. Each lobe of the right lung was separated and then snapped-frozen in liquid nitrogen for further molecular biology analysis. The remaining left lobe was inflated with 4% formalin as following. A small incision was made in the trachea which was then intubated and the lung was inflated with a pressure of 30 cmH_20, which corresponds to approximately 22 mmHg. The inflated lobe and the heart were then dissected from the chest. The heart was kept in PBS for the assessment of the hypertrophy and then fixed in formalin. The left lobe was placed in a formalin containing tube for 24 hours, changed then to PBS solution for additional 24 hours, followed by 70% and 50 % ethanol and finally fixed in the hystokinette machine. Tissue samples were then stored until used for molecular biological analysis or histological staining as described below.

3.1.6 Assessment of the right ventricular hypertrophy

The heart was dissected from the left lung, the atria were removed and a pair of fine scissors was inserted in the right ventricle. The right ventricle (RV) was then carefully dissected from the left ventricle (LV). The separated tissues (RV and the remaining LV plus septum (S)) were weighed to obtain the total heart weight and the right-to-left ventricle plus septum ratio (RV/ (LV+S)).

3.2 Human material

3.2.1 Human lung samples

Lung samples were obtained from patients (n=9) with idiopathic pulmonary arterial hypertension (IPAH) which were transplanted at the Division of Thoracic Surgery, Medical University of Vienna, Austria (Director W. Klepetko). Downsized non-transplantable donor lungs were used as controls lungs (n=10). The studies were approved by the ethics committee of the Justus-Liebig-University School of Medicine, Giessen (Germany) and by the Institutional Review Board of the Medical University of Vienna in accordance with the national law and the guidelines on Good Clinical Practice/International Conference on Harmonization. A written informed consent was

obtained from each diseased patient, while no informed consent was necessary from the donors. The lung samples collected were processed in small pieces and either fixed in 4% (m/v) paraformaldehyde (PFA) or snap-frozen in liquid nitrogen. The patients' characteristics are described in table 2 and have been already reported elsewhere (122). In case of missing mPAP value available, we referred to the diagnosis stated in the pathology report.

Table 2: Patient characteristics for lung tissues

IPAH Patient*	Age (years)	Sex	Echo mPAP § (mmHg)	Invasive mPAP (mmHg)
1	27	F†	80	82
2	28	F	86	-
3	45	M‡	81	-
4	20	F	90	73
5	14	F	125	114
6	44	M	-	83
7	37	F	-	88
8	14	F	-	-
9	43	F	-	88

Footnotes: *IPAH, idiopathic pulmonary arterial hypertension; †F, female; ‡M, male; §mPAP, mean pulmonary arterial pressure.

3.2.2 Isolation of human pulmonary artery smooth muscle cells (hPASMC)

Human PASMCs were isolated from the pulmonary arteries of downsized non-transplantable donor lungs (n=10). Pulmonary arteries were carefully isolated from the lung parenchyma, with the help of a stereomicroscope (Leica, Germany). The adventitial layer was removed from the arteries with a fine forceps. The isolated pulmonary arteries were then cut longitudinally and the endothelial cell layer was wiped off from the luminal side of the vessel. The remaining smooth muscle layer was cut in small squares and plated in a 75 mm^3 flask. To each square of tissue a drop of full media (VascuLife® Basal Medium containing 20%FCS; LifeLine Technology, Walkersville) was added. Cells outgrew from the tissue and when reached confluence cells were trypsinized and kept in liquid nitrogen for further studies. The purity of hPASMC cultures was confirmed using immunofluorescence staining against α-smooth muscle actin (minimum 95% of cells stained positive), as described below (section 3.3.2)

3.3 Cell culture experiments

3.3.1 Cell culture

Human PASMC were cultured in SMC Full Media (VascuLife® SMC Complete Medium, 0.2%antibiotics). For the experiments, hPASMC were changed to basal medium (VascuLife® Basal Medium, 0% FCS, 0.2% antibiotics, LifeLine Technology, Walkersville) for 12 hours before the experiments and maintained in basal medium for the duration of the whole experiment. Human pulmonary artery endothelial cells (hPAEC) were purchased from Lonza (Basel, Switzerland) and cultured in EC Full Media (VascuLife® VEGF-Complete Medium, 0,2% Antibiotic, LifeLine Technology, Walkersville). Both cell types were maintained in incubators (Binder, Tuttlingen, Germany) at 37°C and 5% CO_2. All the experiments were performed with hPASMC between passages 1 and 6, and with hPAEC in passages between 1 and 8.

3.3.2 Immunofluorescence staining

For immunofluorescence staining, hPASMC were seeded on 8-well chamber slides with a density of 20.000 cells/well. When confluence was reached, cells were stimulated with platelet derived growth factor (PDGF-BB, Sigma Aldrich, 10 ng/ml) or transforming growth factor (TGF-β, R&D Systems, 10 ng/mml) for 24 and 3 hours respectively or directly fixed for 15 minutes at -20°C with ice-cold methanol. After washing 3 times with ice cold PBS the cells were incubated with 3% BSA with 0.02 % triton X in PBS for 1 hour at room temperature (RT), and incubated for 16 hours at 4°C with the primary antibody (table 5) diluted in 0.1% BSA in PBS. After 3 washing steps of 5 minutes each with PBS, cells were incubated with anti-rabbit Alexa Fluor® Dye 555 (red) or 488 (green) (Invitrogen, Karlsruhe, Germany). Double immunofluorescence staining was performed by mixing the two primary and the two secondary antibodies. For mounting fluorescence vectashield mounting medium was used (Vector, Burlingame, CA) and the nuclei of the cells were counterstained with 4',6-diamidino-2-phenyindole dihydrochloride (DAPI, Sigma-Aldrich). To control, validate and capture the pictures of the stained slides a Leica DMR and an Olympus fluorescence microscope were used. An example picture of hPASMC purity is shown in figure 9.

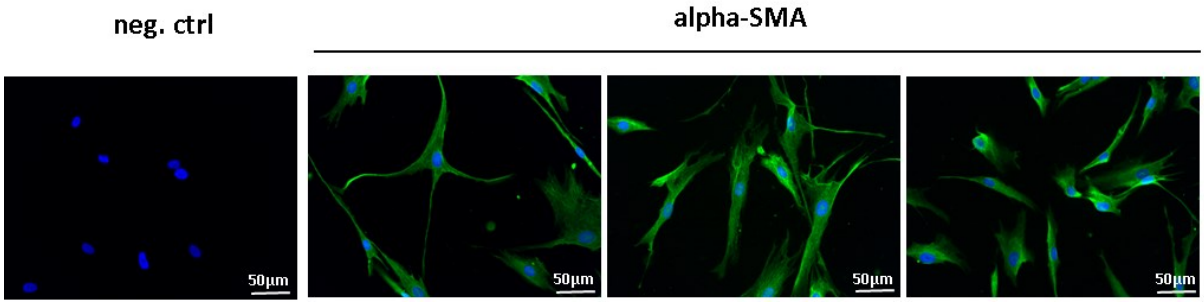

Figure 9: Immunofluorescence staining of hPASMC with α-smooth muscle actin: Staining of α-smooth muscle actin (alpha-SMA) staining in hPASMC (passage 6). The nuclear is stained with DAPI. In the negative control (neg. ctrl) the omission of the primary antibody was applied.

3.3.3 Transfection of primary cells

Silencing of fra-2, jun-B, jun-D, c-fos and c-jun was obtained with pre-designed commercially available siRNAs purchased from Dharmacon (Thermo Scientific, see table 3) used at the concentration of 100 nM. As a control for unspecific gene silencing a universal random negative-control siRNA sequence was applied (Ambion and Qiagen). Effectene Transfection Reagent (Qiagen) was applied to transfect cells. Briefly, the siRNA were mixed with DNA condensation buffer EC and Enhancer solution to allow condensation of the siRNA. The mixture was vortexed for 1 second and incubated at RT for 5 minutes. The condensed siRNA was then mixed with the effectene reagent, vortexed 10 seconds and incubated at RT for 8 minutes. This step allows formation of a condensed complex of siRNA-effectene. In this process micelles structures are formed which contains the siRNA. Post-incubation, basal medium was added and the mixture was applied to the cells. The complexes were left on the cells for 6 hours and afterwards medium was changed to SMC full media. The downregulation of the targeted proteins was verified 48 hours post-transfection by western blotting.

Table 3: Sequences of the siRNAs used for silencing.

Target gene	Targted sequences	Company	Product number
c-jun	GAGCGGACCUUAUGGCUAC GAACAGGUGGCACAGCUUA GAAACGACCUUCUAUGACG UGAAAGCUCAGAACUCGGA	Thermo Scientific (Dharmacon)	L-003268-00-0005
fra-2	GGCCCAGUGUGCAAGAUUA CAGAAAUUCCGGGUAGAUA CCACUCUGCUGGCUCUGUA ACACAUGGCCCUCCCAAGA	Thermo Scientific (Dharmacon)	L-004110-00-0005
c-fos	GGGAUAGCCUCUCUUACUA ACAGUUAUCUCCAGAAGAA GAACCUGUCAAGAGCAUCA GCAAUGAGCCUUCCUCUGA	Thermo Scientific (Dharmacon)	L-003265-00-0005
jun-B	GGACACGCCUUCUGAACGU CAUACACAGCUACGGGAUA GAACAGCCCUUCUACCACG GAGCUGGAACGCCUGAUUG	Thermo Scientific (Dharmacon)	L-003900-00-0005
jun-D	GAAACACCCUUCUACGGCG CCGACGAGCUCACAGUUCC UCAAGAGUCAGAACACGGA GUUCGAUUCUGCCCUAUUU	Thermo Scientific (Dharmacon)	L-003269-00-0005

3.3.4 Stimulation of primary cells

Cells were stimulated with 1% hypoxia, with 10 ng/ml of platelet derived growth factor (PDGF-BB Sigma Aldrich), interleukin-6 (IL-6, Peprotech) and transforming growth factor β (TGF-β, R&D Systems) while endothelin-1 (ET-1, Sigma Aldrich) was used at the concentration of 500nM and connective tissue growth factor (CTGF, Peprotech) at the concentration of 10µg/ml. For pathway inhibitor studies, cells were treated with different inhibitors for 1 hour before addition of the stimulus. The used inhibitors concentrations are: 5 µM SP600126 (inhibitor of JNK), 5 µM BAPTA (chelator of Ca^{2+}), 80 µM Wortmannin (inhibitor of PI3K/AKT), 50 µM U0126 (inhibitor of ERK), 8 µM SB203580 (inhibitor of p38), 1 µM BQ123 (inhibitor of endothelin receptor A), and 1µM BQ788 (inhibitor of endothelin receptor B) (all from Sigma Aldrich) and 10 µM U73122 (inhibitor of PLC) (TOCRIS bioscience).

3.3.5 Proliferation assay

To determine the role of AP-1 transcription family on the proliferation of hPASMC, single (fra-2, c-fos, c-jun, jun-D and jun-B) or double siRNA (fra-2-c-jun, fra-2-jun-B, fra-2-jun-D and c-fos-c-jun) mediated knockdowns were performed as described in section 3.3.3. After 24 hours cells were trypsinized and seeded in a 96 well plate with a density of 10.000 cells/well. After 8-10 hours the cells were changed to basal medium for 12 hours. Subsequently, 500 nM ET-1 or 10 ng/ml PDGF-BB were added for 24 hours together with 1 µCurie/ml of radioactive labeled [3H]-thymidine (BIOTREND Chemikalien GmbH). The proliferation was measured as incorporated radioactivity by a scintillation counter (Wallac 1450 MicroBeta TriLux Liquid Scintillation Counter & Luminometer). The effect of the meprin β inhibitor actinonin (Sigma Aldrich, Taufkirchen, Germany) was determined on proliferation of hPASMC and hPAEC. After starvation for 12 hours (for hPASMC), actinonin and the vehicle were added for 24 hours, before determining the proliferation rate.

3.3.6 Apoptosis assay

To assess the apoptotic effect of actinonin (123), hPASMC and hPAEC were seeded with a cell density of 100.000 cells/well in a 6-well plate. When confluence reached 80%, the complete medium for hPASMC was replaced by basal medium for 12 hours. The duration of treatment for actinonin (Sigma Aldrich) and vehicle was 24 hours. Post-treatment, the supernatant and cells were collected and harvested by trypsinization. The cells were centrifuged at 1200 rpm for 5 minutes and re-suspended in 100 µl of Annexin V buffer (140 mM NaCl, 5mM $CaCl_2$, 10 mM HEPES, pH7.4). Cells were transferred in a 96 well plate and incubated with Annexin V-Alexa 647 (1:20) for 15 minutes at RT in dark to stain apoptotic cells. After washing 2 times with 100 µl of Annexin V buffer (2 cycles of 1200 rpm centrifugation for 3 minutes), cells were re-suspended in 100 µl of Annexin V buffer and transfer in FACS tube. Prior to measurement, propidium iodide (1:20) was add to stain dead cells. Measurement was performed with the FACS Calibur (BD Bioscience).

3.4 Molecular biology techniques

3.4.1 Isolation of RNA and cDNA synthesis

Isolation of total RNA was carried out with the peqGOLD Total RNA isolation kit (PeqLab, Erlangen, Germany). Human or mouse tissue were first minced with pestle and mortar in liquid nitrogen. To preserve the integrity of RNA, RNAses free solutions were used to clean the instruments before and after every sample grinding. The powder obtained from the grinding was re-suspended in 750 µl of lysis buffer. Cell monolayer was lysed directly with 750 µl of lysis buffer. RNA isolation was performed for cells and tissues according to the manufacturer's instructions (PeqLab). The amount and quality of RNA was assessed by measuring the absorbance at 260 nm and the ratio of the absorbance at 280/260 nm respectively (Nanodrop, Rockland, IL). The isolated RNA was reverse transcribed to cDNA with the iScript kit (BioRad, Hercules, CA, USA) according to manufacturer's protocol. The amount of reverse transcribed RNA was 1µg per reaction in a total volume of 20 µl, resulting in a concentration of 50 ng/µl of cDNA.

3.4.2 Real-time PCR

Real-time PCR was performed using a LightCycler 480 (Roche). The reactions for the PCR were prepared using QuantiFast SYBR PCR kit (Qiagen, Hilden, Germany) in 384 well plates with a total volume of 4 µl/well and were carried out in duplicate to control pipetting errors. The PCR conditions were the following: 5 minutes at 95°C, [5 seconds at 95°C, 5 seconds at 60°C, and 10 seconds at 72°C] x45 cycles. As unspecific binding of SYBR®Green to double strand DNA can take place, the specific amplified PCR product was confirmed by analysis of the melting curve and gel electrophoresis. Expression of the analysed genes is shown as ΔCt value normalized to the housekeeping gene (beta-2 microglobulin (β2m) or hydroxymethylbilane synthase (HMBS), which was calculated as following: ΔCt = Ct value (housekeeping gene) – Ct value (gene of interest). For expression analysis in fra-2 TG mice lung homogenate, the WT group values were pooled as no significant difference in the ΔCt values was noticed between WT mice of different ages (8, 12 and 16 weeks). Therefore we compared the fra-2 TG mice of each time point to the pooled WT mice for ΔΔCt analysis. ΔCt was calculated as previously described and the ΔΔCt was calculated with the following formula: ΔCt of the interested gene in fra-2 TG group- ΔCt (average value) of the WT group. Primer sequences are provided in table 4.

Table 4: Primer sequences

Gene name	Species	Access. No.	Forward primer (5´- 3´)	Reverse primer (5´- 3´)
FOS	Human	NM_005252.3	GGGATAGCCTCTCTTACTACCACT	GAAGTTGGCACTGGAGACGG
JUN	Human	NM_002228.3	CCAAGTGCCGGAAAAGGAAG	ACCTGTTCCCTGAGCATGTTG
PCNA	Human	NM_002592.2	CTAAAATGCGCCGGCAATGA	TTCTCCTGGTTTGGTGCTTCA
MKI67	Human	NM_002417.4	TGACCCTGATGAGAAAGCTCAA	ACGTCCAGCATGTTCTGAGG
CCND1	Human	NM_053056.2	AGTGGAAACCATCCGCCG	TCTGTTCCTCGCAGACCTCCA
TGFB1	Human	NM_000660.5	GCCTTTCCTGCTTCTCATGG	TTGCGGAAGTCAATGTAC
CTGF	Human	HM015591.1	GTGAGCCTCGTGCTGGAC	GAGCACCATCTTTGGCGGT
EDN1	Human	NM_001955	Hs_EDN1_1_SG QuantiTect Primer Assay	
HMBS	Human	NM_000190.3	CCCACGCGAATCACTCTCAT	TGTCTGGTAACGGCAATGCG
FOSL2	Human	NM_005253.3	CGGCCAGCAGAAATTCCGGGTAG	GTAGGGGTGCGAGCGAGGGT
JUND	Human	NM_005354.4	GCCTGAGTGAGCAGGTGGCG	GGAGGCCAGCTTCAGCAGCC
JUNB	Human	NM_002229.2	CCTCCCACTGGGGTCCAGGG	AGGTGGAAGGACTGGGCGCA
MEP1A	Human	NM_005588.2	GCTGCAGGTGCATCTCTGGAC	AGCCGTGCCTCCGATCACCA
MEP1B	Human	NM_005925.2	TCAGTAGGAAATAGGCGGGT	CTGCCTGACAGAATTCTGT
JUN	Human	NM_002228.3	CCAAGTGCCGGAAAAGGAAG	ACCTGTTCCCTGAGCATGTTG
B2M	Human	NM_004048.2	CCTGGAGGCTATCCAGCGTACTCC	TGTCGGATGGATGAAACCCAGACA
HMBS	Human	NM_001258209.1	TCGGAGCCATCTGCAAGCGG	GCCGGGTGTTGAGGTTTCCCC
Fos	Mouse	NM_010234.2	AACGCCGACTACGAGGCGTC	GGACAGATCTGCGCAAAAGTCCTGT
Jun	Mouse	NM_010591.2	AGGGGGAAGCACTGCCGTCT	GTCCGTCACTTCACGCGGGG
Etn1	Mouse	NM_010104	Mm_Edn1_1_SG QuantiTect Primer Assay (200)	
B2m	Mouse	NM_009735.3	CGGCCTGTATGCTATCCAGAAAACC	TGTGAGGCGGGTGGAACTGTG
Mep1b	Mouse	NM_008586.2	TCAAGGGCAGTGGGTGCTGGT	ATGCCAGAATCCCAGGGCGTG
Col1a2	Mouse	NM_007743.2	TGTTGGCCCATCTGGTAAAGA	CAGGGAATCCGATGTTGCC
Col1a1	Mouse	NM_000088.3	AATGGCACGGCTGTGTGCGA	AACGGGTCCCCTTGGGCCTT
Col3a1	Mouse	NM_009930.2	GCCCTCCCGGGAATAACGGC	TGGCTCTCCCTTCGCACCGT
Mep1a	Mouse	NM_008585.2	TCTACGCAGGGGAGCGCTGT	GGGTAGCTGCTCACTGCCGC
Mmp9	Mouse	NM_013599.2	GGCCGCTCGGATGGTTACCG	TACGGTCGCGTCCACTCGGG
Pdgfb	Mouse	NM_011057.3	CAGCGAGCCAAGACGCCTCAA	ACACTCTTGCCGACGCCCCT
Tgfb	Mouse	NM_011577.1	GTGGACCGCAACAACGCCATCT	GCAATGGGGGTTCGGGCACT
Pdgfrb	Mouse	NM_001146268.1	GCAGGTCAATGTCCCCGTCCG	GGTCTCTGCAGGTAGACCAGGTG

Mmp7	Mouse	NM_010810.4	TCATGCCTTCGCACCTGGGC	GTTCACTCCTGCGTCCTCACCA
Mmp2	Mouse	NM_008610.2	TGGCAGCCCATGAGTTCGGC	CGGGGGAGGGCCCATAGAGC
Tnc	Mouse	NM_011607	Qiagen custom primer QT00106176	
Anp	Mouse	NM_008725	CCAGCTGCTTCGGGGGTAGGA	TTCGGTACCGGAAGCTGTTGC
Bnp	Mouse	NM_008726	TCGTTTGGGCTGTAACGCACTGA	GCTGGGGAAAGAGACCCAGGC
Hmbs	Mouse	NM_001110251.1	GCCAGAGAAAAGTGCCGTGGG	TCCGGAGGCGGGTGTTGAGG
Fos	Rat	NM_022197.2	AACGCCGACTACGAGGCGTC	GGACAGATCTGCGCAAAAGTCCTGT
Jun	Rat	NM_021835.3	CCAAGTGCCGGAAAAGGAAG	ACCTGTTCCCTGAGCATGTTG
Edn1	Rat	NM_012548.2	GACAAAGAACTCCGAGCCCA	AGCTTGGGACAGGGTTTTCC
Hmbs	Rat	NM_013168.2|	GCCAGAGAAAAGTGCCGTGGGG	CCAGCTTCCGTAGGCGGGTG

3.4.3 Microarray

The total RNA from lung homogenate samples from 4 fra-2 TG and 4 WT littermate control mice (8 weeks old) was isolated with the RNeasy Mini kit (Peqlab) as described in section 1.4.1. The Agilent Low-Input QuickAmp Kit was used to pre-amplify and label 1 µg of total RNA per sample with Cy5. Hybridizations were carried out in Agilent hybridization chambers at 42°C overnight on Agilent 6x80K mouse microarrays. Analysis of the data was performed with the limma package in the software R (124),(125). Intensity values were quantile normalized and corrected for the background. Moderated t statistic was applied to estimate significant differential expression. (Experiments and analysis were performed by Jochen Wilhelm, Universities of Giessen and Marburg Lung Center (UGMLC), Giessen, Germany)

3.4.4 Protein isolation and western blot

To isolate proteins 250 µl of ice-cold RIPA buffer (25mM Tris-HCl (pH 7.6), 150mM NaCl, 1% sodium deoxycholate, 1% NP-40, 0.1% SDS supplemented with protease and phosphatase inhibitors (Thermo Scientific)) was applied to the cell monolayers. The monolayer was destroyed with the help of a cell scraper. Human or mouse tissue were first ground with pestle and mortar in liquid nitrogen to preserve the protein integrity and the post translational modifications of the proteins. The collected powder was then re-suspended in 250 µl RIPA buffer and kept for 30 minutes on ice, vortexing every 10 minutes. The lysate (from tissue or cells) was then centrifuged at 13.000 rpm for 15

minutes at 4°C and the protein extract (supernatant) was collected. The protein lysate were separated on a 10-12% SDS polyacrylamide gel, depending on the size of the protein which was investigated. After gel separation protein were blotted on a nitrocellulose membrane for 1 hour and 30 minutes at 4°C at 100V by electro-transfer. To verify the transfer of the proteins, after the blotting the membranes were stained with the reversible staining, Red Ponceau. The membranes were then washed from the staining with distilled water and blocked for 1 hour at RT with 5% non-fat dry milk in TBS-T (TBS + 0,1% tween 20) buffer. Subsequently, the membranes were incubated for 16 hours at 4°C with primary antibody (table 5). After washing of the membranes with TBS-T 3 times for 5 minutes, they were incubated 1 hour with the corresponding peroxidase-labelled secondary antibody (Pierce). Finally, membranes were incubated with 1 ml of ECL solution (Prime Kit, Amersham Biosciences, Freiburg, Germany) for 5 minutes at RT. Chemiluminescence was detected on Kodak films and developed with an AGFA Curix 60 Film Processor.

3.4.5 Electrophoretic mobility shift assay (EMSA)

To confirm AP-1-meprin promoter interaction we performed electrophoretic mobility shift assays (EMSA) using the LightShift Chemiluminescent EMSA Kit (Thermo Scientific, Rockford, IL). 300.000 hPASMC were seeded in a 60 mm dish and when confluence was reached they were changed to starvation medium overnight. Cells were then stimulated with 10 ng/ml TGF-β for 1 or 2 hours. After stimulation cells were trypsinized and centrifuged at 500g for 5 minutes. Nuclear protein extracts were isolated with the NE-PER Nuclear and Cytoplasmic Extraction Kit, according to the manufacturer's instructions (Pierce, Thermo Scientific). Briefly, the cell pellet was dissolved in a volume of ice cold cytoplasmic extraction reagent I (CER I). The cells were vortexed for 15 seconds and incubated on ice for 10 minutes. The second cytoplasmic extraction reagent (CER II) was added and again the tube was vortexed for 5 seconds and incubated on ice for 1 minute. The tube was then centrifuged at 16000g for 5 minutes and the supernatant, containing the cytoplasmic fraction of protein, was separated. The remaining pellet was then suspended in ice-cold nuclear extraction reagent (NER I). Four cycles of vortexing (15 seconds) and incubation on ice (10 minutes) were carried out before a centrifugation step at 16000g for 10 minutes. The supernatant (nuclear extracts) was then transferred in a new tube and placed on ice. The nuclear extract was then incubated with the labelled and unlabelled probes corresponding to the AP-1 predicted binding site (126) in the human meprin β promoter, and incubated for 20 minutes at RT. The following 3′-biotin–labeled or

unlabeled probes (NC_000018.9) were used: forward primer 5′-CTA CTT TTA TGA CCCA TGT CCC ACC-3′ and reverse primer 5′-GGT GGG ACA TGG GTC ATA AAA GTA G-3′ for position -451, forward primer 5′-AAT TGT TGA CAC AGG AAA AAA AAA A-3′ and reverse primer 5′ -TTT TTT TTT CCT GTG TCA ACA ATT-3′ for the -81 position. After incubation the reactions were loaded in a native 5% polyacrylamide gel and run at 100V for ~2 hours. The DNA-protein complexes were then transferred to a nylon membrane with an electrophoretic transfer at 100V for 30 minutes. After transfer, the complexes were crosslinked on the membrane using a UV-crosslinker (Labortechnik) (45-60 second exposure at 120 mJ/cm^2). Finally the membrane was incubated for 15 minutes with the Blocking Buffer, 15 minutes with the Conjugate/Blocking solution; it was washed 4 times for 5 minutes with washing solution 1X and incubated 5 minutes with the Substrate Equilibration Buffer. DNA-protein complex was detected with Luminol/Enhancer Solution. This protocol was performed according to the manufacturer's instructions of the applied kit (Thermo Scientific).

3.4.6 Hydroxyproline assay

Lungs of WT and fra-2 TG mice at different age (8, 12 and 16 weeks) previously collected were minced with mortar and pestle and proteins were isolated with complete RIPA buffer (see section 3.4.4). 50 µg of protein extracts were incubated with 12 M HCl in a volume ration of 1:1 and mixed at 450 rpm for 20 hours at 95°C. The samples were cooled to 25°C and centrifuged at 13.000 rpm for 10 minutes. The supernatant containing the hydrolysed collagens was then transferred in a plate and incubated with the detection reagents at 60°C for 1 hour and 45 minutes. Consequently the plate was cooled on ice to RT. This protocol was carried out following manufacturer's instruction (Quickzyme Biosciences, Leiden). The absorbance was measured at 570 nm with a spectrophotometer and, based on the standard curve; the concentration of hydroxyproline was calculated.

3.4.7 Tissue staining and immunohistochemistry

Formalin-fixed paraffin embedded lung tissues (mouse, rat, human) were sliced to 2 µm thickness. Incubation of the slides at 60°C for 16 hours followed by xylol incubation and decreasing percentage of ethanol (100%, 90%, 70%, 50% and distilled water) enabled removal of the paraffin from the tissue and rehydrate the slides. After this process the slides underwent Haematoxilin-eosin (H&E), Masson`s trichrome or immunohistochemistry staining.

3.4.7.1 Hematoxylin-eosin staining (H&E)

For the H&E staining slides from fra-2 TG mice were incubated for 5 minute in Mayer`s Hematoxylin solution (Roth) followed by 2 minutes of hot running water. Slides were then incubated 1 minute in Eosin Phloxine (Roth) mixed with 96% ethanol (1:1) and then washed some seconds in distilled water, dehydrated in 96% ethanol and xylol. Finally, they were mounted in xylol based mounting media (Thermo Scientific).

3.4.7.2 Masson`s trichrome

For the Masson`s trichrome the slides from fra-2 TG mice, were deparaffinised, re-fixed in Bouin's solution (75% saturated picric acid, 25% formaldehyde (37-40%), 5% glacial acetic acid) and then washed for 5-10 minutes in running tap water. Afterwards, the nuclei were stained in the Weigert`s iron-hematoxylin (1:1 mixture of 1% hematoxylin in 95% ethanol and 4% of Ferric chloride (29%), 1% HCl in distilled water) solution for 10 minutes, washed and incubated 10 to 15 minutes in Biebrich scarlet acid fuchsin (90% Biebrich scarlet (1% acqueous), 9% Acid fuchsin (1% acqueous) and 1% glacial acetic acid) to stain red the acidophilic elements such as collagen and cytoplasm. After washing, the red staining of the collagen is removed by incubation with the phosphomolybdic-phosphotungstic acid solution (1:1 ratio of 5% Phosphomolybdic acid and 5% of Phosphotungstic acid) for 10 to 15 minutes. Slides are transferred in the Aniline blue solution (2.5% Aniline blue, 2% glacial acetic acid in distilled water) where the collagen will to be stained in blue. The staining is differentiated in 1% acetic solution for 3 minutes, the slides dehydrated in increasing percentage of ethanol and mounted with xylol-based mounting media (Thermo Scientific). Following Masson`s trichrome staining, slides were scanned with an Aperio slide scanner microscope (Aperio Oxford, UK) and the collagen content was quantified by semi-automated images analysis using the Visiopharm software (Hoersholm). The quantification of collagen was calculated as the percentage of collagen (blue staining) to the total area analyzed for each lung specimen. To maintain consistency between samples always the left lobe was analyzed for each mouse.

3.4.7.3 Immunohistochemistry

Immunohistochemistry stainings were performed on human, mouse and rat slides using ZytoChem Plus AP-Fast Red Kit (Zymed Laboratories Inc., San Francisco, CA) or ImmPACT^{TM} VIP Kit (Vector Laboratories) according to the manufacturer's instruction. For both protocols the antigen retrieval step was performed at 95°C for 45 minutes with 10mM Sodium Citrate pH6 and the tissue marked with a Dako pen (Dako). For the

ZytoChem Plus AP-Fast Red Kit, slides were incubated with the blocking solution for 5 minutes, washed 2 minutes in TBS and incubated 1 hour with the primary antibody (table 5). After incubation, the slides were washed again 3 times 5 minutes with TBS, incubated 20 minutes with the Post-Block reagent, washed and incubated with the AP polymer reagent for 30 minutes. After a final washing step, the Fast Red developing reagent was applied on the slides and the reaction was stopped with distilled water when the desired intensity was obtained. Counterstaining was performed with Heamatoxylin for 45 seconds and mounting with aqueous medium (Merck). For the ImmPress kit before blocking slides were incubated in 15% H_2O_2 in methanol to block the endogenous peroxidase and therefore reduce unspecific staining. Blocking was performed with 10% BSA for 1 hour, followed by 2.5% serum block normal horse serum for 20 minutes. Primary antibody was incubated overnight (table 5) and after incubation with the secondary reagent peroxidase for 30 minutes the NovaRed substrate was applied on the slides. The reaction was stopped with distilled water when the desired intensity was obtained. Counterstaining was performed with Heamatoxylin for 45 seconds, slides where dehydrated and mounted with xylol based medium (Thermo Scientific). Details of antibodies and dilution applied are reported in the table 5. Negative controls were performed with the omission of the primary antibody. Aperio slide scanner or Olympus scanner microscope was used to scan the stained slides and snapshots were captured with OlyVIA 2.6 viewer (Olympus Soft Imaging Solutions) and Image Scope software (Aperio Oxford, UK).

Table 5: List of antibodies

Antibody	Source	Application	Dilution	Company	Product Nr.	used in
c-fos	rabbit	IHC	1:50	Cell signaling	#4384	Hu
c-fos	rabbit	ICH	1:100	Atlas antibody	HPA018531	Mu/Ra
c-fos	rabbit	WB	1:500	Novus Biological	NB100-91772	Hu
α-SMA	goat	IHC	1:100	Sigma Aldrich	#2228	Hu/Mu/Ra
p-c-fos(ser32)	rabbit	IHC/ WB	1:50	Cell signaling	#5348	Hu/Mu/Ra
c-jun	rabbit	IHC/ WB	1:100/1:1000	Cell signaling	#9165	Hu/Mu/Ra
p-c-jun(Ser73)	rabbit	IHC/ WB	1:100/1:1000	Cell signaling	#3270	Hu/Mu/Ra
Fra2 (L15)	rabbit	IHC/ WB	1:200/1:1000	Santa Cruz B.	sc-171	Hu/Mu/Ra
Meprin β	rabbit	IHC	1:250	Abcam	ab42743	Hu
Meprin β	goat	IHC	1:100	R&D	AF3300	Mu
JunD	rabbit	WB	1:1000	Abcam	ab28837	Hu
JunB	rabbit	IHC/ WB/IF	1:100/1:1000/1:100	Cell signaling	#3753	Hu/Mu
PCNA	rabbit	IHC	1:100	Santa Cruz B.	sc79027	Mu
TGF-β	rabbit	IHC	1:200	Cell signaling	#3711	Mu
Erk1/2	rabbit	WB	1:1000	Cell signaling	#9102	Hu/Mu
p-Erk1/2(Thr202/Tyr204)	rabbit	WB	1:1000	Cell signaling	#9101	Hu/Mu
SAPK/JNK	rabbit	WB	1:1000	Cell signaling	#9252	Hu/Mu
p-SAPK/JNK(Thr183/tyr185)	rabbit	WB	1:1000	Cell signaling	#4671	Hu/Mu
Akt	rabbit	WB	1:1000	Cell signaling	#9272	Hu/Mu
p-Akt(Thr308)	rabbit	WB	1:1000	Cell signaling	#9275	Hu/Mu
p38	rabbit	WB	1:1000	Cell signaling	#9212	Hu/Mu
p-p38(Thr180/Tyr182)	rabbit	WB	1:1000	Cell signaling	#9211	Hu/Mu
α-tubulin	rabbit	WB	1:2000	Cell signaling	#2125	Hu/Mu

3.5 Statistical analysis

Statistical analysis was performed with the software GraphPad Prism 5. To enable statistical analysis, experiments were designed and performed with matched control condition/animals. For all analysis p-values < 0.05 were considered significant and statistical significance is marked by an asterisk on the graphs.

3.5.1 Animal studies

Data for animal experiments (hemodynamic measurements, collagen quantification and expression analysis) are shown as scattered dot plots with a mean line ± SEM. The difference between the two groups was assessed by Student's t-test (hemodynamic measurement and collagen quantification). Regarding the expression studies for fra-2 TG mice as ΔΔCt was calculated and WT were pooled (see section 3.4.1), significant difference was assessed by one way ANOVA with the Dunnett`s post hoc test, comparing all the TG conditions to the WT.

3.5.2 Studies using human samples

For human samples (expression data) data are shown as scattered dot plot with a mean line ± SEM. Significance difference was determined by Student's t-test.

3.5.3 *In vitro* experiments

For *in vitro* experiments all expression analysis are presented as box-whiskers plot while the proliferation studies and the protein quantification for western blots are presented as column bar graph and in both cases the estimates are shown as mean with SEM. In general, significant differences within two groups were determined by Student's t-test while comparison of one group to multiple groups was performed by one-way ANOVA with the post-hoc test Dunnett's multiple-to-one comparison. For *in vitro* inhibitor studies, difference between multiple groups was assessed with Bonferroni test.

4 Results

4.1 AP-1 regulation by hypoxia

In order to understand the triggering molecular mechanism of the vascular remodeling in pulmonary hypertension it is necessary to investigate the early phase of the disease before the manifestation. This is not feasible in human, as pulmonary hypertension presents symptoms just when the disease is fully developed, however it is possible in animal models. The most frequently used animal model to study pulmonary hypertension is the chronic hypoxic (10% ambient oxygen which corresponds to Aspen altitude) exposure over several weeks in mice. However, a very short time exposure to hypoxia might help to find the triggering molecules. Chronic hypoxia has been previously shown to increase AP-1 transcription factors expression, leading to proliferation and migration of hPASMC (127); however it is not known whether these transcription factors are regulated *in vivo* upon short hypoxia exposure.

In order to evaluate the effects of the short term hypoxia, we exposed the mice to 12 and 24 hours hypoxia and we analysed the expression level of AP-1 transcription factors. Our results showed that the jun family (c-jun, jun-B and jun-D) was not affected by hypoxia at the investigated time points as shown in figure 10 A, B and C.

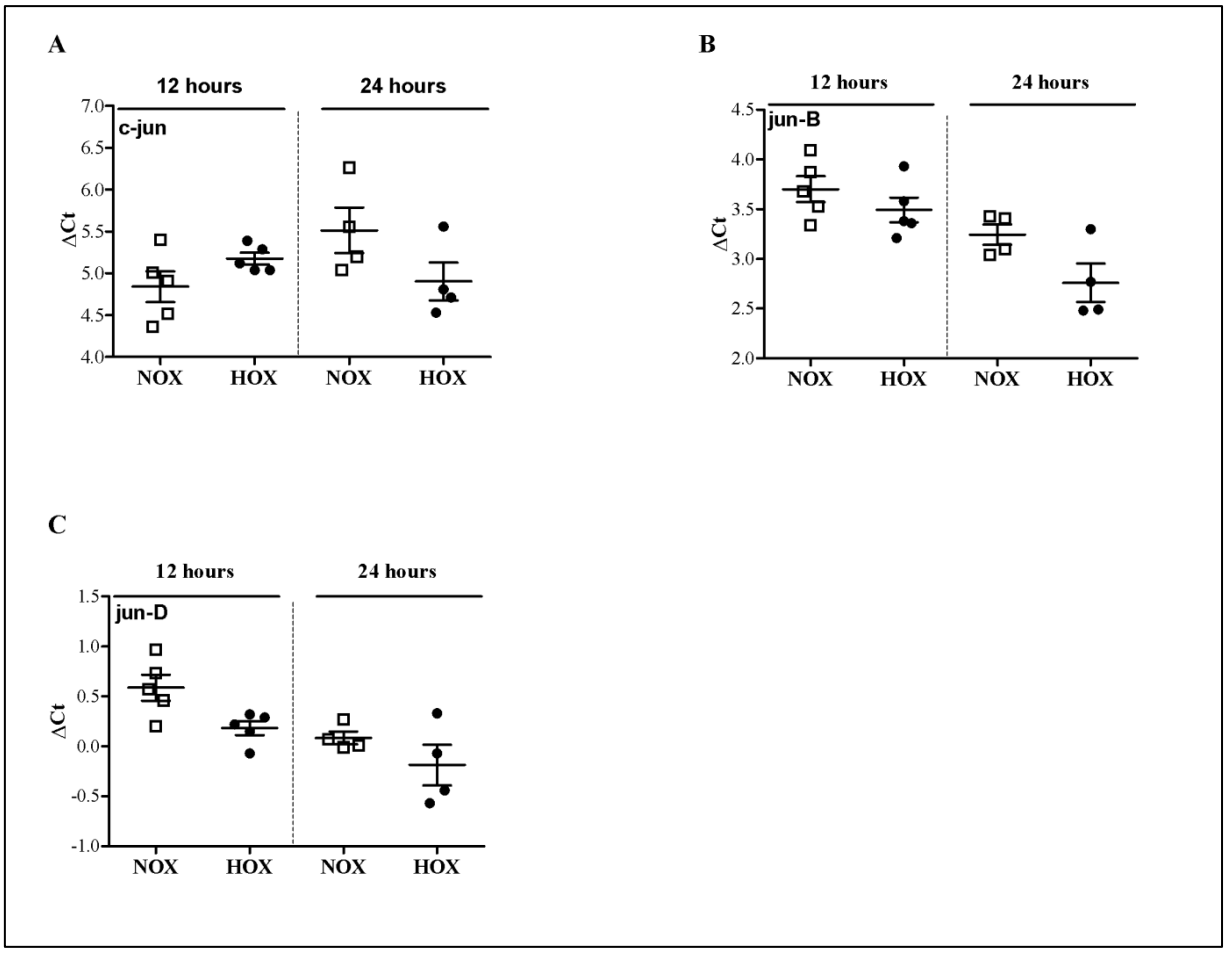

Figure 10: jun family regulation in hypoxia-exposed mice. Mice were exposed to hypoxia and normoxia for 12 (n=5) and 24 hours (n=4). Relative expression assessed by real-time PCR of A) c-jun, B) jun-B, and C) jun-D is presented,

Contrary, as depicted in figure 11, some members of the fos family were affected by short hypoxia exposure. Upon 12 hours hypoxia fra-2 and fra-1 were up-regulated (Figure 11A, B), while no change in the other components was observed at both investigated time points (Figure 11C, D).

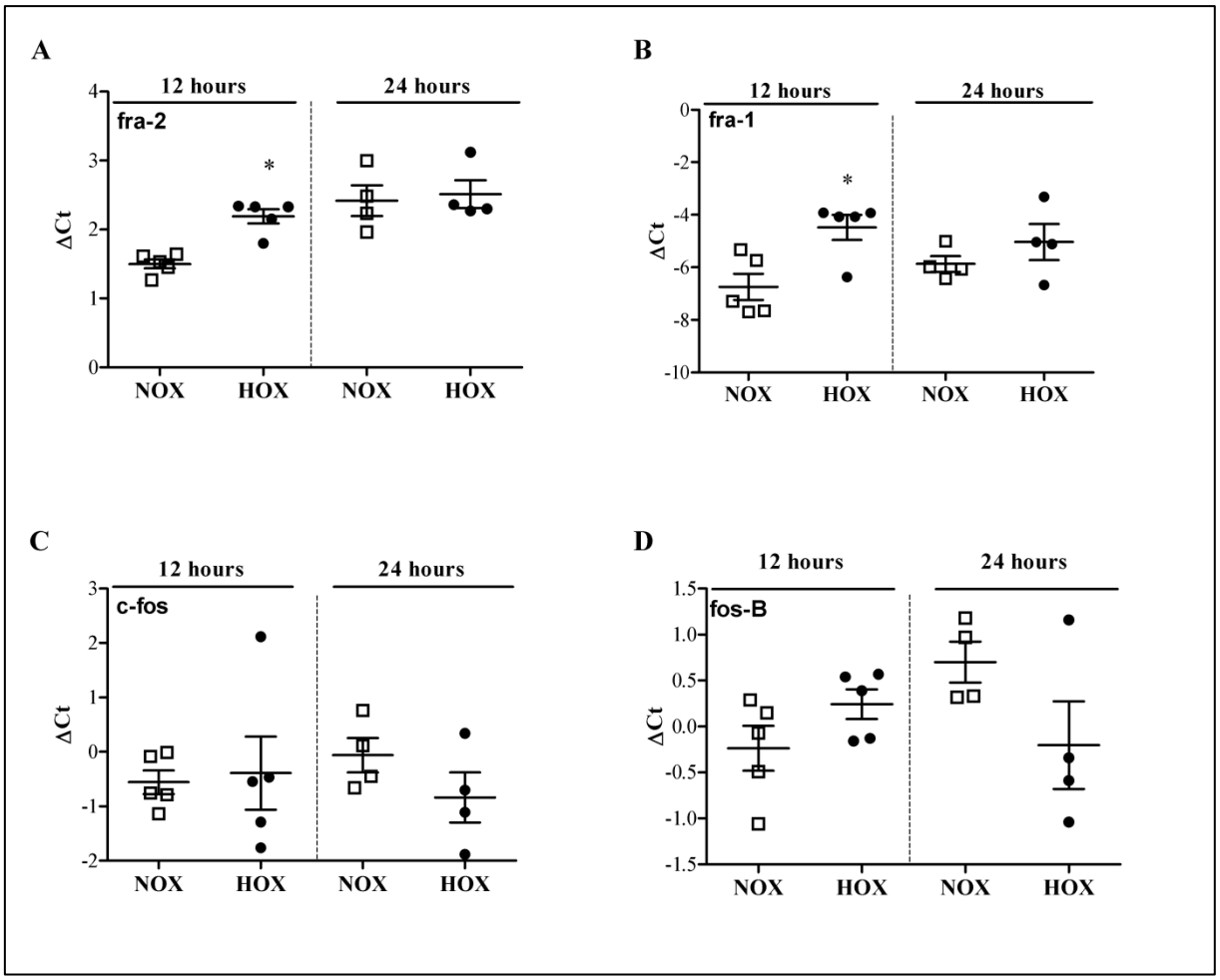

Figure 11: fos family regulation in hypoxia-exposed mice. Mice were exposed to hypoxia and normoxia for 12 (n=5) and 24 hours (n=4). Relative expression assessed by real-time PCR of A) fra-2, B) fra-1, C) c-fos and D) fos-B.

Importantly, AP-1 transcription factor expressions are influenced in a very fast manner (128), therefore even shorter exposure time could affect the AP-1 complex. Thus, in collaboration with Dr. Jochen Wilhelm from the University of Giessen and Marburg Lung Center (UGMLC, Giessen, Germany), a microarray analysis in RNA from lung homogenate of mice exposed for 3 hours to hypoxia was performed. Amongst other regulated genes, this analysis revealed that c-fos and c-jun were significantly up-regulated (Table 6 and GEO record GSE56698).

Gene Name	p-value	adjusted p-value
Proto-oncogene protein c-fos	0.000454843	0.032465787
Proto-oncogene c-jun	0.002268897	0.08238952

Table 6: Upregulation of c-fos and c-jun from the microarray analysis. P-value and adjusted p-value of c-fos and c-jun are reported. The adjusted p-value is adjusted to the number of listed genes, to have a more stringent p-value in order to reduce the false discovery.

4.2 Fra-2 in experimental pulmonary hypertension

Fra-2 (member of the fos family) overexpressing transgenic (TG) mice has been shown previously to develop pulmonary vascular remodeling (100). We hypothesized that this mouse model could exhibit pulmonary hypertension phenotype including increased pulmonary pressure and that fra-2, as a transcription factor, can regulate some key molecules involved in vascular remodeling.

4.2.1 Fra-2 is expressed in smooth muscle cells of human pulmonary vessels

To confirm the overexpression of fra-2 in our model we perform western blot and immunohistochemical staining in lung from fra-2 TG mice. As shown in figure 12A, fra-2 protein level is highly expressed in the lung of fra-2 TG mice in comparison to WT mice. Similar result can be observed in the immunohistochemical staining, where fra-2 is highly expressed in nearly every cell of the lung (Figure 12B). In WT mice fra-2 is not highly expressed, but positive cells are present (Figure 12B arrowheads).

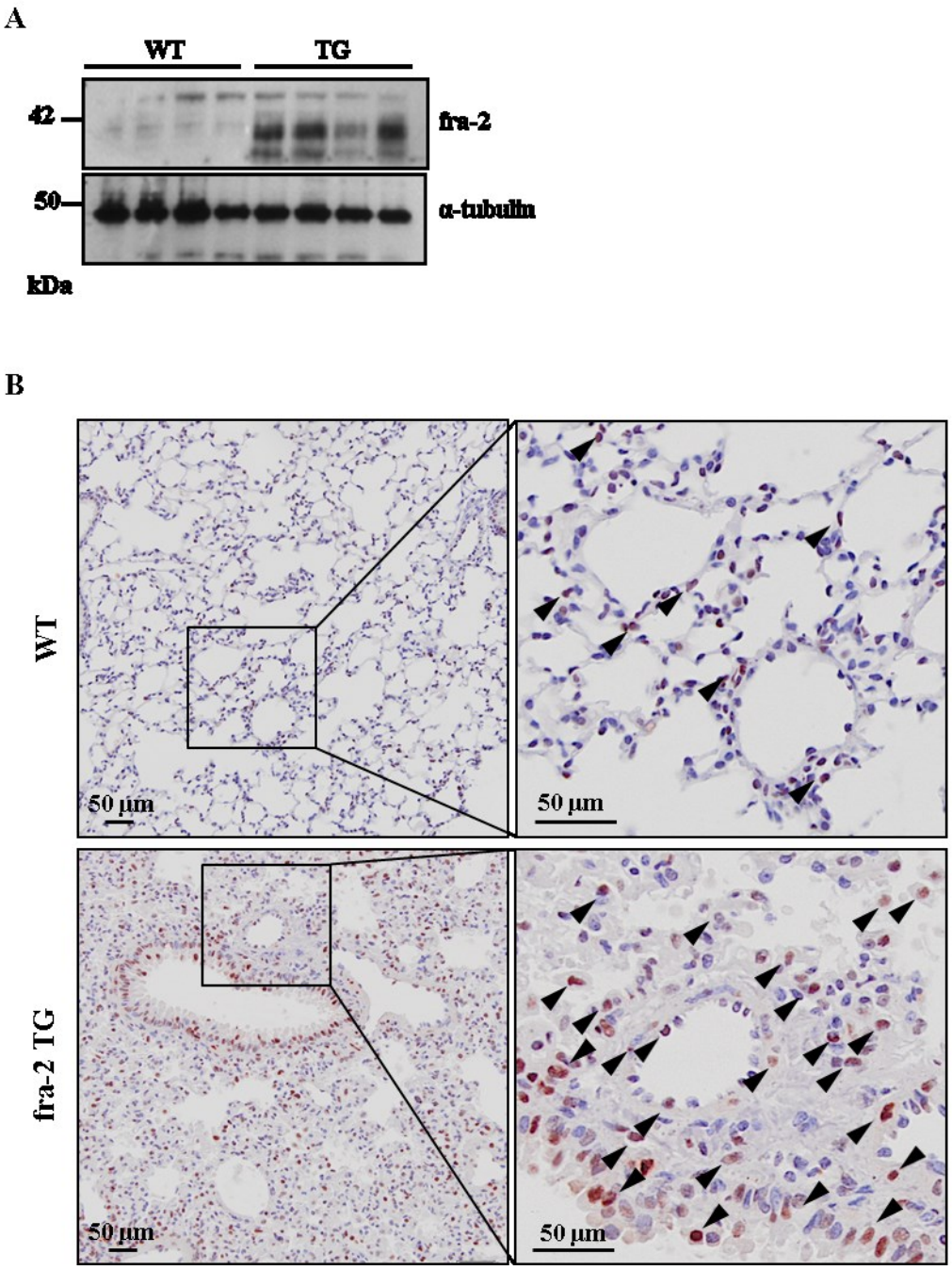

Figure 12: Fra-2 is overexpressed in fra-2 TG mice. A) Western blot analysis of fra-2 in lung homogenate from wild type-WT (n=4) and fra-2 TG mice (n=4), α-tubulin shows the loading control. B) Representative picture of fra-2 immunohistochemical staining in wild type (WT, arrowheads; n=3) and fra-2 TG (arrowheads, n=3). Western blot modified from (129).

To confirm the localization of fra-2 in human samples, we performed immunohistochemical staining in human donor and PAH patients' lung specimen. In figure 13, it is notable that fra-2 is mainly expressed in smooth muscle cells as shown by staining of serial slides with alpha-smooth muscle actin (α-sma) and fra-2. To note, fra-2 is also

expressed in epithelial cells and endothelial cells. The localization of fra-2 in smooth muscle cells suggests a possible role of this transcription factor in the remodeling process.

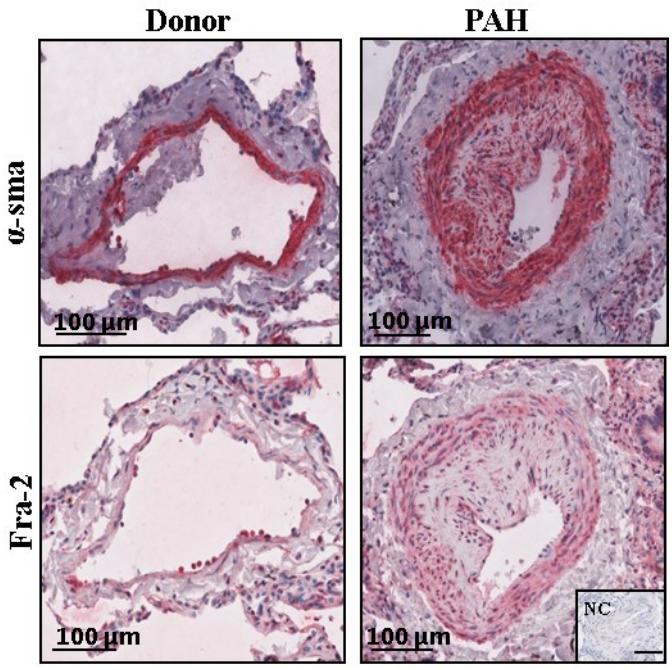

Figure 13: Fra-2 is expressed in smooth muscle cells. Representative lung vessel from donor and PAH patients stained with α-sma and fra-2. Serial slides were stained to be able to compare localization of fra-2. NC represents the negative control. PAH, pulmonary arterial hypertension (n=3). Figure modified from (129)

4.2.2 Fra-2 TG mice show increase of the right ventricular systolic pressure

In order to assess whether fra-2 TG mice develop pulmonary hypertension we performed hemodynamic measurement at different ages of the mice. In this way we analysed the development of the disease and we examined at each time point the pressure and the remodeling process. Accordingly to the previous publication (100), we have chosen the 8 weeks (early stage) 12 (middle stage) and 16 weeks (developed remodeling) time point. We observed that the right ventricular systolic pressure (RVSP) was elevated at each time point, starting form 8 weeks (Figure 14A). The Fulton index, indicating the heart hypertrophy was statistically elevated just at 8 weeks' time point while no difference at later time points was observed (Figure 14B). Most importantly no change was observed in the systemic arterial pressure (SAP) (Figure 14C), indicating that even though these mice globally over expressed fra-2, this transcription factor affect specifically the pulmonary circulation.

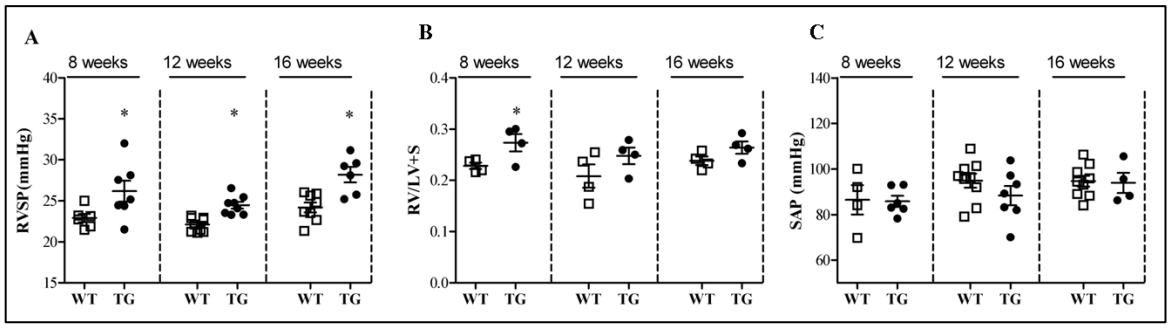

Figure 14: Fra-2 TG mice develop increased RVSP. Measurement of A) Right ventricular systolic pressure (RVSP), B) Fulton index (Right ventricle/Left ventricle plus septum; RV/LV+S) and C) systemic arterial pressure (SAP). (n= 4-8). Figure modified from (129)

Further confirming the hemodynamic data and the fulton index, we performed expression analysis of atrial natriuretic peptide (ANP) and brain natriuretic peptide (BNP) level from the heart of fra-2 TG and WT mice. These two proteins are considered to be markers of volume or pressure overload in the heart (130). ANP (Figure 15A) was significantly elevated at all-time point investigated, suggesting a direct regulation of ANP gene by fra-2. BNP (Figure 15B) was elevated only at 8 weeks, in accordance to the fulton index.

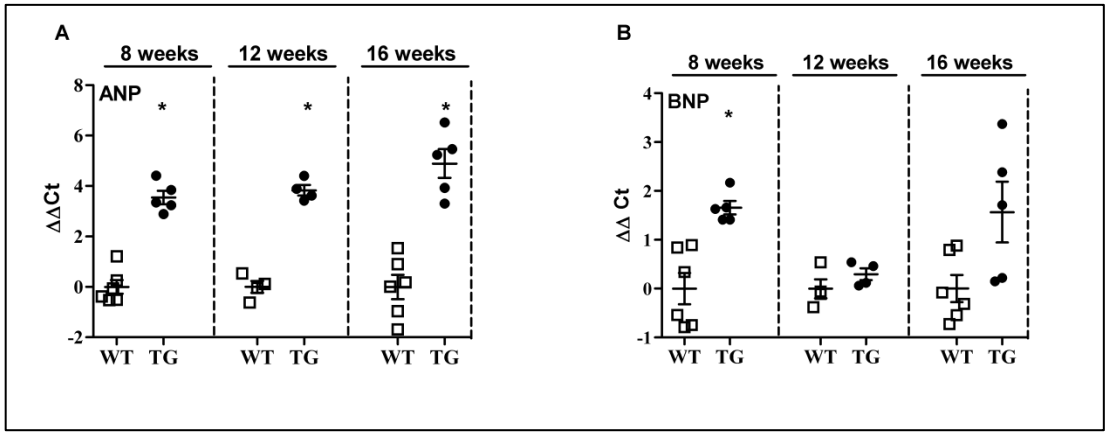

Figure 15: Fra-2 TG mice show increase ANP and BNP. Relative expression of A) atrial natriuretic peptide (ANP) and B) brain natriuretic peptide (BNP) in heart tissue from WT and fra-2 TG mice assessed by real-time PCR (n= 4-6). Figure modified from (129)

4.2.3 Fra-2 TG mice show pronounced pulmonary vascular remodeling

To characterize the mice and compare the elevated pressure with the remodeling process we performed hematoxilin and eosin (H&E), alpha smooth muscle actin (α-sma) and Masson's trichrome staining on serial slides from 8, 12 and 16 weeks' fra-2 TG and WT

mice. In figure 16A and B, it is possible to notice that fra-2 TG mice showed increased thickening of the vessels (arrows) starting already at 8 weeks and a strong inflammatory infiltrate at 16 weeks (arrowheads). It is important to mention that the remodeling at 8 weeks is limited at some vessel and is not as homogenous as at 16 weeks. Moreover, in figure 16C the Masson's trichrome staining clearly showed a high amount of collagen deposition around the vessel of the fra-2 TG mice lungs.

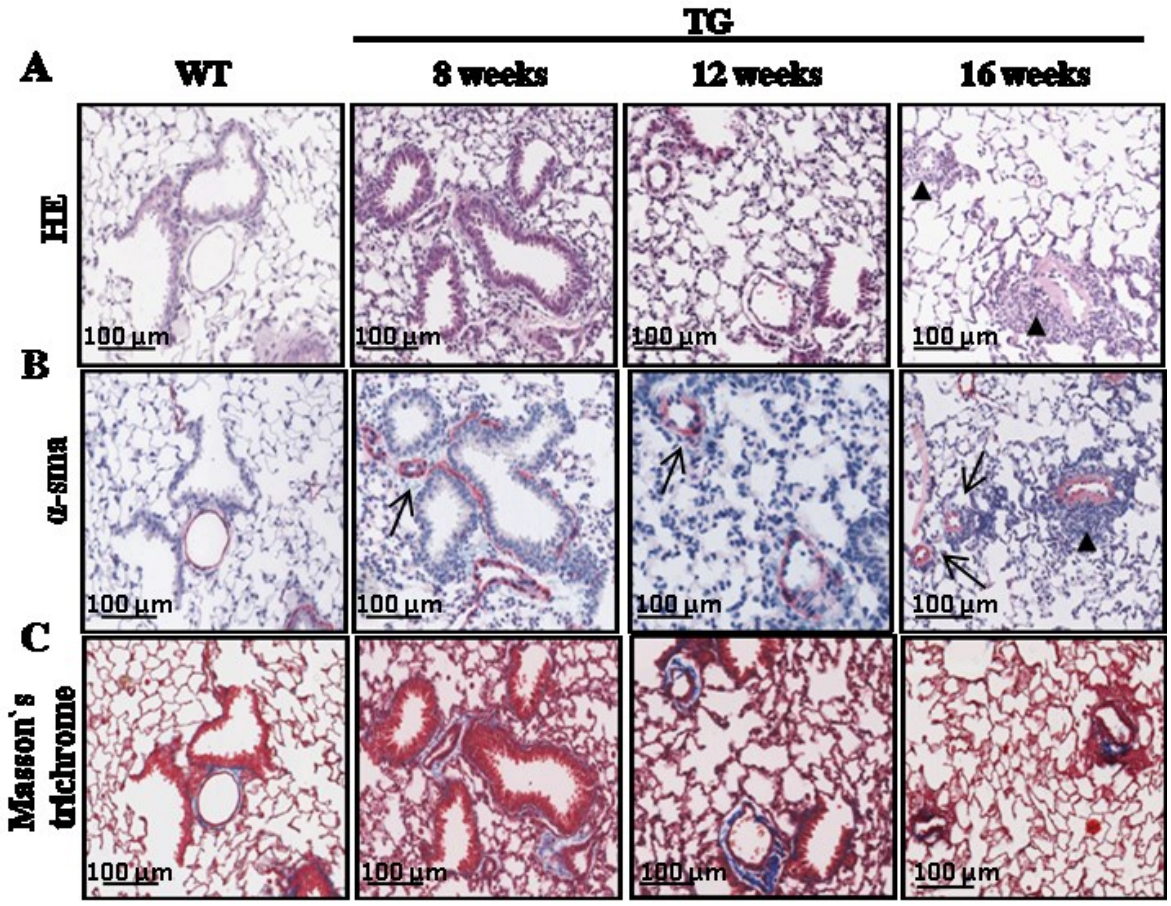

Figure 16: Fra-2 TG mice have increased vessel wall thickness, inflammatory infiltrate and collagen deposition. Serial slides from WT and fra-2 TG mice with A) hematoxylin and eosin (H&E); B) alpha smooth muscle actin (α-sma) and C) Masson's tricrhome staining (n=4). Figure modified from (129)

In addition, analysis of the lung parenchyma of fra-2 TG and WT mice revealed higher number of muscularized vessel in the TG mice in compared to WT (Figure 17), which can contribute to the increased pulmonary pressure.

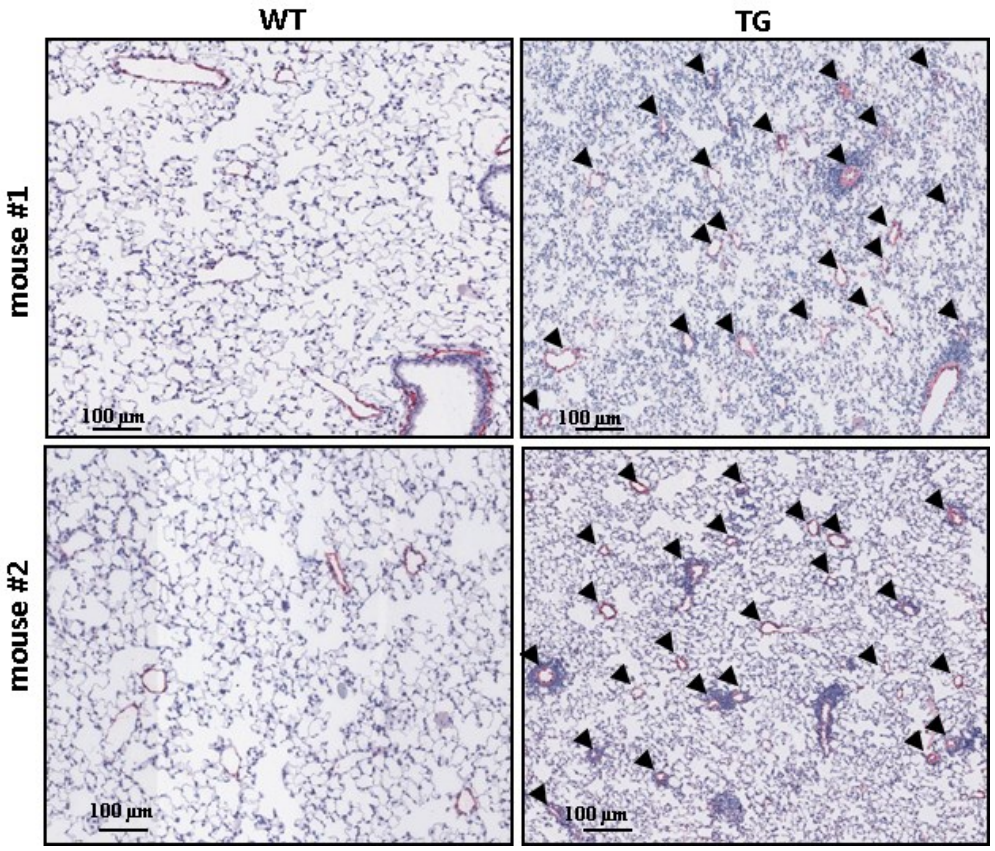

Figure 17: Fra-2 TG mice have increased number of α-sma actin positive vessel. Representative region of lung parenchyma from WT and fra-2 TG mice revealing an increased number of muscularized vessels in fra-2 TG mice (indicated by arrowheads) in comparison to WT (n=4, WT and fra-2 TG mice at 16 weeks). Figure modified from (129)

To characterize the phenotype from the molecular point of view, we performed western blot analysis on fra-2 TG mice lung homogenate to check whether some pathways resulted to be de-regulated in comparison to WT mice. As shown in figure 18, AKT pathway resulted to be strongly activated at all examined time points and p38 pathway revealed higher phosphorylation in 8 weeks' fra-2 TG mice in comparison to WT.

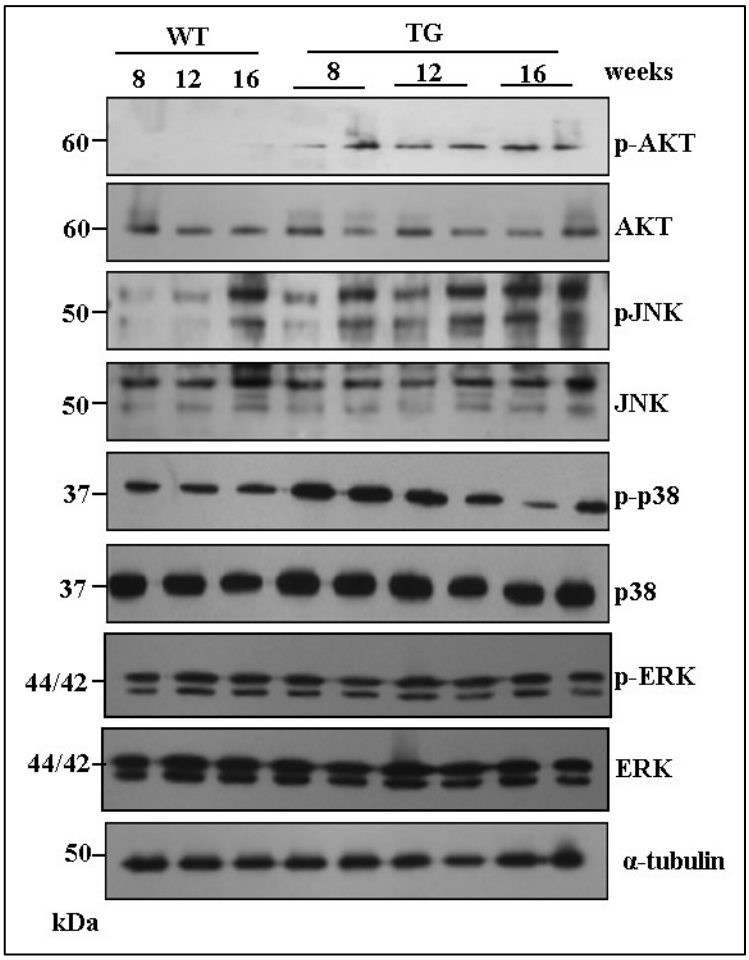

Figure 18: Fra-2 TG mice show activated AKT and p38. Representative western blot analysis of protein lysates in lung homogenate of WT and fra-2 TG mice for the following pathways: p-AKT/AKT, p-JNK/JNK, p-p38/p38, p-ERK/ERK; phosphorylated-p; α-tubulin shows the loading control (n=4 individual experiments were performed, 4 different animals/group). Figure modified from (129).

Importantly, AKT pathway is known to be a pro-survival pathway (131) which is in accordance with the positivity of smooth muscle cells to proliferating cell nuclear antigen (PCNA), shown in figure 19 by arrowheads. In this figure, beside the collagen deposition around the smooth muscle cells it is clearly visible that several smooth muscle cells are in the proliferating phase.

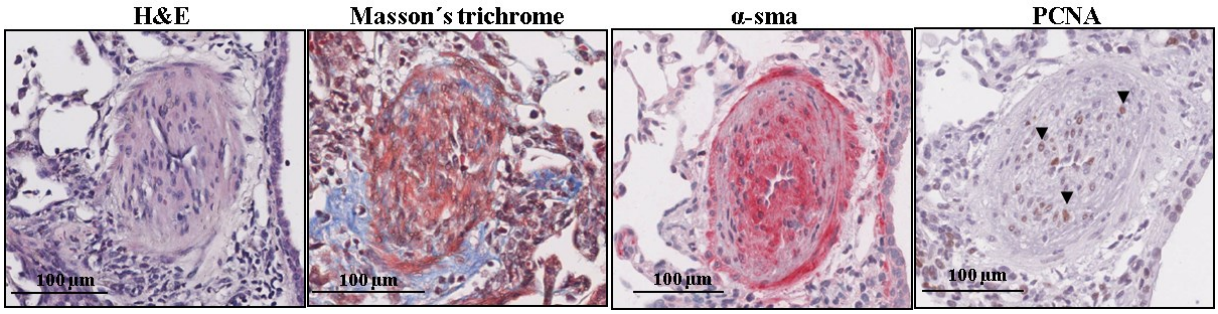

Figure 19: Smooth muscle actin positive cells from fra-2 TG mice are positive for proliferative marker. Serial slides from fra-2 TG mice with H&E; Masson's tricrhome, α-sma and PCNA staining (n=3). Figure modified from (129)

4.2.4 Pathways leading to pulmonary vascular remodeling in the fra-2 TG mice

Collagens are up-regulated in fra-2 TG mice

As we observed pronounced collagen deposition around the vessel in fra-2 TG (Figure 19 and 20) mice we performed expression analysis of different collagens in the lung homogenate in order to assess which collagen is responsible for the high perivascular deposition.

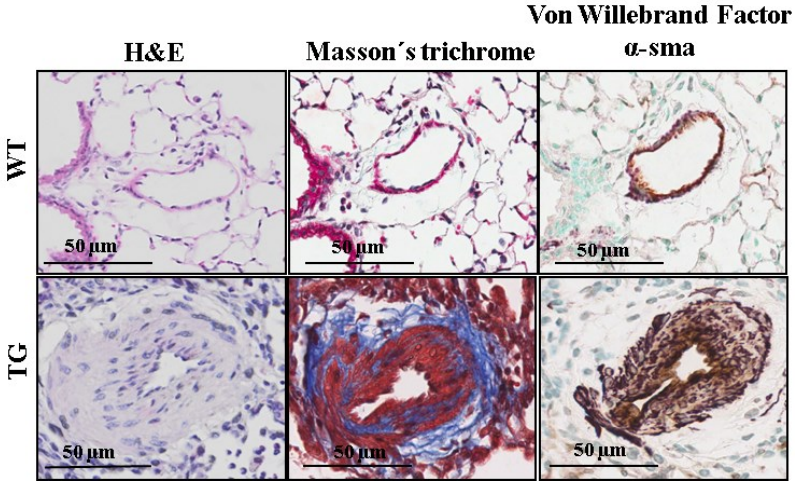

Figure 20: Fra-2 TG mice display perivascular collagen deposition. Serial slides from WT and fra-2 TG mice with H&E; Masson's tricrhome, and Von-Willebrand/α-sma double staining (n=4). Figure modified from (129).

We observed that collagen 1alpha1 (1α1) and 3alpha1 (3α1) were up-regulated at 16 weeks' time point but no change was observed on collagen 1alpha2 (1α2) (Figure 21).

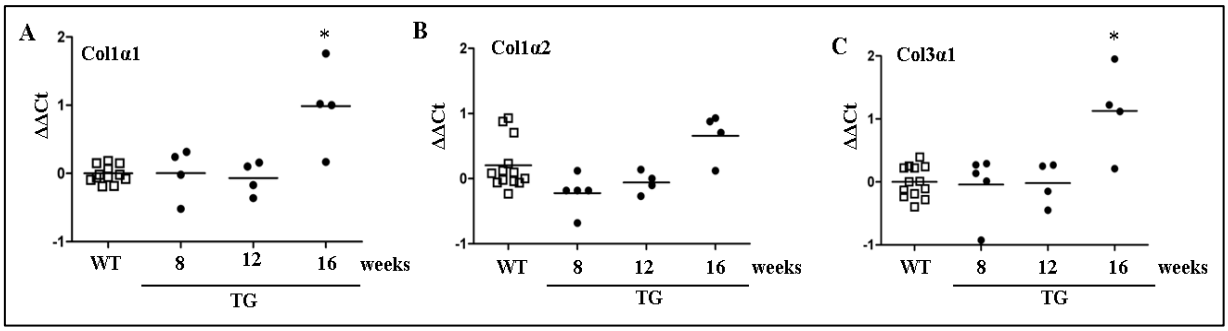

Figure 21: Collagens 1alpha1 and 3alpha1 are upregulated in fra-2 TG mice. Relative expression of A) collagen 1alpha1 (1α1); B) collagen 1alpha2 (1α2) and C) collagen 3alpha1 (3α1) assessed by real-time PCR in lung homogenate. (n=4 animals/group for fra-2 TG mice, n=13 pooled WT). Figure modified from (129).

MMPs are down-regulated in fra-2 TG mice

In addition, we observed decreased expression of collagen degrading enzyme such as MMP2 and MMP9 (Figure 22)

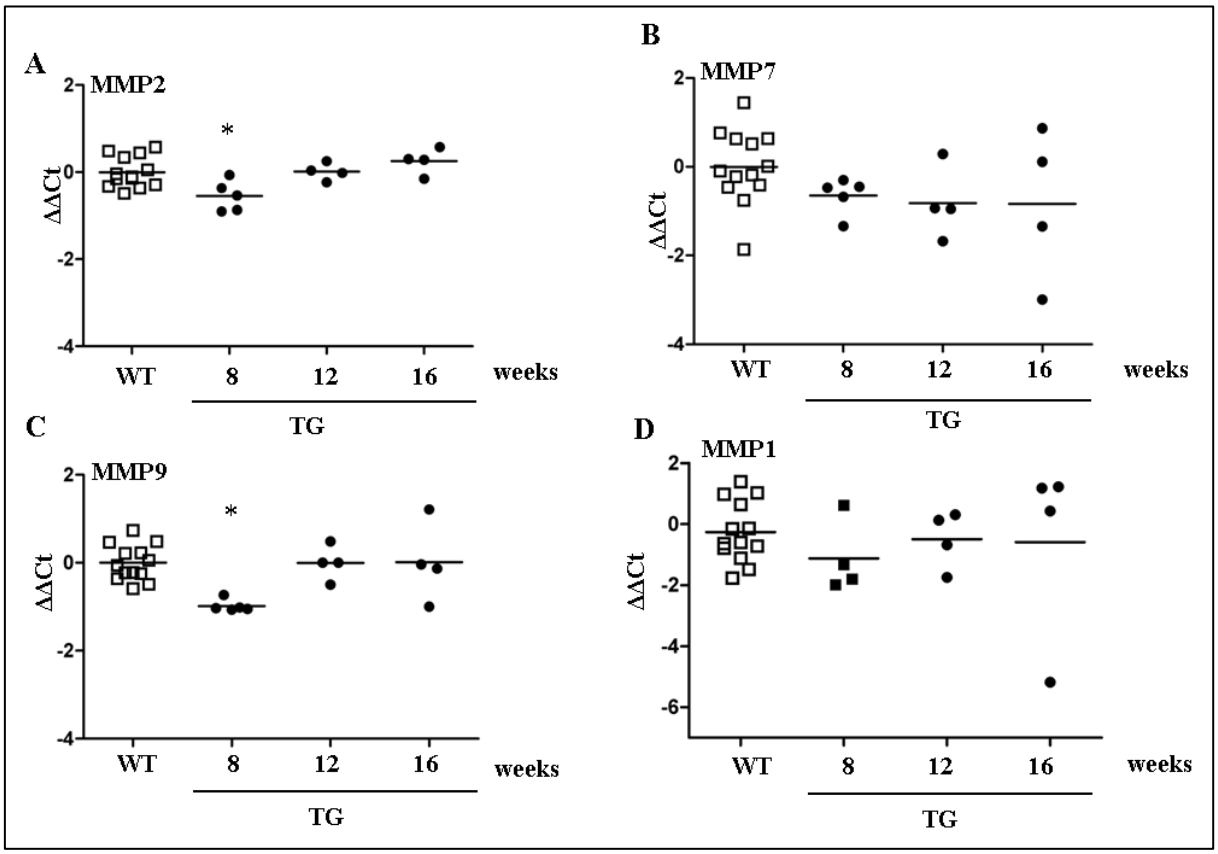

Figure 22: MMP2 and MMP7 are downregulated in fra-2 TG mice. Relative expression of A)MMP2; B) MMP7; C) MMP9 and D) MMP1 assessed by real-time PCR (n=4 animals /group for fra-2 TG mice, n=13 pooled WT). Figure modified from (129).

The increase in collagen expression and the concomitant decrease of MMP enzymes may represent the cause of the enhanced perivascular collagen deposition. To rule out the possibility that the change in expression level of collagen was due to the fibrotic phenotype of the mice, we performed fibrosis quantification and hydroxyproline assay on the lung. As depicted in figure 23 there was no change in fra-2 TG mice in comparison to WT mice regarding the hydroxiproline content (Figure 23A) and the amount of fibrosis (Figure 23B). This suggests that the fibrotic process at the analysed points was still not apparent and that the vessel thickening and the perivascular collagen deposition was before the onset of fibrosis.

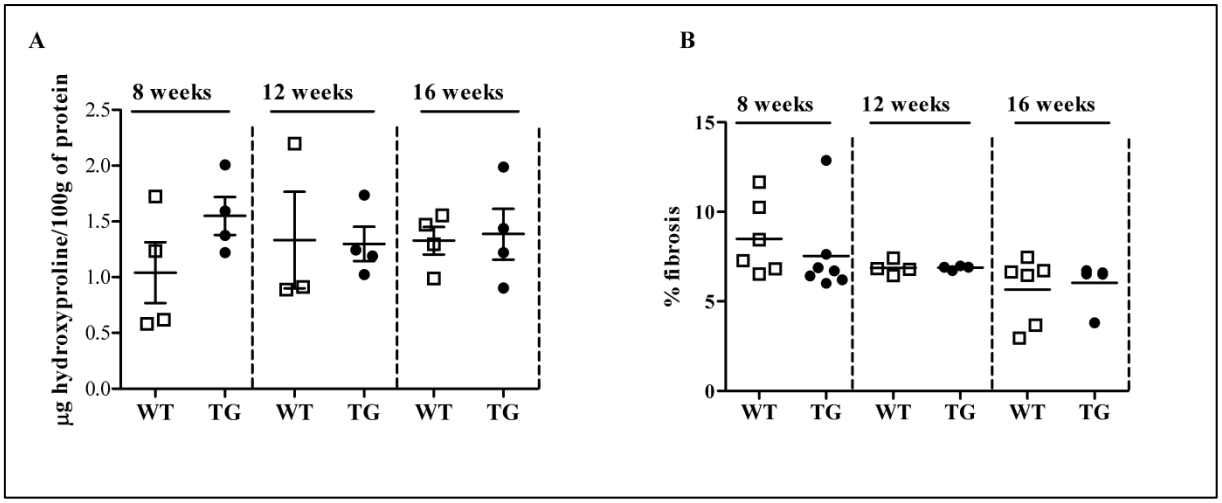

Figure 23: The lungs of fra-2 TG mice do not show any parenchymal fibrotic changes. Quantification in fra-2 TG and WT mice at 8, 12 and 16 weeks of A) hydroxyproline content (n= 3 or 4 animals/group); and of B) fibrosis as a percentage of the whole area (n=3-6 animals/group). Figure modified from (129).

4.2.5 Fra-2 signaling in human pulmonary artery smooth muscle cells, the role of PDGF-BB

As fra-2 was mainly expressed in the smooth muscle layer of pulmonary vessels in PAH patients (Figure 4), we aimed to identify which factors can regulate fra-2 in human pulmonary artery smooth muscle cells (hPASMC). Fra-2, as a transcription factor, can be directly activated by MAP kinases; therefore we tested factors known to activate MAPK pathways and which have relevance in PH. We tested PDGF-BB, ET-1 and TGF-β on

hPASMC, and the stimulation revealed that PDGF-BB was the only growth factor able to increase fra-2 expression level (Figure 24A, B, and C).

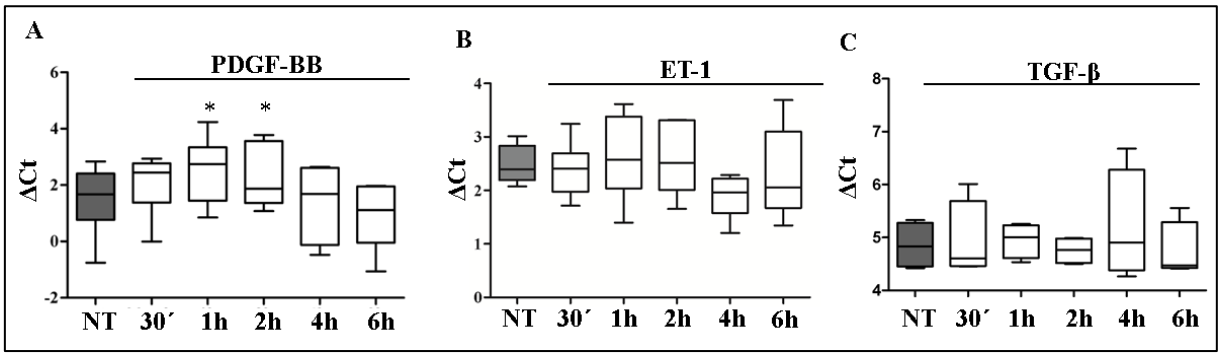

Figure 24: PDGF-BB increases expression of fra-2 in hPASMC. Relative expression of fra-2 upon stimulation with A) PDGF-BB (10ng/ml); B) ET-1 (100nM) and C) TGF-β1 (10ng/ml) by real-time PCR at the indicated time points (n=4-5 individual experiments). Figure modified from (129).

This result was further confirmed at the protein level (Figure 25A). As shown in figure 25A fra-2 protein level increased after 3hour stimulation with PDGF-BB. Molecular pathway analysis revealed that treatment of cells with JNK inhibitor (SP), blocked the PDGF-BB induced upregulation of fra-2 (Figure 25B), while no suppression resulted when cells were treated with ERK inhibitor (U) or PI3K/AKT inhibitor (W).

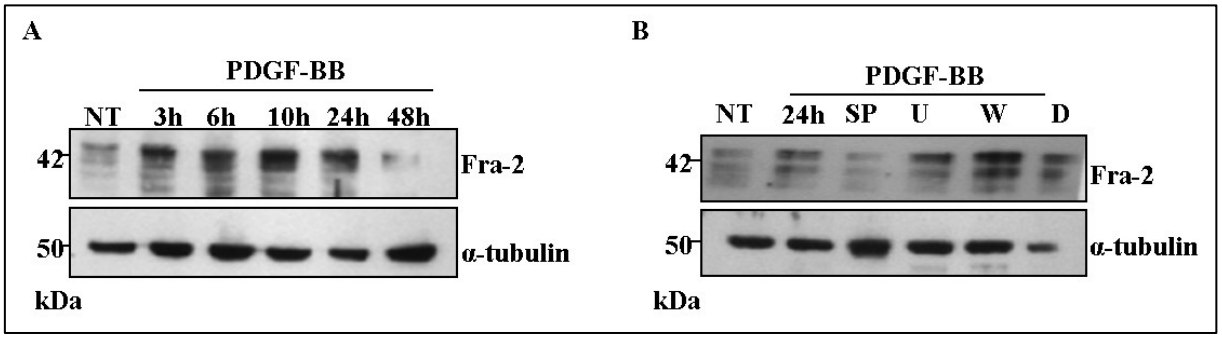

Figure 25: PDGF-BB increases protein level of fra-2 in a JNK dependant manner. A) Western blot showing the protein level of fra-2 in hPASMC upon treatment with PDGF-BB for the indicated time points, α-tubulin shows the loading control, (n=3 individual experiments); B) Western blot analysis of fra-2 expression induced by PDGF-BB upon inhibitors treatment. Cells were treated with JNK inhibitor ((S): SP600125); ERK1/2 inhibitor ((U): UO126), PI3K/AKT inhibitor ((W): Wortmannin,) vehicle (DMSO (D)) for 1 hour before treatment with PDGF-BB, α-tubulin display the loading control (n=3 individual experiments). Figure modified from (129).

Transcription factors are generally binding to target genes promoters, therefore they need to translocate into the nucleus (132). In the next step we checked whether PDGF-BB stimulation induced fra-2 nuclear translocation in hPASMC. As shown in figure 26, stimulation of hPASMC with PDGF-BB for 24 hours induced fra-2 nuclear localization.

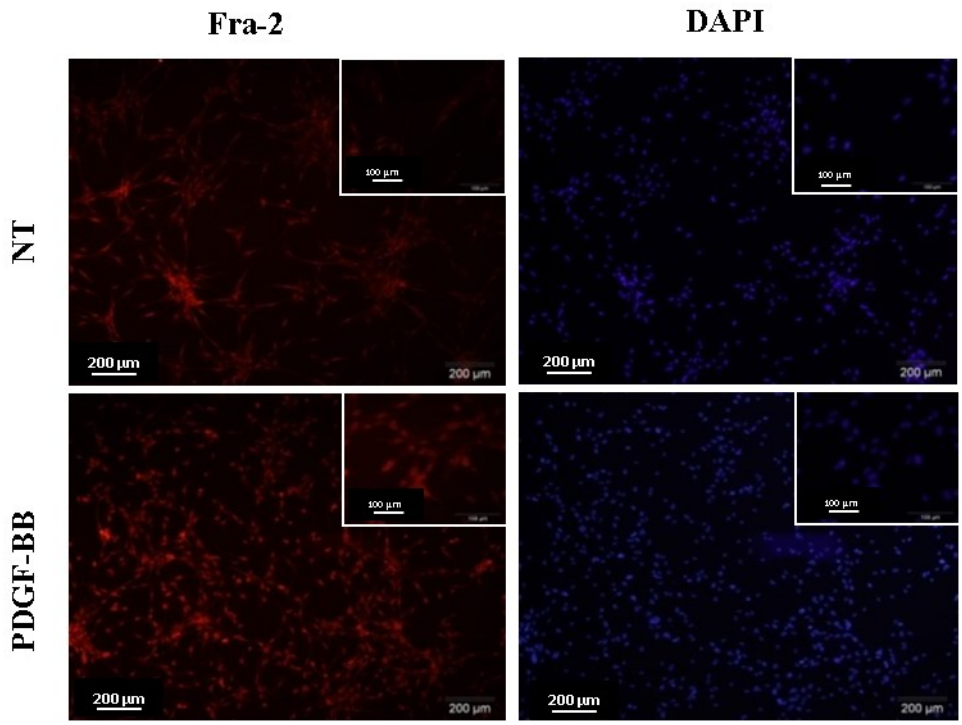

Figure 26: Fra-2 translocates into the nucleus upon PDGF-BB stimulation. Immunofluorescence staining showing fra-2 localization into the nucleus in PDGF-BB treated hPASMC. The picture with scale bar 200µm corresponds to 10X magnification, the inset to 40X magnification (n=3). Figure modified from (129).

PDGF-BB is known to be a mitogenic factor for hPASMC in pulmonary hypertension (54) and fra-2, as a transcription factor, could induce target genes involved in proliferation. Therefore, we aimed to assess the role of fra-2 in PDGF-BB induced proliferation. Fra-2 does not have a transactivation domain, which implies that it cannot activate transcription by itself but it needs to form a dimer with another member of AP-1 family. Accordingly we did not observe any change in proliferation when only fra-2 was silenced (Figure 27). Silencing efficiency for fra-2 is shown in figure 28.

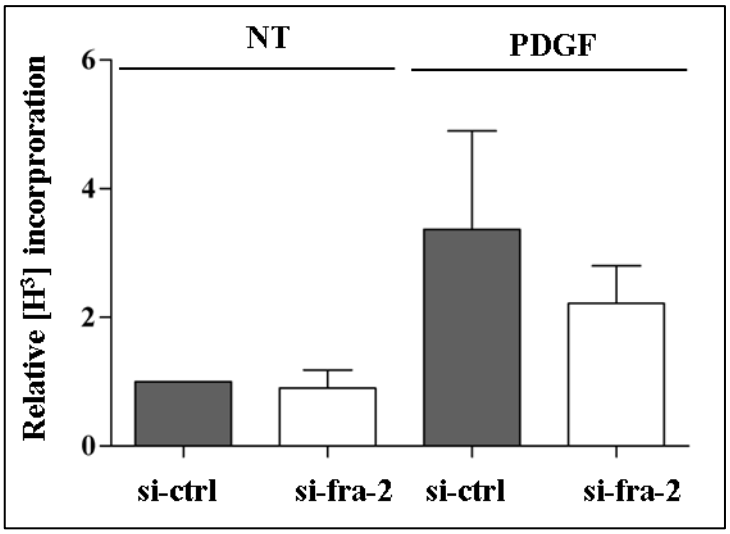

Figure 27: Proliferation of hPASMC is not affected by silencing of fra-2. Proliferation was assessed by thymidine incorporation in PDGF-BB treated and untreated hPASMC which were silenced with fra-2 or ctrl siRNA (n= 4 individual experiments). Figure modified from (129).

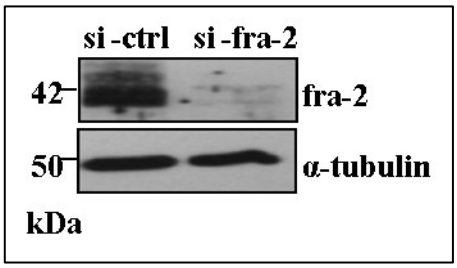

Figure 28: Silencing efficiency of the fra-2. Western blot showing the silencing efficiency of fra-2 after 48 hours silencing, α-tubulin shows the loading control (n=3 individual experiments). Figure modified from (129).

As fra-2 needs an interaction with a second AP-1 member to activate transcription processes, we next investigated which of the jun components could be regulated by PDGF-BB and therefore be interacting with fra-2. As shown in figure 29, c-jun and jun-B were regulated by PDGF-BB already after 30 minutes stimulation (Figure 29A and C). Jun-D level was not regulated by PDGF-BB (Figure 29B).

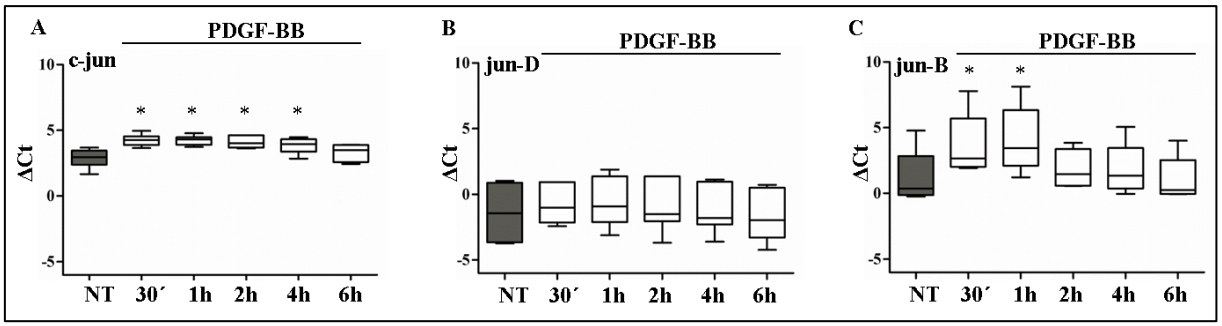

Figure 29: PDGF-BB increases expression of c-jun and jun-B in hPASMC. Relative expression assessed by real-time PCR of A) c-jun, B) jun-D and C) jun-B upon stimulation with PDGF-BB (n=4 individual experiments). Figure modified from (129).

Similarly, c-jun and jun-B protein levels were increased upon PDGF-BB stimulation, while no change in jun-D level was observed (Figure 30A). Interestingly, our inhibitor studies revealed that PDGF-BB induced c-jun protein was mediated by JNK pathway (Figure 30B) while jun-B protein was mediated via JNK and ERK pathway (Figure 21B).

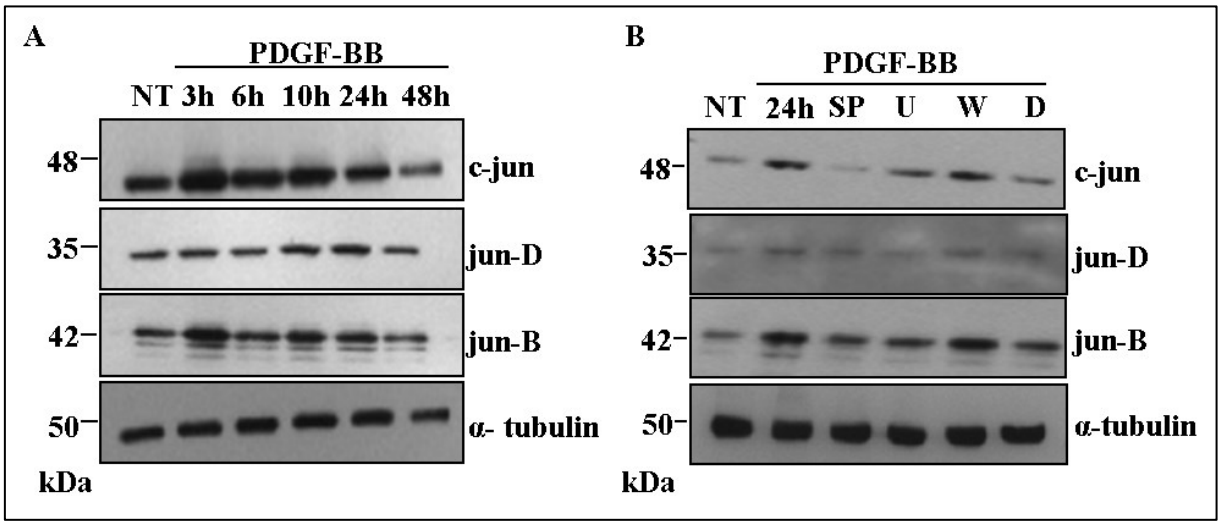

Figure 30: PDGF-BB increases protein level of c-jun and jun-B via JNK and ERK. A) Western blot showing the protein level of c-jun, jun-D and jun-B in hPASMC upon treatment with PDGF-BB for the indicated time points, α-tubulin shows the loading control, (n=3 individual experiments); B) Western blot analysis of c-jun, jun-D and jun-B expression induced by PDGF-BB. Cells were treated with JNK inhibitor ((S): SP600125); ERK1/2 inhibitor ((U): UO126), PI3K/AKT inhibitor ((W): Wortmannin,) or vehicle (DMSO (D)) for 1 hour before treatment, α-tubulin shows the loading control (n=3 individual experiments). Figure modified from (129).

The next step was to assess whether double silencing of fra-2 with each of the jun components would affect hPASMC proliferation induced by PDGF-BB. We observed that

silencing of each of the dimer (fra-2-c-jun, fra-2-jun-D and fra-2/jun-B) reduced significantly the PDGF-BB induced proliferation of hPASMC (Figure 31). To note, no significant difference was noticed on proliferation if cells were silenced but not subjected to PDGF-BB, implying a specific effect of PDGF-BB on these AP-1 components.

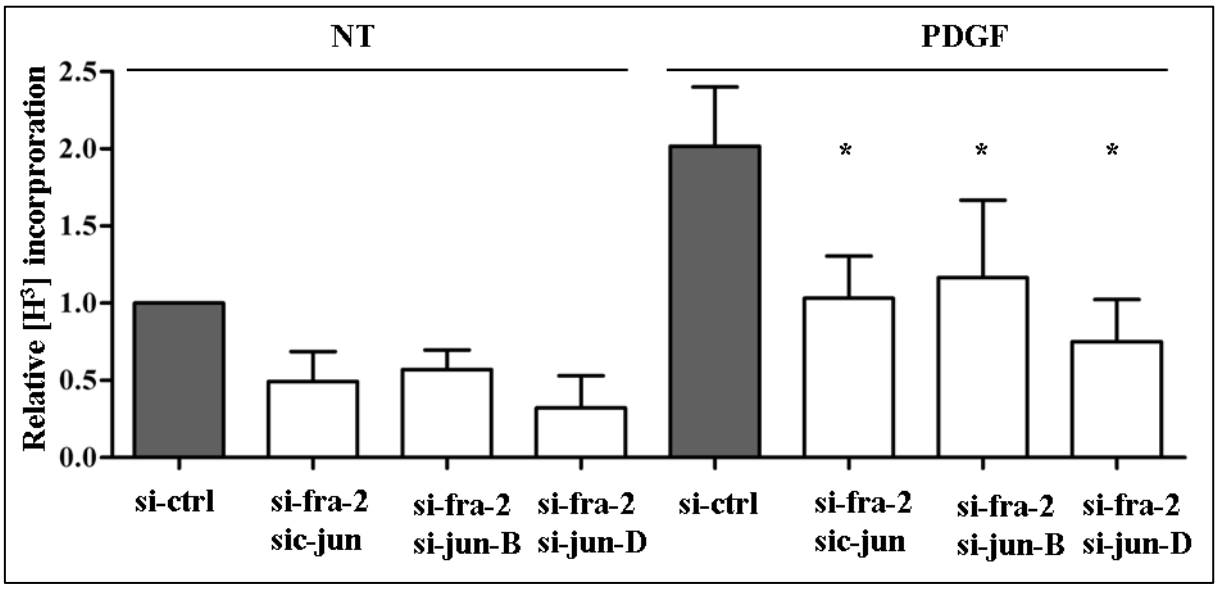

Figure 31: Proliferation of hPASMC is affected by double silencing of fra-2 with any of the jun components. Proliferation was assessed by thymidine incorporation in PDGF-BB treated and untreated hPASMC which were silenced with the following combination of siRNA: si-fra-2/si-c-jun; si-fra-2/si-junB, si-fra-2/si-JunD or si-ctrl (n=4 individual experiments). Figure modified from (129).

Silencing efficiency of the different AP-1 components is represented in figure 32.

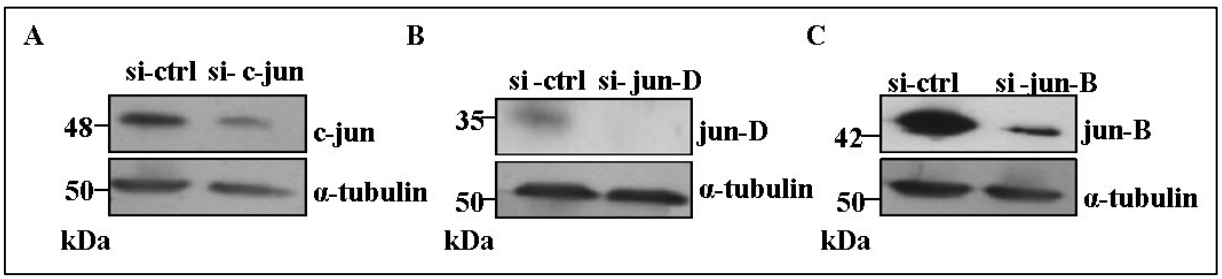

Figure 32: Silencing efficiency of the different AP-1 components. Western blot representation of silencing efficiency of A) c-jun, B) jun-D and C) jun-B after 48 hours silencing. α-tubulin shows the loading control (n=3 individual experiments). Figure modified from (129).

4.3 Fra-2/Ap-1 target gene: Meprin β

In order to identify which genes fra-2 and jun components could regulate in fra-2 TG mice which also might be involved in the remodeling process, we performed a microarray from the lung homogenate of fra-2 TG and WT.

4.3.1 Meprin β is the most up-regulated gene in fra-2 TG mice lung

In collaboration with Dr.Jochen Willhelm form Giessen University, Germany, we performed a microarray analysis in fra-2 TG mice and WT, which revealed that the most up-regulated gene in the lungs of fra-2 TG mice was meprin β (Figure 33A). The microarray analysis was performed on 8 weeks old mice. The real time PCR data showed the upregulation also at 12 and 16 weeks (Figure 33B).

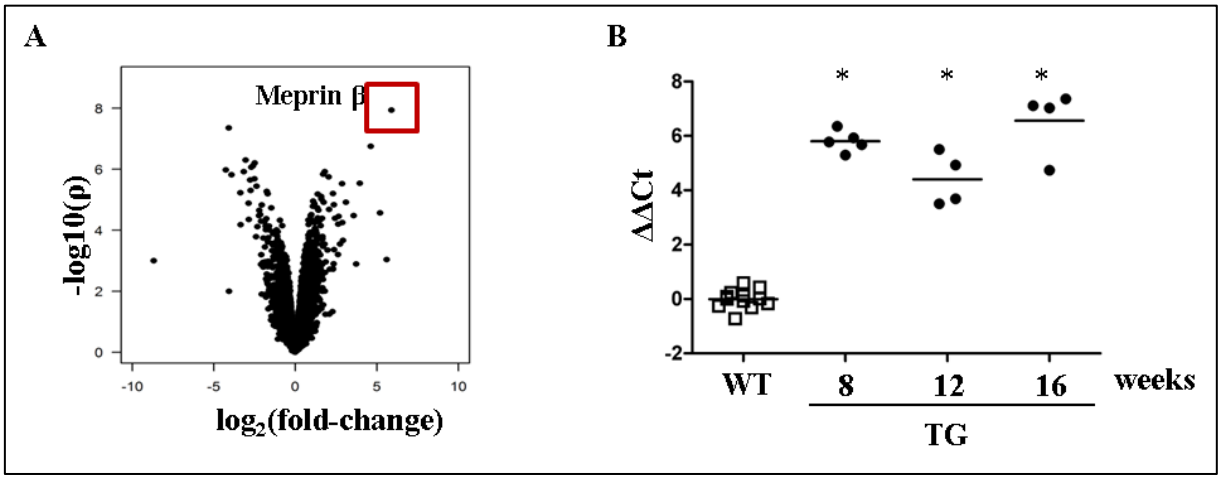

Figure 33: Meprin β is the most upregulated gene in fra-2 TG mice. A) Volcano plot representing the regulation of all the genes plotted as significance of regulation versus log2-fold regulation. B) Relative expression assessed by real-time PCR of meprin β in WT and 8,12,and 16 weeks old fra-2 TG mice (n=4 animals /group for fra-2 TG mice, n=13 pooled WT). Figure modified from (129).

4.3.2 Meprin β is expressed in the endothelial, smooth muscle and inflammatory cells in fra-2 TG mice lung

Meprin β is a protease which can process a plethora of different substrate, such as pro-collagen (133). To assess the localization of meprin β in fra-2 TG mice we performed immunohistochemical staining on fra-2 TG mice lung at different time points (8, 12 and 16 weeks). The staining revealed that meprin β is highly expressed in the vessel wall, and

specifically in the smooth muscle, endothelial cells but also in the epithelium and inflammatory cells (Figure 34).

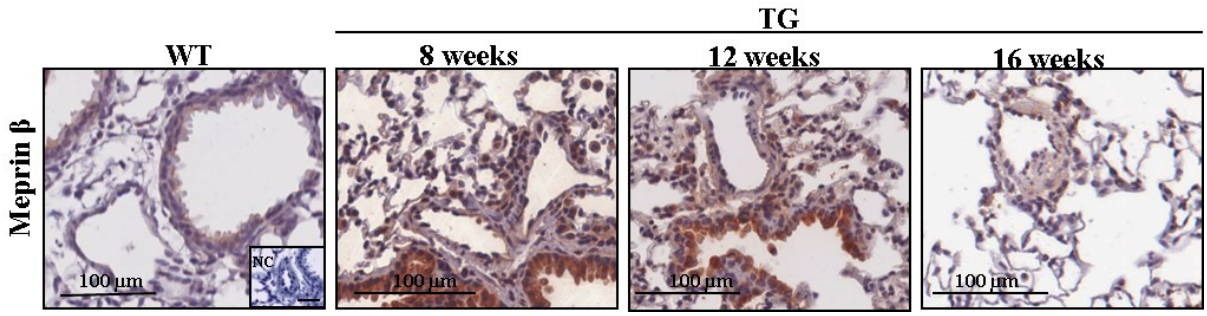

Figure 34: Meprin β is expressed in smooth muscle, endothelial cells, ephitelium and inflammatory cells. Representative pictures of the immunohistochemical staining on WT and fra-2 TG (8, 12 and 16 weeks) mice lung with meprin β (n=4). Figure modified from (129).

To confirm localization of meprin β in the vasculature wall, next we performed real-time PCR in pulmonary arteries isolated from WT and fra-2 TG mice. Our results showed that the expression level of meprin β was strongly increased in the pulmonary arteries of fra-2 TG mice in comparison to WT mice (Figure 35)

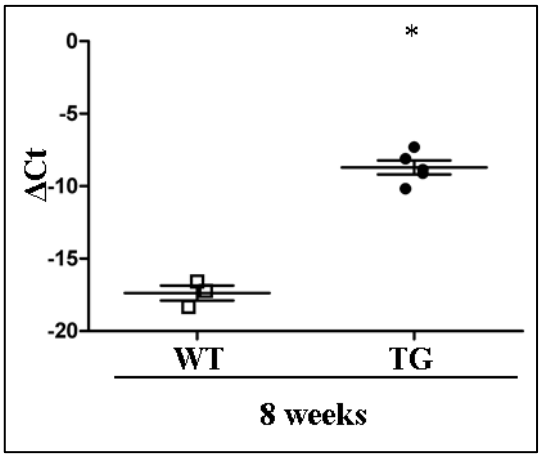

Figure 35: Meprin β is up-regulated in the isolated pulmonary arteries of fra-2 TG mice. Relative expression assessed by real-time PCR of meprin β in pulmonary arteries isolated from WT and fra-2 TG mice (8 weeks) (n=4 animals/group for fra-2 TG mice, n=13 pooled WT). Figure modified from (129).

4.3.3 Regulation of meprin β by TGF-β in human pulmonary artery smooth muscle cells

To investigate which factors can regulate meprin β, we stimulated hPASMC with PDGF-BB and TGF-β. We found that meprin β was not regulated by PDGF-BB (Figure 36A) but by TGF-β (Figure 36B), another important growth factor in pulmonary hypertension. TGF-β increased meprin β expression in a time dependent manner, as shown in figure 36B.

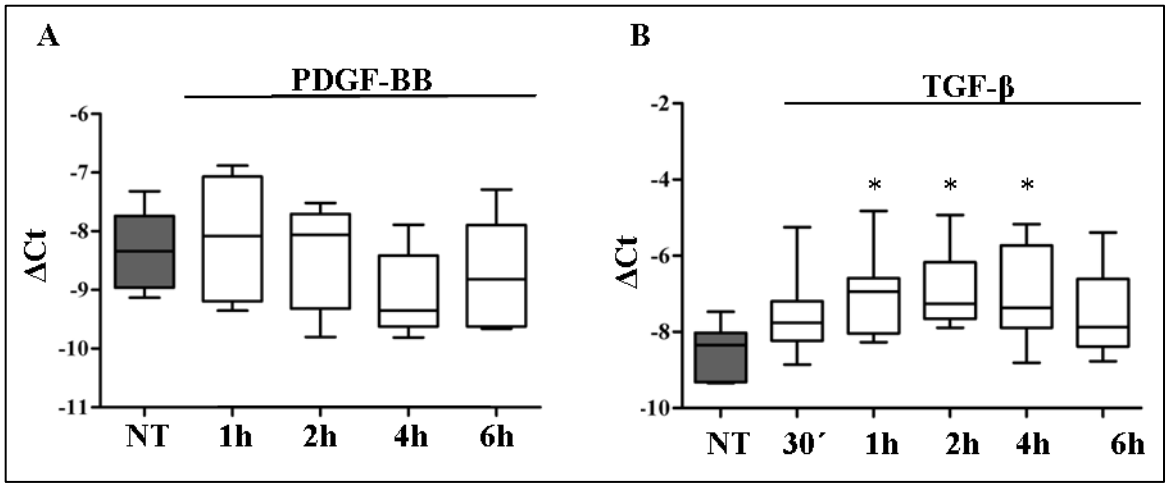

Figure 36: Meprin β is regulated by TGFβ. Relative expression of meprin β assessed by real-time PCR in hPASMC stimulated with A) PDGF-BB and B) TGF-β for the indicated time points (n=4-6 individual experiments). Figure modified from (129).

In silico analysis of the meprin β promoter revealed that it contains two predicted AP-1 binding sites at the position -451 and -81 (Figure 37).

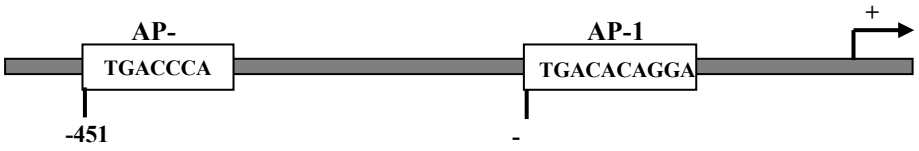

Figure 37: Meprin β promoter contains two AP-1 binding sites. Representation of the meprin β promoter. AP-1 binding sites are present at position -451 and -81; the sequence is reported in the box. +1 indicates the starting codon for the transcription of the gene. Figure modified from (129).

As AP-1 binding sites are present in the meprin-β promoter and meprin β was regulated by TGF-β at the mRNA level, in the next series of experiments we investigated whether TGFβ treatment increased meprin β expression by an enhanced binding of AP-1 to its promoter. First, we performed electromobility shift assay, which revealed that upon 1 and 2 hours

TGFβ treatment AP-1 binding to -451 was enhanced in comparison to untreated cells (Figure 38). The binding site -81 showed enhanced binding as well, even though to a lesser extent.

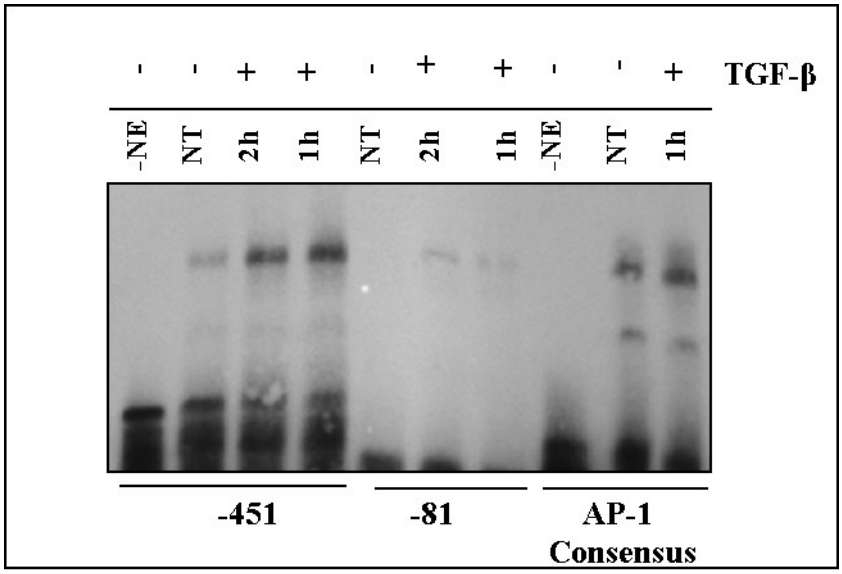

Figure 38: Ap-1 complex binds to meprin β promoter upon TGF-β stimulation. Electromobility shift assay (EMSA) showing the binding of AP-1 to the meprin β promoter sequences at the sites -451 and -81. AP-1 consensus is used a positive control. –NE, without nuclear extract, NT, untreated hPASMC, 2h and 1h, 2 hours and 1 hour treatment of hPASMC with TGF-β (n=3 individual experiments). Figure modified from (129).

As meprin β was regulated in vitro by TGF-β, next we wanted to investigate the level of TGF-β in fra-2 TG mice. Our expression analysis show, that TGF-β was upregulated in 12 and 16 weeks old fra-2 TG mice lung homogenate (Figure 39), confirming the *in vivo* relevance of this factor.

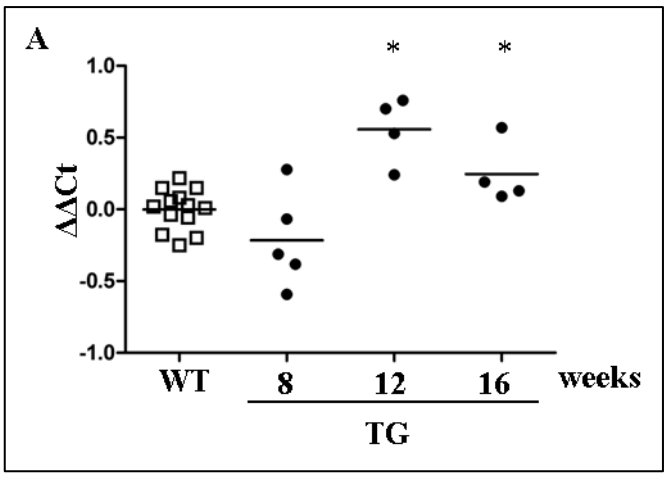

Figure 39: TGF-β is up-regulated in fra-2 TG mice. Relative expression assessed by real-time PCR of TGF-β assessed in WT and 8,12,and 16 weeks old fra-2 TG mice (n=4 animals/group for fra-2 TG mice, n=13 pooled WT). Figure modified from (129).

Immunohistochemical staining of TGF-β in fra-2 TG mice confirmed the real time PCR result, with increased expression of TGF-β in 12 and 16 weeks old mice. Moreover, TGF-β was mainly expressed in the remodelled vessels and in the inflammatory cells (Figure 40).

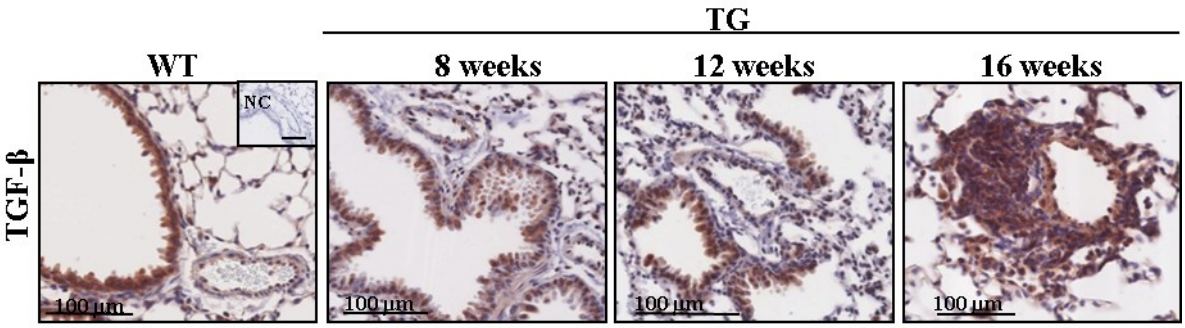

Figure 40: TGF-β is expressed in lung vessel wall and in inflammatory cells. Representative pictures of the immunohistochemical staining on WT and fra-2 TG (8, 12 and 16 weeks) mice lung with meprin β (n=3). Figure modified from (129).

TGF-β was previously shown to regulate AP-1 components, in particular the jun family (134). We then investigated the effect of TGF-β on jun components in hPASMC. As shown in figure 41A, TGF-β increased the mRNA level of jun-B in a time dependent manner. The same result was confirmed in western blot analysis, where jun-B protein level was increased already after 2 hours TGF-β stimulation (Figure 41B).

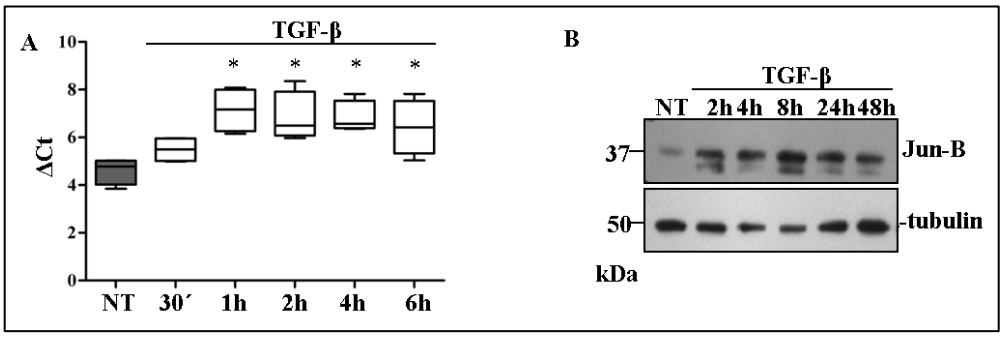

Figure 41: TGF-β increases expression of jun-B in hPASMC. A) Relative expression of jun-B upon stimulation with TGF-β assessed by real time PCR (n=4 individual experiments); B) Western blot showing the protein level of jun-B in hPASMC upon treatment with TGF-β for the indicated time points, α-tubulin shows the loading control (n=3 individual experiments). Figure modified from (129).

Importantly, TGF-β stimulation on hPASMC induced jun-B nuclear localization as shown in figure 42.

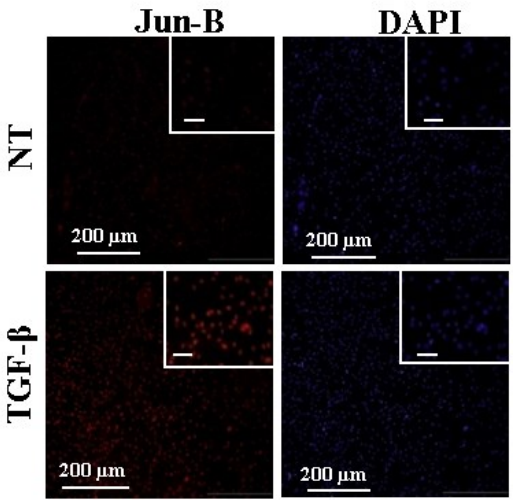

Figure 42: TGF-β induces nuclear localization of jun-B in hPASMC. Immunofluorescence staining showing jun-B localization into the nucleus in TGF-β treated hPASMC. Cells were stimulated for 3 hours. The picture with scale bar 200µm corresponds to 10X magnification, the inset to 40X magnification (n=3 individual experiments). Figure modified from (129).

Finally, staining of jun-B on human lungs revealed that jun-B localized predominantly in smooth muscle actin positive cells, as shown by staining of serial slides with jun-B and α-sma (Figure 43). These results altogether suggest a possible role of jun-B and fra-2 in mediating meprin β expression upon TGF-β.

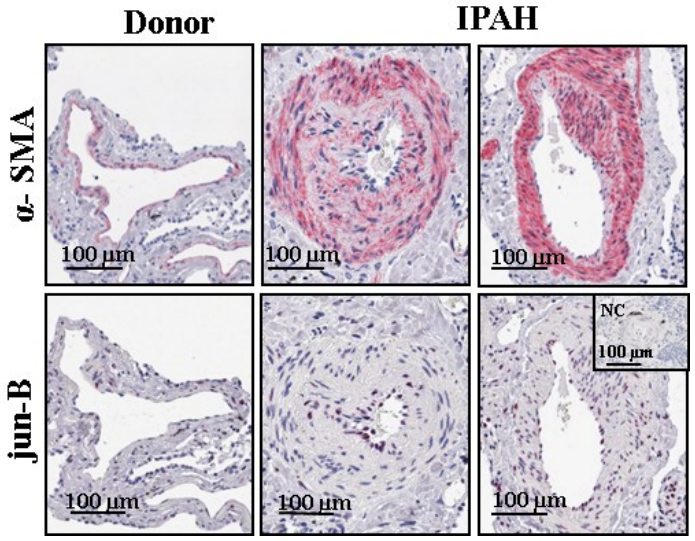

Figure 43: Jun-B is expressed in smooth muscle cells. Representative vessel from donor and PAH patients lungs stained with α-sma and jun-B. Serial slides were stained to be able to define

localization of jun-B. NC represents the negative control. PAH, pulmonary arterial hypertension. (n=3). Figure modified from (129).

4.3.4 The role of meprin β for the human disease

In order to verify the clinical importance of meprin β, we used human lung samples to assess the expression level in donor versus PAH patients. Our results showed that meprin β levels were significantly higher in the PAH patients in comparison to donor (figure 44).

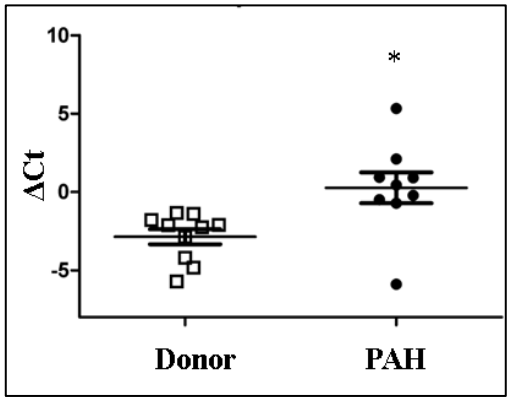

Figure 44: Meprin β is up-regulated in PAH patients in comparison to donors. Relative expression assessed by real-time PCR of meprin β in donor lung (n=10) and PAH patients (n=9) homogenates. Figure modified from (129).

Staining of meprin β in human lungs showed that meprin β was very low expressed in normal condition (donors) but strongly expressed in the vasculature of PAH lungs (Figure 45).

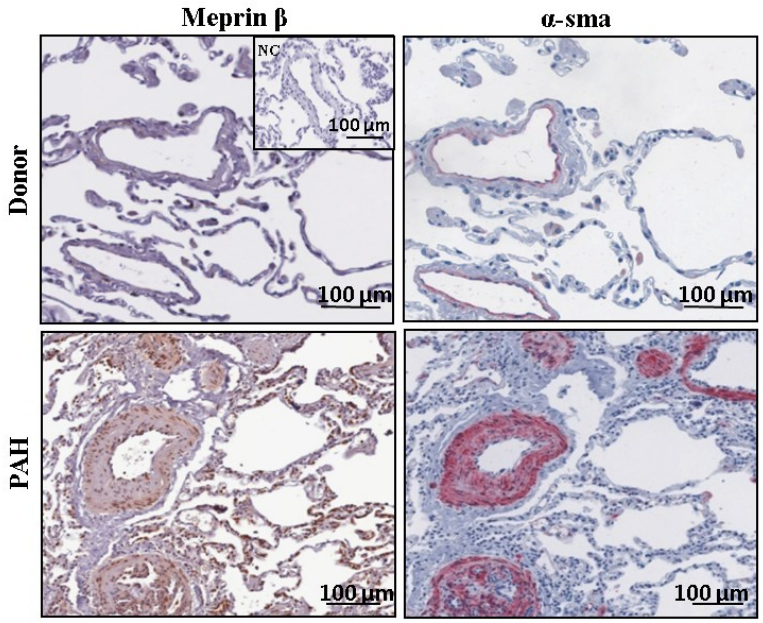

Figure 45: Meprin β is expressed predominantly in the vasculature of PAH patient lungs. Representative vessel from donor and PAH patients lungs stained with α-sma and meprin β. Serial slides were stained to be able to compare localization of meprin β. NC represents the negative control. PAH, pulmonary arterial hypertension (n=3). Figure modified from (129).

As meprin β was predominantly expressed in hPASMC and hPAEC in human lungs, we aimed to investigate meprin β inhibition effect on proliferation and apoptosis of these two cells types using pharmacological tools. Actinonin, the inhibitor of meprin β, reduced PDGF-B-induced proliferation of hPASMC in a dose dependent manner (Figure 46A). Similarly, hPAEC proliferation was also inhibited by actinonin (Figure 46B).

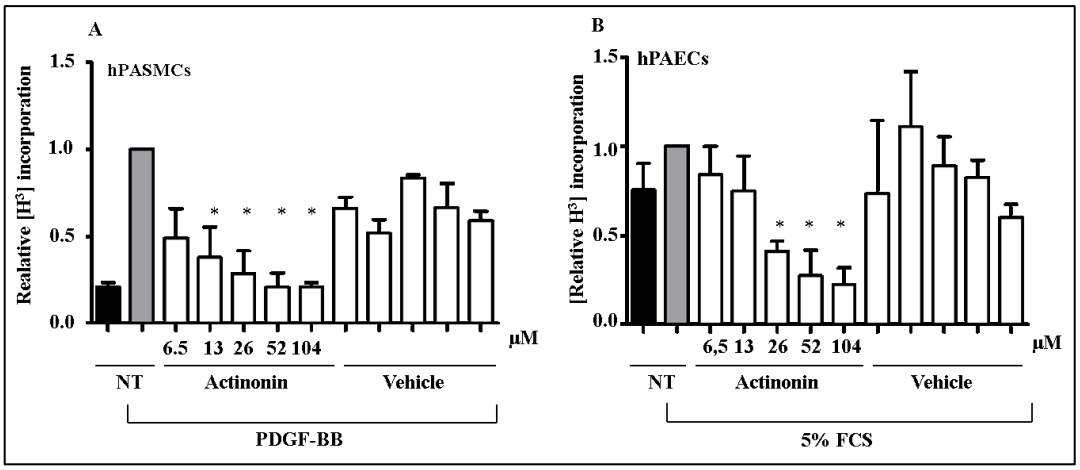

Figure 46: Inhibition of meprin β reduces hPASMC and hPAEC proliferation. Proliferation was assessed by thymidine incorporation in PDGF-BB or 5% FCS for hPASMC and hPAEC respectively. Cells were treated with actinonin and the corresponding vehicle at the indicated concentration. Black column: untreated cells without PDGF-BB, grey column: untreated cells with PDGF-BB (n= 3 individual experiments). Figure modified from (129).

Actinonin was already reported to induce apoptosis in tumor cells (123), therefore in order to investigate whether the decreased proliferation was caused by an increase apoptosis, we performed apoptosis assay. No change in the apoptosis rate was observed in both cell types analysed (Figure 47A and B). These results suggest a role of meprin β in proliferation of hPAEC and hPASMC.

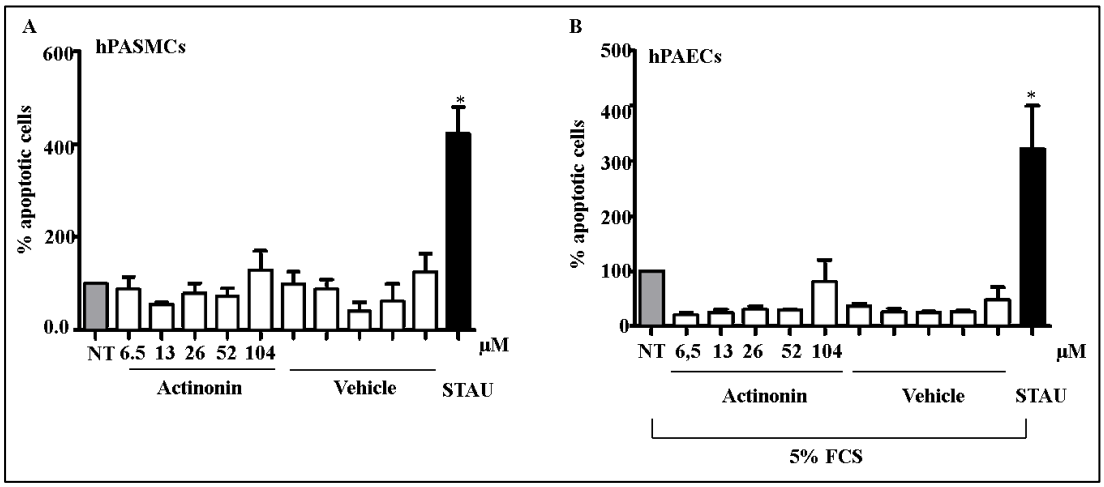

Figure 47: Inhibition of meprin β does not induce apoptosis of hPASMC and hPAEC. Percentage of A) hPASMC and B) hPAEC apoptotic cells, determined upon treatment with actinonin or vehicle for the indicated concentrations. Staurosporin (black column) (STAU, 0. 5 mg/ml) has been used as a positive control for the assay, grey column untreated cells (NT) (n= 3 individual experiments). Figure modified from (129).

4.4 The role of the AP-1 members c-fos/c-jun in hypoxia induced vascular remodeling

Our previous results show an upregulation of c-fos and c-jun upon 3h hypoxia in the microarray analysis (Table 6) and the regulation of c-fos and c-jun in hypoxia was also described earlier (94). We aimed to decipher the role of these two transcription factors in hypoxia induced vascular remodeling.

4.4.1 Hypoxia regulates factors responsible for the development of PAH

The microarray analysis performed in lung homogenate from mice exposed 3 hours to hypoxia, revealed not only that c-jun and c-fos were up-regulated but that endothelin-1 (ET-1) was the strongest up-regulated gene (Figure 48). ET-1 is an important vasoconstrictor which inhibition is currently used as a therapy for PH (135).

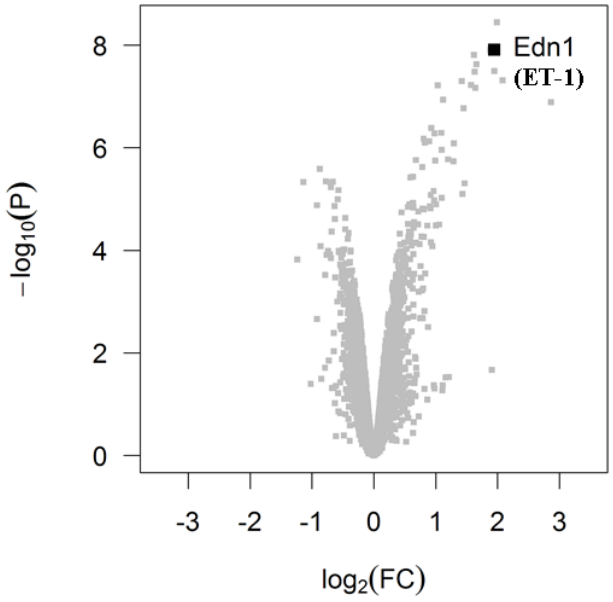

Figure 48: ET-1 is the most up-regulated gene upon 3 hours hypoxia exposure. Volcano plot representing the regulation of all the genes plotted as significance of regulation versus log2-fold regulation. Figure from (136).

In addition, molecular pathway analysis showed that upon 3 hours hypoxia exposure in mice the mitogen activated protein kinase (MAPK) pathway was the most differentially regulated (Table 7).

Pathway name	Impact factor	#Genes in Pathway	#Input Genes in Pathway	#Pathway Genes on chip	%Input Genes in Pathway	%Pathway Genes in Pathway	p-value	corrected p-value
MAPK signaling pathway	23.656	258	13	258	9.155	5.039	4.04E-10	4.04E-10
p53 signaling pathway	22.045	65	8	65	5.634	12.308	9.32E-10	9.32E-10
Cytokine-cytokine receptor interaction	14.153	242	9	242	6.338	3.719	2.77E-06	2.77E-06
TGF-beta signaling pathway	10.875	89	3	89	2.113	3.371	9.13E-03	9.13E-03
Melanogenesis	10.116	98	3	98	2.113	3.061	1.18E-02	1.18E-02

Table 7: MAPK is the most differentially regulated pathway in 3 hour hypoxia microarray. Table represents the most differentially regulated signaling pathway analysis in hypoxic mice versus normoxic mice lungs. Figure modified from (136).

MAPK pathway is known to be activated by mitogen factors and to affect transcription factors, such as AP-1(128). Therefore, we aimed to delineate whether the intracellular molecular pathway activated by ET-1 affected c-fos and c-jun transcription factors and how it influences hPASMC behaviour.

Et-1 is secreted by endothelial cells and it mainly acts on smooth muscle cells, where its receptors are mostly expressed (137). We first examined the effect of ET-1 on proliferation of hPAMSC. As shown in figure 49, ET-1 increased mRNA level of proliferation markers such as KI67 and cyclind D1, in a time dependent manner.

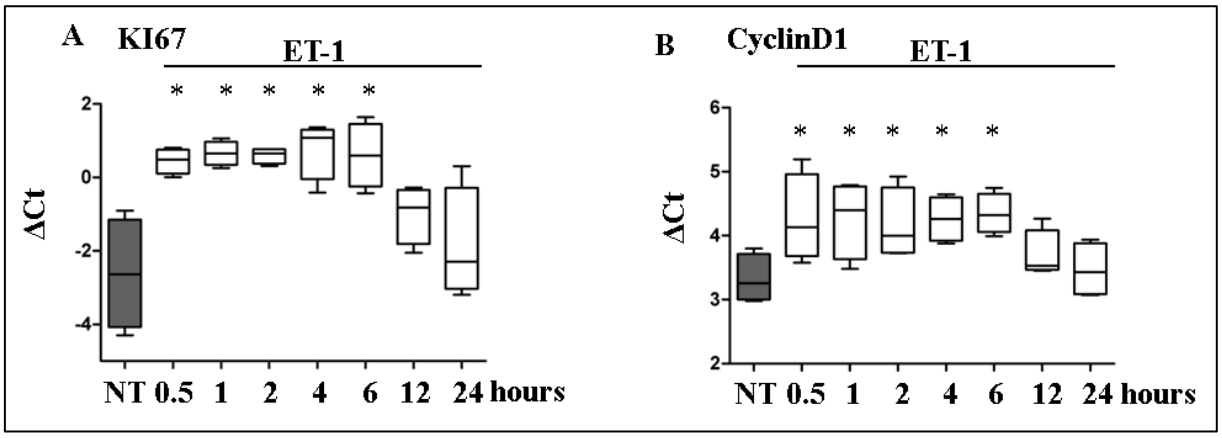

Figure 49: KI67 and CyclinD1 expression is increased by ET-1 in hPASMC. Relative expression of A) KI67 and B) CyclinD1 upon stimulation with ET-1 assessed by real time PCR (n=4 individual experiments). Figure modified from (136).

Accordingly, dose dependent stimulation showed that at the concentration of 500nM, ET-1 increased hPASMC proliferation rate (Figure 50). The proliferative effect was not pronounced however significant.

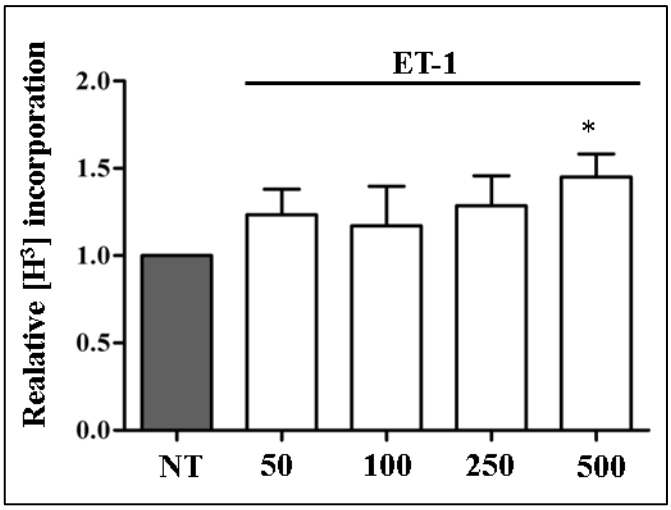

Figure 50: ET-1 induces proliferation of hPASMC. Proliferation was assessed by thymidine incorporation upon dose dependent ET-1 stimulation on hPASMC (n= 5 individual experiments). Figure modified from (136).

4.4.2 The regulation of c-jun/c-fos by ET-1

As c-fos/c-jun resulted to be up-regulated in the lung homogenate of mice exposed to 3 hours hypoxia, and ET-1 induced proliferation on hPASMC, next we aimed to delineate whether ET-1 has an influence on c-fos and c-jun. Stimulation of hPASMC with ET-1 increased the mRNA expression level of c-fos (Figure 51A) but not of c-jun (Figure 51B) .

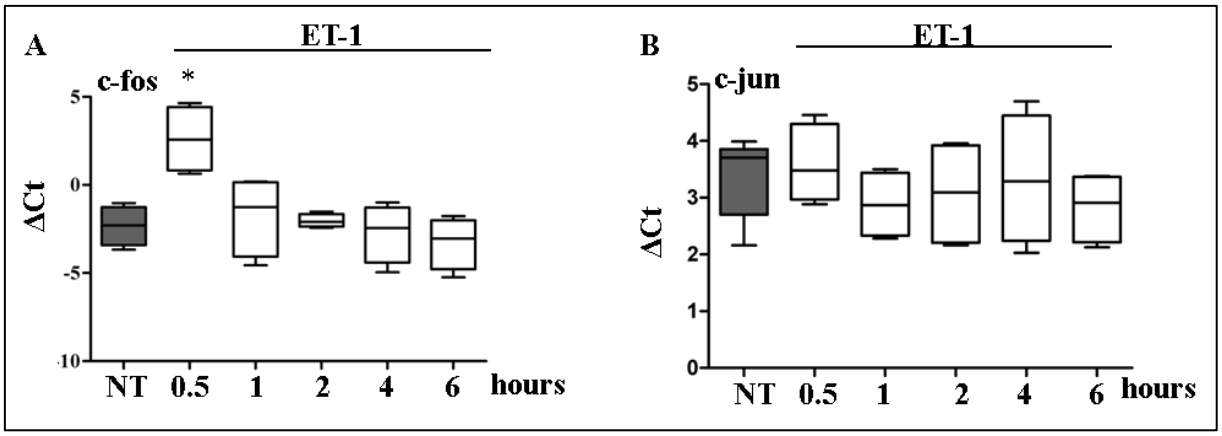

Figure 51: c-fos but not c-jun expression is increased by ET-1. Relative expression of A) c-fos and B) c-jun upon stimulation with ET-1 assessed by real time PCR (n=4 individual experiments). Figure modified from (136).

Similarly, the protein level of c-fos was significantly increased upon 24 hours ET-1 treatment (Figure 52A), however no change was observed on c-jun levels at all investigated time points (Figure 52B).

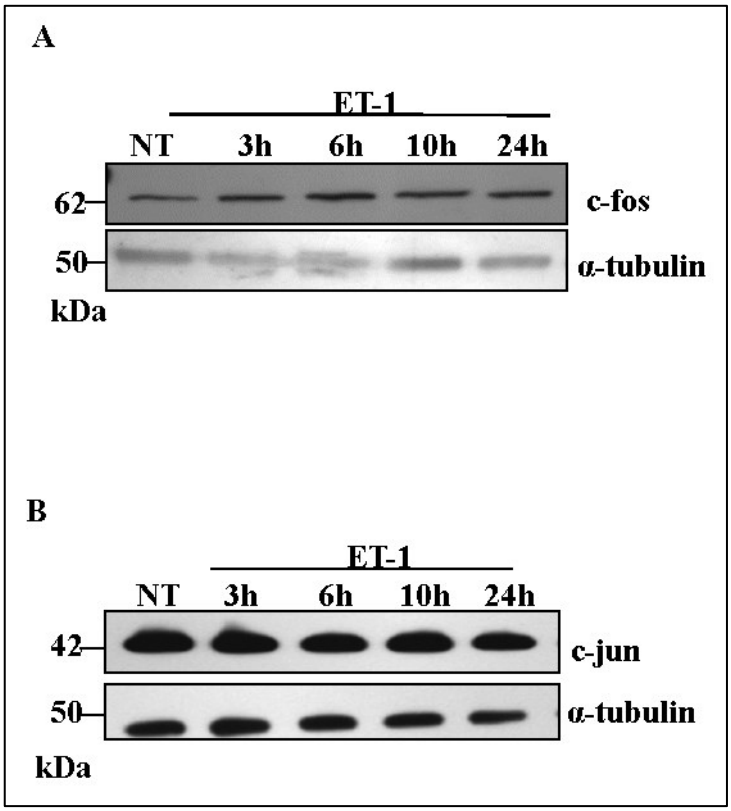

Figure 52: ET-1 increases protein level of c-fos. A) Western blot showing the protein level of A) c-fos and B) c-jun on hPASMC upon treatment with ET-1 for the indicated time points; α-tubulin shows the loading control (n=4 individual experiments). Figure modified from (136).

In order to determine which pathway is involved in the regulation of c-fos via ET-1 we performed several pharmacological studies. Different inhibitors, acting on different pathways, were applied and expression of c-fos was analysed upon ET-1 treatment. According to our results, c-fos induction is mediated via endothelin receptor A (inhibitor BQ123) rather than B (inhibitor BQ788) (Figure 53). Moreover, we also observed that when ERK1/2 a MAPK, was inhibited (U0126), c-fos induction was abolished (Figure 53). These results indicate that the increased expression of c-fos is mediated via the endothelin receptor A and ERK 1/2 pathway.

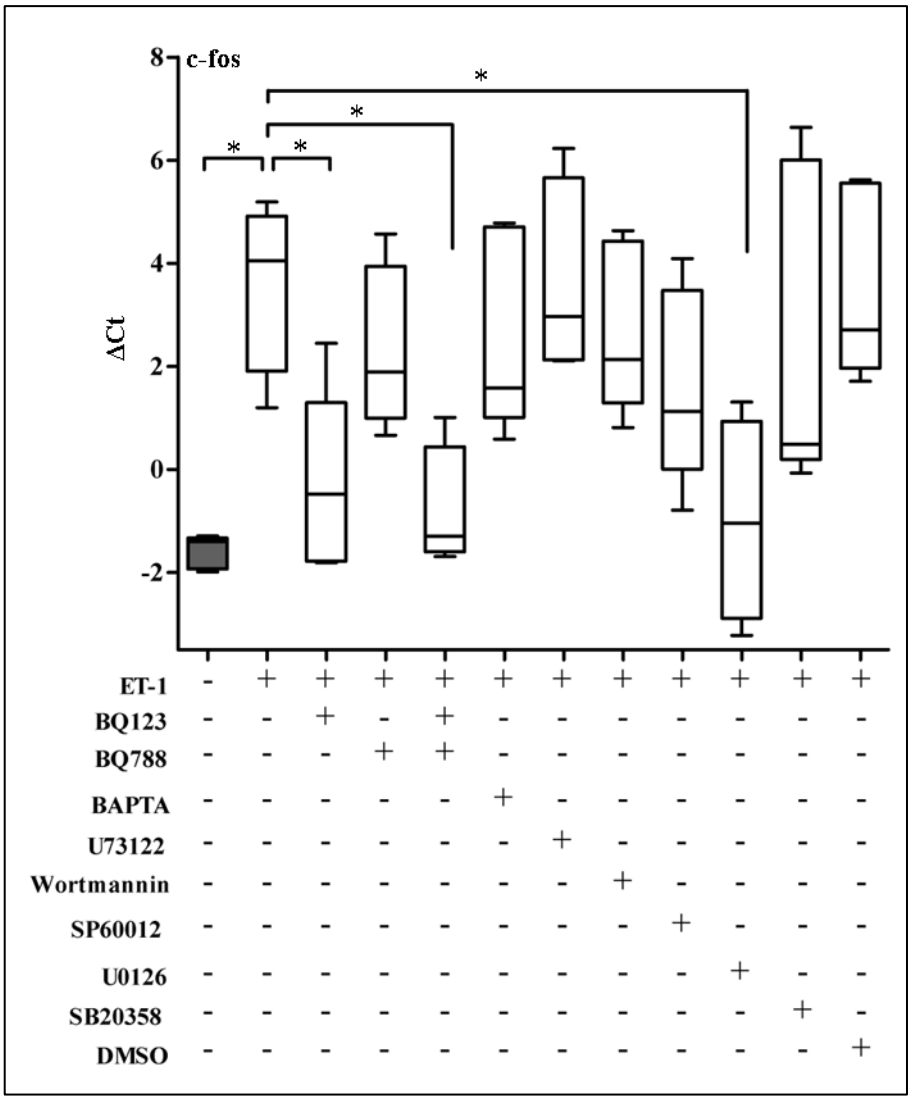

Figure 53: ET-1 increases c-fos via endothelin receptor A and ERK. Expression level of c-fos assessed upon ET-1 stimulation and different inhibitor treatment. hPASMC were treated with endothelin antagonist A (BQ123, 1 µM), endothelin antagonist B (BQ788, 1µM); calcium chelator (BAPTA), PLC inhibitor (U73122), PI3K/AKT inhibitor (Wortmannin), JNK inhibitor (SP60012), ERK1/2 inhibitor (UO126), p38 inhibitor (SB20358) or vehicle (DMSO) for 1 hour before treatment with ET-1 (n=4 individual experiments). Figure modified from (136).

In the next step, we determined whether ERK pathway is activated (phosphorylated) by ET-1. Western blot analysis of ET-1 stimulation on hPASMC revealed that indeed, ERK is transiently phosphorylated (after 5 minutes) by ET-1 (Figure 54)

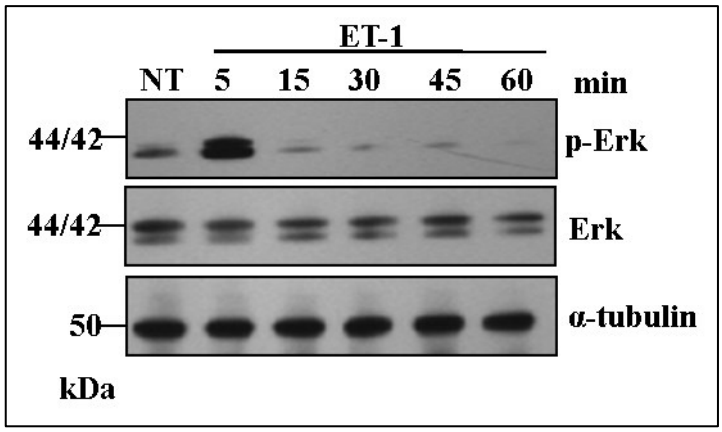

Figure 54: ET-1 increases phosphorylation of ERK. Western blot showing the phosphorylated form of ERK1/2 upon treatment with ET-1 for the indicated time points in hPASMC (n=4 individual experiments). Figure modified from (136).

In order to assess the functional relevance of the ET-1/ERK/c-fos axis, we performed proliferation assay in c-fos and control (ctrl) silenced cells using si-RNA. Accordingly to our previous results silencing of c-fos diminished the ET-1 induced proliferation. However, c-jun silencing did not affect DNA synthesis of hPASMC (Figure 55).

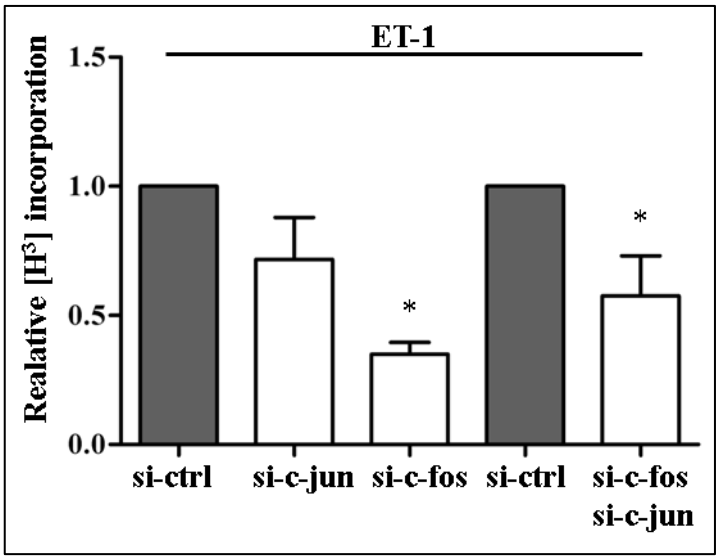

Figure 55: Proliferation of hPASMC is reduced by silencing of c-fos. Proliferation was assessed by thymidine incorporation in ET-1 treated hPASMC which were silenced with c-fos and c-jun singularly or in combination (n= 4 individual experiments). Figure modified from (136).

Silencing efficiency is shown at the protein level 48 hours after treatment with the corresponding siRNA in figure 56.

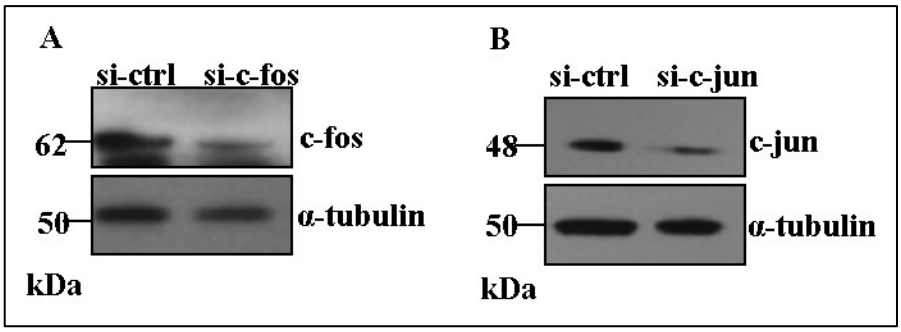

Figure 56: Silencing efficiency of c-fos and c-jun. Western blot representing the silencing efficiency of A) c-fos and B) c-jun after 48 hours silencing in hPASMC. α-tubulin shows the loading control (n=3 individual experiments). Figure modified from (136).

Increased total protein level of transcription factors can lead to an enhanced activity, however higher phosphorylation status without protein amount affection can also enhance their stability. In addition, interaction with other transcription factors can influence their transcriptional activity (138). Therefore, in the next step we analysed the phosphorylation status of c-fos and c-jun upon ET-1. As shown in figure 57, short ET-1 stimulation led to an increase phosphorylation of c-jun and c-fos. The dynamic of the phosphorylation for c-jun and c-fos resulted to be different. C-jun was phosphorylated at serine 73 already after 15 minutes stimulation and reached the peack at 30 minutes. At later time point the phosphorylation status was slowly back to normal level. On the other side, c-fos phosphorylation on serine 32 was strongly induced after 45 and 60 minutes. The two different dynamics indicate a more direct ET-1 induced mechanism for c-jun and a secondary ET-1 induced mechanism for c-fos (Figure 57).

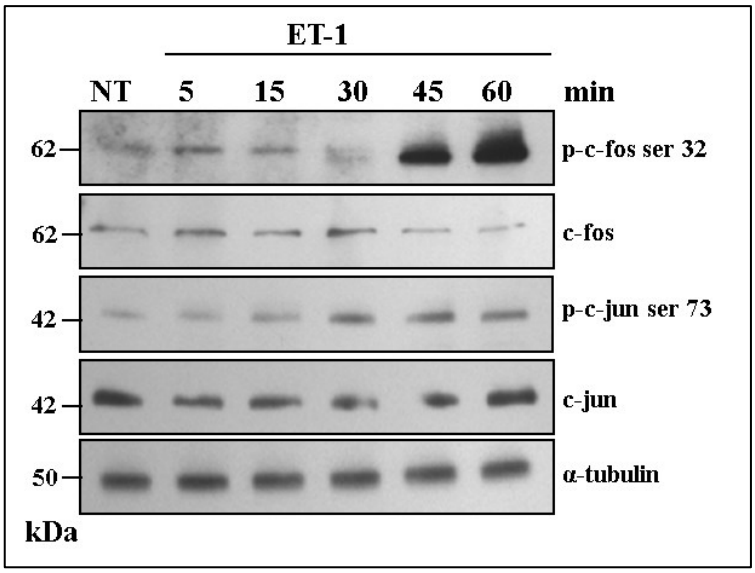

Figure 57: ET-1 induces phosphorylation of c-jun and c-fos. Western blot showing the phosphorylated form of c-fos and c-jun upon treatment with ET-1 for the indicated time points in hPASMC. α-tubulin shows the loading control (n=5 individual experiments). Figure modified from (136).

4.4.3 The regulation of c-jun/c-fos by CTGF

As the second most upregulated gene in the microarray analysis was CTGF, we hypothesize that CTGF might be responsible for induction of c-jun, which then together with c-fos could increase proliferation of hPASMCs in a cumulative manner. Analysis of the expression level of c-jun in hPASMC treated with CTGF did not show any change due to the stimulation (Figure 58A). Of note, no change was also observed in the c-fos level (Figure 58B).

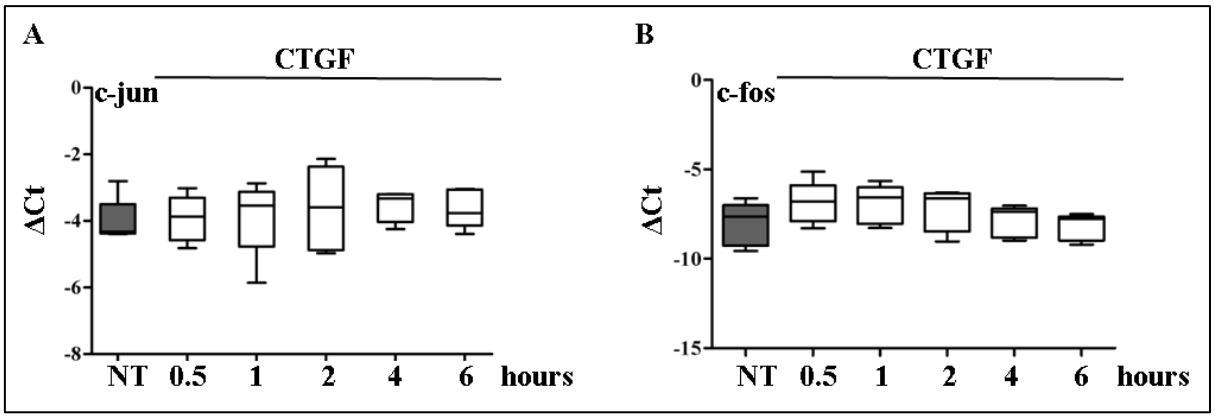

Figure 58: CTGF does not influence c-jun and c-fos expression level. Relative expression of A) c-jun and B) c-fos upon stimulation with CTGF assessed by real time PCR (n=4 individual experiments). Figure modified from (136).

One of the kinases which can phosphorylate c-jun is JNK kinase (139), therefore we checked the phosphorylation status of JNK and c-jun upon CTGF treatment. Analysis of the western blot revealed that phosphorylation status of JNK kinase and c-jun are not affected by CTGF (Figure 59 A and B).

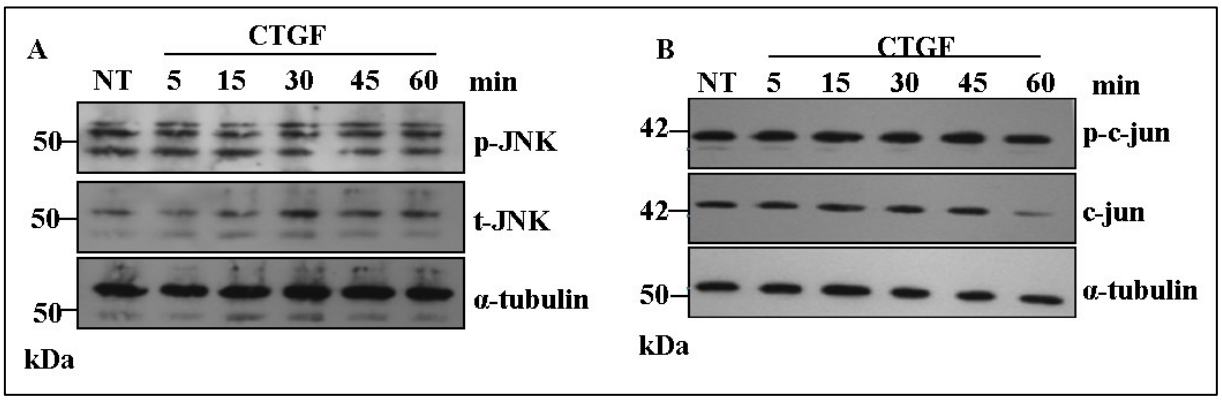

Figure 59: CTGF does not increase protein level of c-jun. A) Western blot showing the phosphorylated protein level of c-jun in hPASMC upon treatment with CTGF for the indicated time points. α-tubulin shows the loading control (n=3 individual experiments). Figure modified from (136).

In addition, the role of CTGF in proliferation was also investigated. We observed no change in the proliferation rate of hPASMC when stimulated with CTGF alone or in combination with ET-1 (Figure 60).

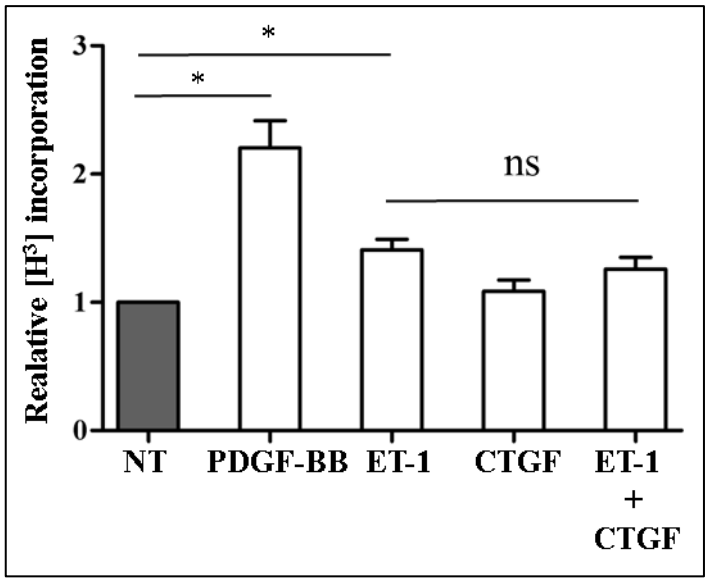

Figure 60: CTGF does not affect proliferation of hPASMC. Proliferation was assessed by thymidine incorporation with PDGF-BB (used as a positive control), ET-1, CTGF and ET-1/CTGF treated hPASMC (n= 4 individual experiments). Figure modified from (136).

Accordingly, expression levels of proliferation markers were also not affected by CTGF (Figure 61). These results suggest that there is no influence from CTGF on c-jun transcription factor and on hPASMC proliferation.

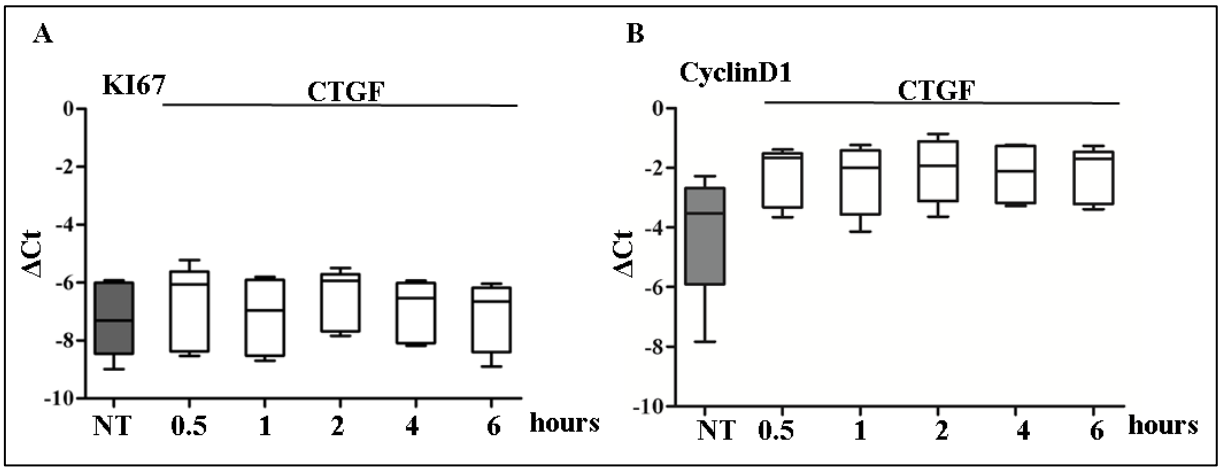

Figure 61: CTGF does not influence proliferating marker expression level. Relative expression of A) KI67 and B) CyclinD1 upon stimulation with CTGF on hPASMC was assessed by real time PCR (n=4-5 individual experiments). Figure modified from (136).

4.4.4 c-jun/c-fos relevance in animal models and in the human

To confirm the relevance of c-fos and c-jun in the disease, we examined their expression and their phosphorylation status in human and animal samples.

4.4.4.1 Animal models

We performed immunohistochemical staining in 2 different animal models used to study pulmonary hypertension: the monocrotaline rat model and the chronic hypoxia exposure model. We observed that in the monocrotaline rat model c-fos, c-jun and their phosphorylated forms were localized in the smooth muscle cell layer of the vessel (Figure 62A, arrowheads). Similarly, in the chronic hypoxia mouse model the staining was in the smooth muscle layer of the vessel wall.

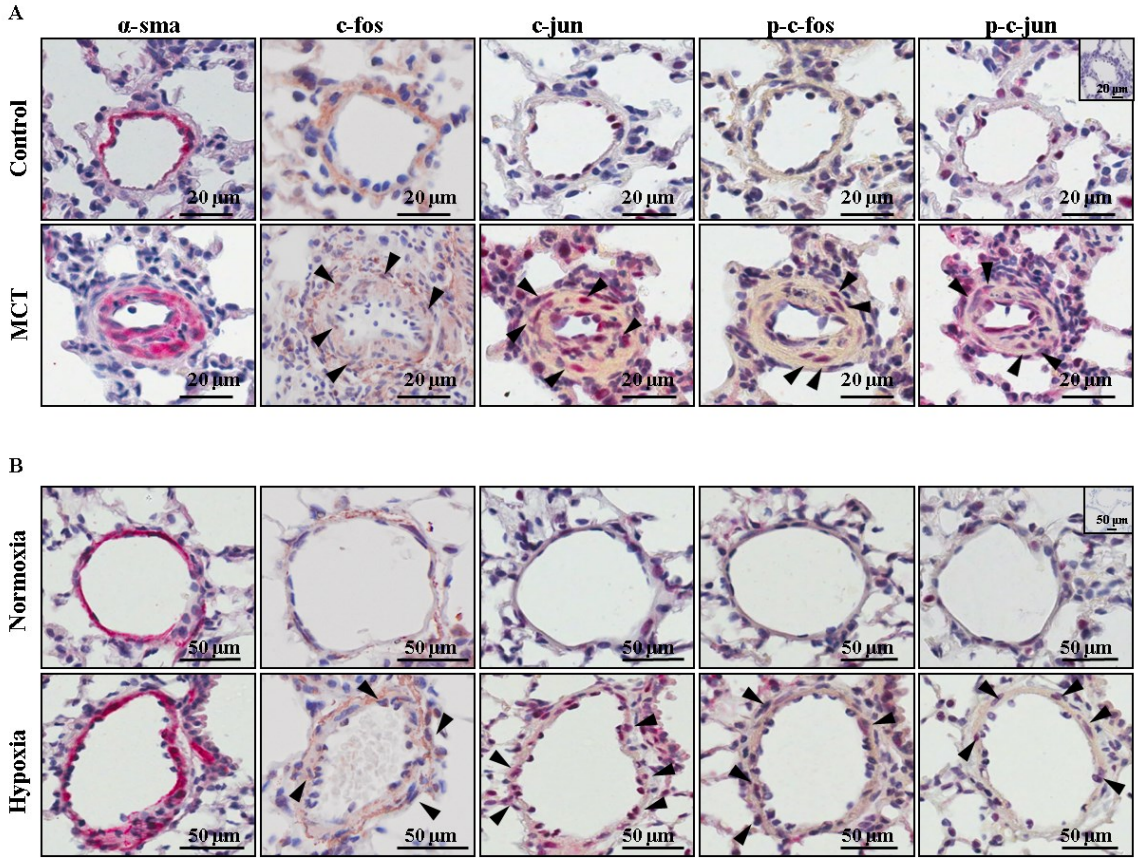

Figure 62: Phosphorylated and total c-jun and c-fos are mainly expressed in the smooth muscle layer of the vessel in the lung of monocrotaline rat and chronic hypoxia mouse model. Representative pictures of the immunohistochemical staining on A) monocrotaline rat model and B) chronic hypoxia mouse model of c-fos, c-jun, phospho (p)-c-fos and phospo (p)-c-jun (n=3). Figure modified from (136).

Similarly to the animal models, in human samples positivity for phosphorylated and total c-fos and c-jun was present mainly in the smooth muscle actin positive cells, as shown in figure 63 by serial slide immunohistochemistry (Figure 63, arrowheads).

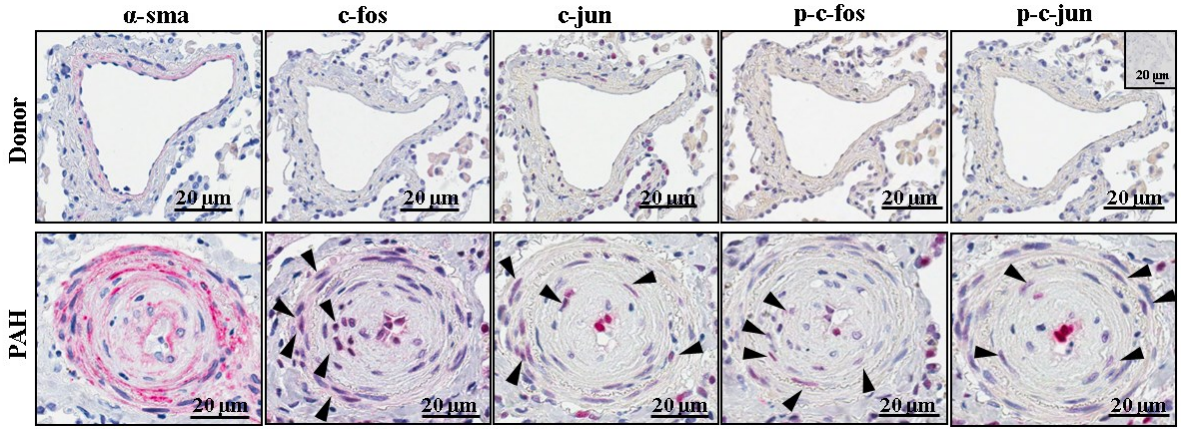

Figure 63: Phosphorylated and total c-jun and c-fos are mainly expressed in the smooth muscle layer in the lung of PAH patients. Representative pictures of the immunohistochemical staining on donor and PAH patients of c-fos, c-jun, phospho (p)-c-fos and phospo (p)-c-jun (n=3). Figure modified from (136).

Taken together, these results demonstrate that c-jun and c-fos are expressed and active in the remodelled pulmonary vessel in the animal model and more importantly in human lung samples. This, suggest a relevant role of these two transcription factors in regulating remodeling of the vessel wall, partly via the presented ET-1 driven molecular mechanism.

5 Discussion

In this study we analyzed and identified two molecular mechanisms which contribute to the vascular remodeling process occurring in the lung of PH patients. We used two different mice model: the Fra-2 TG mice and the hypoxic exposed mice. These two models enabled us to characterize vessel wall thickness, identify new molecular player and study the early stage of the remodeling process.

5.1 AP-1 regulation

AP-1 transcription factors are a family of protein which in response to different stimuli can bind DNA and induce or repress transcription of specific target genes (93). AP-1 is induced by many different stimuli mostly via activation of MAPK (92). Therefore these transcription factors are considered to be key proteins in many different molecular mechanisms (89). As AP-1 regulates a plethora of different mechanisms, inhibition of this molecule as a possible therapeutic target would affect too many cell processes simultaneously. Therefore in order to gain specific response to different stimuli, the AP-1 is regulated at many levels, starting with cell type, triggering stimulus, expression level, post-translation modification and protein dimerization combination. We could show that upon same stimulus, not all the AP-1 members were affected and that different stimuli have influenced different members. In hPASMC, we observed that PDGF-BB regulated fra-2, c-jun and jun-B but not jun-D and that TGF-β was important for jun-B induction but not for other jun family members. We could also show that c-fos and c-jun were upregulated by short time hypoxia exposure (microarray), together with ET-1. In addition ET-1 induced c-fos expression via ERK1/2 while c-jun was not affected. It has been shown that hypoxia enhances levels of different factors such as ET-1, PDGF-BB and TGF-β (111), therefore it might be plausible that c-jun increased expression was mediated by other factors which were not investigated in this study. c-jun was previously shown to be regulated by CTGF in human lung fibroblast (23906792), however we could not see any regulation of c-jun in hPASMC upon CTGF. The remodeling mechanism and process is very complex and influenced by many different stimuli simultaneously {Yuan, 2005 #36), therefore it is very challenging to recapitulate *in vitro* the disease conditions. Taken together, these data suggest a very fine regulation of AP-1 members by different stimuli, and moreover a specificity of response depending on the applied stimulus and on the cell type analysed. In addition to the transcriptional level, the phosphorylation, as a post-

translational modification, has been shown to enhance AP-1 DNA binding affinity and therefore their stability (140).We observed that PDGF-BB and TGF-β enhanced nuclear localization of fra-2 and jun-B respectively and that ET-1 affected phosphorylation of c-fos in ser32, and of c-jun in ser73. There are other regulatory levels, such as different interactions protein or specific DNA binding sequence, which make AP-1 an extremely complex protein family (138).

AP-1 is a convergent point for different signaling pathway. This is important, as these three analysed pathway (PDGF-BB, ET-1 and TGF-β) are known to be crucial and relevant for the development and progression of vascular remodeling in PH. PDGF-BB is a very strong mitogen and, as its receptors are found to be highly expressed in the vessel of PH patients (62), it has a crucial role in proliferation of hPASMC. ET-1 is a strong vasoconstrictor and at high concentration it can affect proliferation. Normally the circulating level of ET-1 is very low and it is secreted in response to specific situation. It is known that there is an increase of ET-1 in PH (22), which maintains a constant constriction of the vessel and to some extend contributes to the proliferative aspect of the disease. TGF-β is a pro-fibrotic factor involved in ECM remodeling, rearrangement and collagen deposition (82). Its importance in PH is related to the collagen deposition and ECM remodeling within the vessel wall. The involvement of AP-1 in each of these pathways, highlight the central role of this family of transcription factors in mediating many different processes and in connecting different pathways.

5.2 AP-1 in cell proliferation

AP-1 family is known to be involved in cell proliferation (141),(85) and the underlying mechanisms are carefully regulated. The proliferative state of a cell is in generally influeced via MAPK activation, and transcription factors which in turn induce expression of the proliferating markers, such as cyclinD1 (142). In this study we have delineated the role of AP-1 transcription factors in mediating hPASMC proliferation induced by PDGF-BB and ET-1. We have observed that fra-2 TG mice develop remodeling of the vessel wall, which was characterized by PCNA positive smooth muscle cells. Moreover, we observed activation of the pro-survival AKT pathway in the lung homogenate of fra-2 TG mice. Activation of AKT can be mediated by different factors, such as PDGF-BB and TGF-β which were identified as trigger factors (143). Importantly, we observed that fra-2 was directly regulated by PDGF-BB. Moreover, we could show that fra-2 can bind to the

jun components and induce proliferation. Silencing of fra-2 with each of the jun components decreased PDGF-BB induced proliferation. Importantly, we could observe lower proliferation rate just in the silenced PDGF-BB treated cells and not in the silenced untreated cells, underlying that PDGF-BB specifically influenced these AP-1 transcription factors. The decreased proliferation due to silencing of each jun components with fra-2, should not be interpreted as an effect caused by lack of specificity. Proliferation was the final read out of the functional study, however we cannot exclude that each complex leaded to different response which consequently reduced proliferation. For instance it has been shown that c-jun and jun-D can directly act on the cell cycle regulatory protein ((144) (145). However, c-jun and also jun-B can enhance transcription of pro-proliferative factors (146). It is plausible that PDG-BB induced different molecular pathways activation in which fra-2 and the jun components resulted to be involved affecting ultimately hPASMC proliferation. In the second part of the study we examined the ET-1 induced proliferation. ET-1 level has been reported to be elevated in the serum of PAH patients and locally on the vascular EC, suggesting that hPAECs might produce more ET-1 in PAH disease condition (22), (73). ET-1 can influence cell growth (71); however the ET-1 role on mediating the proliferation of hPASMC is controversial. A previous study showed that ET-1 does not increase hPASMCs proliferation (147), whilst our results and other studies (148) revealed that ET-1 at high concentration can affects proliferation in previously starved hPASMCs. Accordingly we could show that ET-1 increased expression of the proliferative markers Ki67 and Cyclin D1. The ET-1 induced proliferation was mediated by c-fos. We could not observe any significant effect on ET-1 driven proliferation upon silencing of c-jun, although its role on cell growth has been previously demonstrated (95). To test the hypothesis that c-jun could be induced by other factors and therefore it could affect cumulatively proliferation, we investigated the effect of CTGF (second most up-regulated gene in the microarray) on c-jun. CTGF did not affect neither c-jun expression or phosphorylation nor proliferation of hPASMC. Taken together, these results underlie the importance of the applied stimulus and functional read out considered on the induction of AP-1. Moreover, in order to explain how the AP-1 can mediate cell behavior (eg. proliferation); the molecular mechanism should be profoundly studied.

5.3 AP-1 and target genes

Among the many different mechanisms regulating AP-1, it is also important to identify which are the final targets of the analysed complex.

In the first part of the study we have showed that global over expression of fra-2 (AP-1 component) induced not only vascular remodeling phenotype in the lung of the mice (100) but also increased RVSP. For the first time we characterized fra-2 TG mice with a physiological relevant parameter. Moreover, we also identified a new AP-1 target gene which is important in the vascular remodeling process. Our microarray analysis revealed that meprin β was the most up-regulated gene in the lung homogenate of fra-2 TG mice. This result was confounded in pulmonary arteries from mice and in human IPAH samples where we observed smooth muscle cell and endothelial cell localization. In addition we examined a novel mechanism where fra-2/meprin β pathway resulted to be regulated in an AP-1 dependent manner by a complementary influence of TGF-β and PDGF-BB.

5.3.1 Meprins: structure

Meprins are proteases which belong to the astacin family. There are 6 components of the astacin proteinases, which include the two meprins, three BMP1 and an ovastacin (149). Their structure is very similar (Figure 64); they both have a protease domain protected by a pro-domain which has to be cleaved off, in order to activate their catalytic domain. They possess a MAM domain (meprin, A5 protein receptor-associated tyrosine phosphatase μ) and a TRAF domain (TNF receptor associated factor) which are important for their oligomerization, trough formation of sulfide bonds (150). They have an EGF-like domain, a transmembrane domain and a cytosolic domain (149). The α subunit contains an additional sequence before the EGF-like domain, called inserted sequence, which is constitutively cleaved in the process of protein maturation and it allows meprin α to be released if not forming a heterodimer with meprin β (Figure 64). Contrary meprin β, which lack this sequence can be anchored to the membrane, but it can be shed by different proteases, such as ADAMs (151) (152).

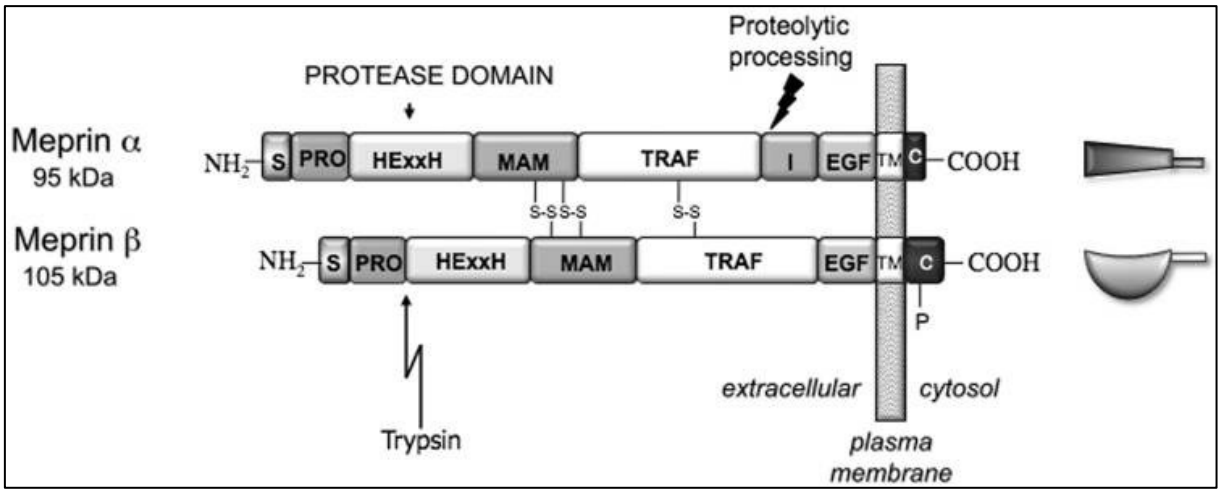

Figure 64: Structural domains of human meprins. Representation of the structural domain present in meprin α and meprin β. PRO: pro domain; HExxH: catalytic domain with HExxH domain; MAM: meprin, A5 protein receptor-associated tyrosine phosphatase μ; TRAF: TNF receptor associated factor; I: inserted domain; EGF: epithelial growth factor-like domain; TM: transmembrane domain; C: cytosolic domain (Figure from (149)).

The cytosolic domain is different between the two meprins. While the meprin α cytosolic domain is just 6 aminoacids, the meprin β is 28 aminoacids long and possess a PKC consensus sequence containing a phosphorylation site (Ser 687) (153). Meprin α and β are encoded by different gene and they can form hetero or homodimer. Moreover, meprin α homodimers can interact in a no-covalent way to form more complex multimers (154). The pro-enzyme is not self-activated, as for MMPs and ADAMs, but activated by trypsin like enzymes, such as kallikrein-4 (155). In details, it has been shown that kallikrein 4 and 8 activates specifically meprin β, while meprin α is activated by kallikrein 5 (156).

5.3.2 Meprins: functions

Meprins are highly expressed in epithelial cells of kidney, skin and intestine, where their function was, to date, mainly studied and where they have a polarized expression, mostly restricted to the apical membrane (157). For instance in the kidney, the specific localization allows meprins to cleave peptide and proteins, which can be re-absorbed. However, in disease condition, meprins can be re-localized in the cell and be more active or change the substrate specificity (149). In these circumstances meprin activity has been shown to be deleterious, as it damages the epithelial barrier, cleaving cell-cell contact or adhesion molecules (158), (159), (160). Many substrates of meprins have been identified in

in vitro studies (151). ECM proteins, such as tenascin C (161)and fibronectin or cell cell contact molecules such as CD99 (151) are cleaved by meprins. Additionally, meprins can process growth factors such as CTGF, TGFβ-1 and VEGF-A (162), (151). The broad spectrum of substrate which has been identified to date, make meprins very interesting but also very complex proteases to study especially in the context of pulmonary hypertension and vascular remodeling.

5.3.3 Meprins in the lung

Meprin were extensively studied in kidney disease and just few studied have addressed their role in lung. It has been shown that meprin α increases secretion of IL-8 and TGF-α from bronchial epithelial cells. Moreover, epithelial cells stimulated with meprin α showed activated EGFR pathway and NFkB(163). In this context meprin α appear to be relevant for inflammatory lung diseases. Another study revealed a role of meprin β in activating the epithelial sodium channel (ENa) in the lung. It has been shown that the c-terminal domain of meprin β interact with the cytosolic domain of one of the subunit of the ENa which consequently leads to increase current (164). These finding suggest that meprins might have a role in lung epithelial cell physiology; however their role in the pulmonary vasculature was, to date, not investigated.

5.3.4 Meprin β role in vascular remodeling and ECM

Our *in vitro* results showed that inhibition of the protease meprin β reduced the proliferation of smooth muscle and endothelial cells. It has been previously shown, that meprin β can stimulate proliferation trough activation of growth factors, which in turn activate their own receptor (165). We cannot exclude that similar mechanism could explain the effect of proliferation by this protease. To date, only few studies have shown *in vivo* the role of meprin β in ECM processing and none of them addressed its role in human vascular remodeling. Meprin β can cleave basement membrane proteins (eg. collagen IV) (166), but it can also act on the maturation of the collagen. Meprin β can cleave the pro-collagen thus release mature collagen fibrils which can undergo the crosslinking process resulting in collagen deposition (133, 167). Our results are in agreement with the aforementioned studies, as we observed high collagen content within the remodeled vessel of fra-2 TG mice. It is known that collagen amount is regulated by the deposition and the degradation rate (168). While degradation of collagen is mainly controlled by MMPs (MMP-1, MMP-

8, MMP-2, MMP-9) (50), the deposition can be regulated at different stages, such as maturation (meprin β) or crosslinking (Lysisl oxidases). Lysil oxidases (LOX) are enzyme able to catalyze aldehydes group from lysine residues of collagen (51) therefore leading to crosslinking of the mature fibrils. It has been shown that LOX enzymes are up-regulated in hPASMC and adventitial fibroblast from IPAH patients in comparison to donor (169). Moreover inhibition of LOX in animal model resulted in attenuation of the pulmonary hypertension and the vascular remodeling (169). Changes in the ECM components can affect the cellular response and vice-versa. For instance if the ECM become more stiff the cells might migrate less, however if MMPs are highly active in this conditions the migration might even be enhanced (170).In line with this notion, in fra-2 TG mice we detected decreased expression of MMP-2 and MMP-9, collagen-degrading proteases. This finding could further shift the collagen homeostasis towards collagen deposition. Importantly MMP2 and 9 were reported to be relevant for the remodeling process in PH animal models ((171) (172)). The role of fra-2 in mediating collagen expression was previously reported in Fra-2 knock out mice, which exhibited changes in collagen expression (173). As our analysis was performed on lung homogenate, it is important to highlight that at the analyzed time points, no sign of parenchyma fibrosis was noticed. Therefore the detected changes mirrored the changes in the remodeled vessels. Taken together these results suggest a role of fra-2 and jun members in increasing meprin β expression, which would then enhance collagen maturation. This mechanism could be responsible for the alteration of the vessels in their functional and mechanical properties thus contributing to the pathological remodeling process (133). Accordingly, collagen deposition on the vessels wall was shown to be associated with the progression of PAH (174).

In addition to ECM proteins, proteases can act on growth factors. It has been shown that proteases can release growth factors (eg TGF- β) from the ECM (175) which can in turn affect the surrounding cell proliferation or migration (8294500). TGF-β is a very important growth factor in PH, known to induce pro-fibrotic changes in vasculature and parenchyma tissue (176). TGF-β can be stored in the ECM and it can be inhibited by the latent TGF-β binding protein (LTBP) which prevents TGF-β binding to its receptors (15611103). *In vitro* study showed that meprin β can cleave LTBP, therefore enhance activation of TGF β induced pathway (151).

5.3.5 Meprin regulation in hPASMC

In our *in vitro* experiments, we observed that PDGF-BB regulate fra-2 expression in hPASMCs but TGF-β was responsible for regulating meprin β expression in hPASMCs. The explanation for this could lies in the fine regulation which was already addressed in the previous sections. Different transcription factors, from different families, could act together in a cooperative manner to induce a specific response. In detail, a recent study could show that the induction of the PAI-1 and MMP-10 genes was mediated by different transcription factors. They could show that smad2/3 proteins, induced by TGF-β, were able to bind the promoters of PAI and MMP-10 just in presence of other transcription factors such as c-jun, jun-B and fra-1 (177). It is tempting to speculate, that meprin β is induced by TGF-β because the jun members together with the PDGF-BB induced fra-2, can effectively bind to meprin β promoter and enhance its expression. However, we cannot exclude that other transcription factors induced by TGF-β (eg. smad proteins) or by PDGF-BB are important in this mechanism. Another possibility which was reported could be an indirect activation of TGF- β by PDGF-BB. It has been shown that PDGF-BB can activate calpain via increase of the intracellular calcium (178). Calpain, which is an endopeptidase was shown to be able to activate TGF-β intracellulary (179). In this mechanism the activated TGF-β could be responsible for the enhanced expression of the necessary transcription factors for meprin β expression. These results suggest that PDGF-BB acts with TGF-β in a cumulative manner, however further studies would be necessary to delineate whether other pathways or other growth factors are involved in this process. Importantly, we observed that inhibition of meprin β with actinonin affected hPASMC and hPAEC PDGF-BB induced proliferation without influence on their apoptosis rate. Taken our findings together, we could identify in meprin β a new mediator of the remodeling and the proliferating process in PH. This indicates meprin β as multifunctional proteases in regulating different pathways.

In conclusion, we could show that AP-1 transcription family plays an important role in mediating the vascular remodeling process. We also partly delineate the complexity of the regulation of AP-1 and meprin β as a direct target gene. Understanding of the signaling upstream of AP-1 can help identification of stimuli responsible for initiating the remodeling process. More importantly analysis of the downstream signaling of AP-1 can be essential for identification of new target genes which could be targetable. A good understanding of the AP-1 triggered molecular mechanisms could be essential to identify

new players in the development of PAH. In our proposed mechanism, the AP-1 family is induced by different stimuli (PDGF-BB, TGFβ and ET-1) which induce increase expression, phosphorylation and/or nuclear localization of AP-1. These changes enhance AP-1 activity which is affecting proliferation of hPASMC and transcription of target genes. A novel identified target gene is meprin β, which can influence collagen maturation and hPASMC proliferation. Moreover, meprin β could be responsible for increasing the active level of TGF-β further enhancing the pathway in a positive feedback loop manner (Figure 34).

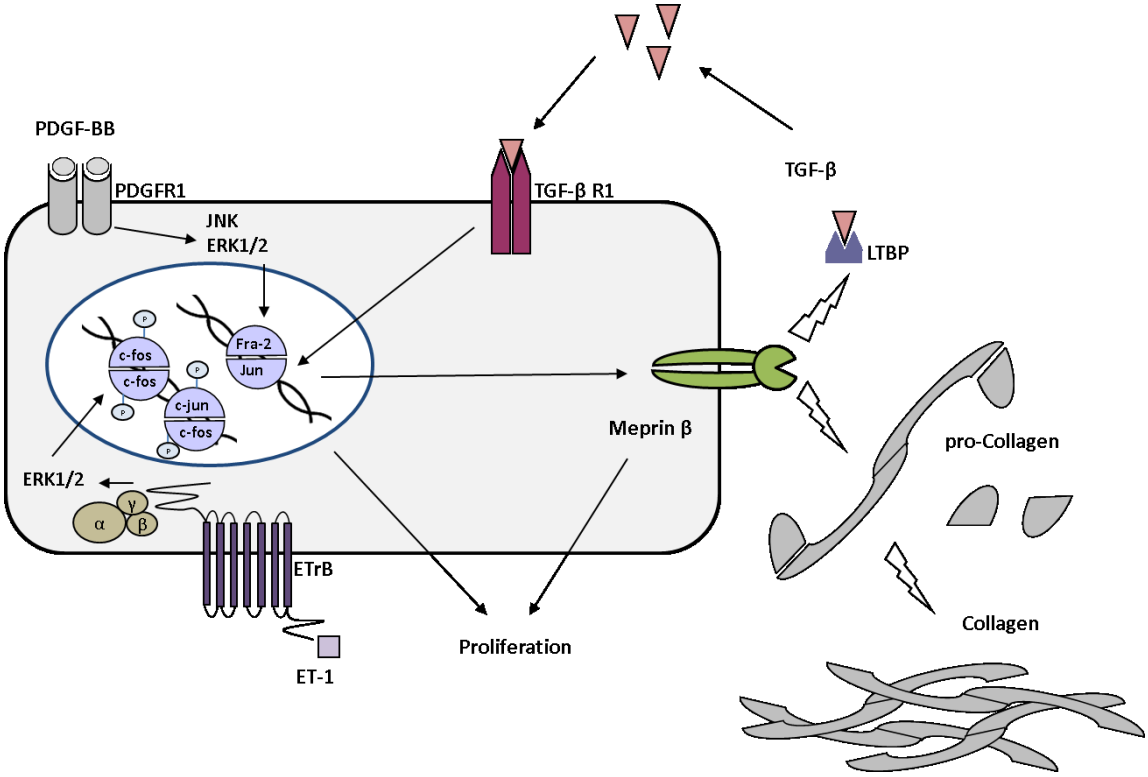

Figure 65: Representation of molecular pathways involved in vascular remodeling. PDGF-BB stimulation on hPASMC induces increase of fra-2 expression. PDGF-BB induced fra-2 which translocate into the nucleus. In the nucleus fra-2 forms a dimer with the jun components leading to enhanced hPASMC proliferation. Moreover, TGF-β stimulation on hPASMC enhances the expression level of jun-B and its nuclear localization. Jun-B and fra-2 could form a dimer and bind to the meprin β promoter, enhancing its expression. In turn meprin β processes pro-collagen, contributing to vascular remodeling and further enhancing its own expression by activating new TGF-β. ET-1 binds to the ETrA which activates ERK1/2 and leads to c-fos increase expression and phosphorylation on hPASMC. c-fos mediates ET-1 induced proliferation of hPASMCs. ET-1 increases c-jun phosphorylation.

6 References

1. Simonneau G, Gatzoulis MA, Adatia I, Celermajer D, Denton C, Ghofrani A, et al. Updated clinical classification of pulmonary hypertension. Journal of the American College of Cardiology. 2013;62(25 Suppl):D34-41.

2. Hoffmann J, Wilhelm J, Marsh LM, Ghanim B, Klepetko W, Kovacs G, et al. Distinct differences in gene expression patterns in pulmonary arteries of patients with chronic obstructive pulmonary disease and idiopathic pulmonary fibrosis with pulmonary hypertension. American journal of respiratory and critical care medicine. 2014;190(1):98-111.

3. Kelly CR, Rabbani LE. Videos in clinical medicine. Pulmonary-artery catheterization. The New England journal of medicine. 2013;369(25):e35.

4. Milan A, Magnino C, Veglio F. Echocardiographic indexes for the non-invasive evaluation of pulmonary hemodynamics. Journal of the American Society of Echocardiography : official publication of the American Society of Echocardiography. 2010;23(3):225-39; quiz 332-4.

5. Pienn M, Kovacs G, Tscherner M, Avian A, Johnson TR, Kullnig P, et al. Non-invasive determination of pulmonary hypertension with dynamic contrast-enhanced computed tomography: a pilot study. European radiology. 2014;24(3):668-76.

6. Reiter U, Reiter G, Kovacs G, Stalder AF, Gulsun MA, Greiser A, et al. Evaluation of elevated mean pulmonary arterial pressure based on magnetic resonance 4D velocity mapping: comparison of visualization techniques. PloS one. 2013;8(12):e82212.

7. Galie N, Hoeper MM, Humbert M, Torbicki A, Vachiery JL, Barbera JA, et al. Guidelines for the diagnosis and treatment of pulmonary hypertension: the Task Force for the Diagnosis and Treatment of Pulmonary Hypertension of the European Society of Cardiology (ESC) and the European Respiratory Society (ERS), endorsed by the International Society of Heart and Lung Transplantation (ISHLT). European heart journal. 2009;30(20):2493-537.

8. McLaughlin VV, McGoon MD. Pulmonary arterial hypertension. Circulation. 2006;114(13):1417-31.

9. Chaumais MC, Macari EA, Sitbon O. Calcium-channel blockers in pulmonary arterial hypertension. Handbook of experimental pharmacology. 2013;218:161-75.

10. Gomberg-Maitland M, Olschewski H. Prostacyclin therapies for the treatment of pulmonary arterial hypertension. The European respiratory journal. 2008;31(4):891-901.

11. Galie N, Corris PA, Frost A, Girgis RE, Granton J, Jing ZC, et al. Updated treatment algorithm of pulmonary arterial hypertension. Journal of the American College of Cardiology. 2013;62(25 Suppl):D60-72.

12. Sitbon O, Morrell N. Pathways in pulmonary arterial hypertension: the future is here. European respiratory review : an official journal of the European Respiratory Society. 2012;21(126):321-7.

13. Olschewski H. Prostacyclins. Handbook of experimental pharmacology. 2013;218:177-98.

14. Clozel M, Maresta A, Humbert M. Endothelin receptor antagonists. Handbook of experimental pharmacology. 2013;218:199-227.

15. Montani D, Chaumais MC, Savale L, Natali D, Price LC, Jais X, et al. Phosphodiesterase type 5 inhibitors in pulmonary arterial hypertension. Advances in therapy. 2009;26(9):813-25.

16. Archer SL, Weir EK, Wilkins MR. Basic science of pulmonary arterial hypertension for clinicians: new concepts and experimental therapies. Circulation. 2010;121(18):2045-66.

17. Michiels C. Endothelial cell functions. Journal of cellular physiology. 2003;196(3):430-43.

18. Tuder RM, Groves B, Badesch DB, Voelkel NF. Exuberant endothelial cell growth and elements of inflammation are present in plexiform lesions of pulmonary hypertension. The American journal of pathology. 1994;144(2):275-85.

19. Tuder RM, Marecki JC, Richter A, Fijalkowska I, Flores S. Pathology of pulmonary hypertension. Clinics in chest medicine. 2007;28(1):23-42, vii.

20. Cool CD, Stewart JS, Werahera P, Miller GJ, Williams RL, Voelkel NF, et al. Three-dimensional reconstruction of pulmonary arteries in plexiform pulmonary hypertension using cell-specific markers. Evidence for a dynamic and heterogeneous process of pulmonary endothelial cell growth. The American journal of pathology. 1999;155(2):411-9.

21. Tuder RM, Stacher E, Robinson J, Kumar R, Graham BB. Pathology of pulmonary hypertension. Clinics in chest medicine. 2013;34(4):639-50.

22. Humbert M, Morrell NW, Archer SL, Stenmark KR, MacLean MR, Lang IM, et al. Cellular and molecular pathobiology of pulmonary arterial hypertension. Journal of the American College of Cardiology. 2004;43(12 Suppl S):13S-24S.

23. Sakao S, Taraseviciene-Stewart L, Lee JD, Wood K, Cool CD, Voelkel NF. Initial apoptosis is followed by increased proliferation of apoptosis-resistant endothelial cells. FASEB journal : official publication of the Federation of American Societies for Experimental Biology. 2005;19(9):1178-80.

24. Townsley MI. Structure and composition of pulmonary arteries, capillaries, and veins. Comprehensive Physiology. 2012;2(1):675-709.

25. Seidelmann SB, Lighthouse JK, Greif DM. Development and pathologies of the arterial wall. Cellular and molecular life sciences : CMLS. 2014;71(11):1977-99.

26. Rensen SS, Doevendans PA, van Eys GJ. Regulation and characteristics of vascular smooth muscle cell phenotypic diversity. Netherlands heart journal : monthly journal of the Netherlands Society of Cardiology and the Netherlands Heart Foundation. 2007;15(3):100-8.

27. Hao H, Gabbiani G, Bochaton-Piallat ML. Arterial smooth muscle cell heterogeneity: implications for atherosclerosis and restenosis development. Arteriosclerosis, thrombosis, and vascular biology. 2003;23(9):1510-20.

28. Frid MG, Moiseeva EP, Stenmark KR. Multiple phenotypically distinct smooth muscle cell populations exist in the adult and developing bovine pulmonary arterial media in vivo. Circulation research. 1994;75(4):669-81.

29. Voelkel NF, Tuder RM. Cellular and molecular biology of vascular smooth muscle cells in pulmonary hypertension. Pulmonary pharmacology & therapeutics. 1997;10(5-6):231-41.

30. Li X, Van Putten V, Zarinetchi F, Nicks ME, Thaler S, Heasley LE, et al. Suppression of smooth-muscle alpha-actin expression by platelet-derived growth factor in vascular smooth-muscle cells involves Ras and cytosolic phospholipase A2. The Biochemical journal. 1997;327 (Pt 3):709-16.

31. Wohrley JD, Frid MG, Moiseeva EP, Orton EC, Belknap JK, Stenmark KR. Hypoxia selectively induces proliferation in a specific subpopulation of smooth muscle cells in the bovine neonatal pulmonary arterial media. The Journal of clinical investigation. 1995;96(1):273-81.

32. Gingras M, Farand P, Safar ME, Plante GE. Adventitia: the vital wall of conduit arteries. Journal of the American Society of Hypertension : JASH. 2009;3(3):166-83.

33. Stenmark KR, Nozik-Grayck E, Gerasimovskaya E, Anwar A, Li M, Riddle S, et al. The adventitia: Essential role in pulmonary vascular remodeling. Comprehensive Physiology. 2011;1(1):141-61.

34. Stenmark KR, Davie N, Frid M, Gerasimovskaya E, Das M. Role of the adventitia in pulmonary vascular remodeling. Physiology. 2006;21:134-45.

35. Meyrick BO, Reid LM. Crotalaria-induced pulmonary hypertension. Uptake of 3H-thymidine by the cells of the pulmonary circulation and alveolar walls. The American journal of pathology. 1982;106(1):84-94.

36. Stenmark KR, Gerasimovskaya E, Nemenoff RA, Das M. Hypoxic activation of adventitial fibroblasts: role in vascular remodeling. Chest. 2002;122(6 Suppl):326S-34S.

37. Orton EC, LaRue SM, Ensley B, Stenmark K. Bromodeoxyuridine labeling and DNA content of pulmonary arterial medial cells from hypoxia-exposed and nonexposed healthy calves. American journal of veterinary research. 1992;53(10):1925-30.

38. Smith P, Heath D, Yacoub M, Madden B, Caslin A, Gosney J. The ultrastructure of plexogenic pulmonary arteriopathy. The Journal of pathology. 1990;160(2):111-21.

39. Gabbiani G. The myofibroblast in wound healing and fibrocontractive diseases. The Journal of pathology. 2003;200(4):500-3.

40. Hynes RO. The extracellular matrix: not just pretty fibrils. Science. 2009;326(5957):1216-9.

41. Kerrigan JJ, Mansell JP, Sandy JR. Matrix turnover. Journal of orthodontics. 2000;27(3):227-33.

42. Hynes RO, Naba A. Overview of the matrisome--an inventory of extracellular matrix constituents and functions. Cold Spring Harbor perspectives in biology. 2012;4(1):a004903.

43. Arribas SM, Hinek A, Gonzalez MC. Elastic fibres and vascular structure in hypertension. Pharmacology & therapeutics. 2006;111(3):771-91.

44. Rabinovitch M, Bothwell T, Hayakawa BN, Williams WG, Trusler GA, Rowe RD, et al. Pulmonary artery endothelial abnormalities in patients with congenital heart defects and pulmonary hypertension. A correlation of light with scanning electron microscopy and transmission electron microscopy. Laboratory investigation; a journal of technical methods and pathology. 1986;55(6):632-53.

45. Zaidi SH, Hui CC, Cheah AY, You XM, Husain M, Rabinovitch M. Targeted overexpression of elafin protects mice against cardiac dysfunction and mortality following viral myocarditis. The Journal of clinical investigation. 1999;103(8):1211-9.

46. Denhardt DT, Feng B, Edwards DR, Cocuzzi ET, Malyankar UM. Tissue inhibitor of metalloproteinases (TIMP, aka EPA): structure, control of expression and biological functions. Pharmacology & therapeutics. 1993;59(3):329-41.

47. Ihida-Stansbury K, McKean DM, Lane KB, Loyd JE, Wheeler LA, Morrell NW, et al. Tenascin-C is induced by mutated BMP type II receptors in familial forms of pulmonary arterial hypertension. American journal of physiology Lung cellular and molecular physiology. 2006;291(4):L694-702.

48. Cummings CL, Gawlitta D, Nerem RM, Stegemann JP. Properties of engineered vascular constructs made from collagen, fibrin, and collagen-fibrin mixtures. Biomaterials. 2004;25(17):3699-706.

49. Tabima DM, Roldan-Alzate A, Wang Z, Hacker TA, Molthen RC, Chesler NC. Persistent vascular collagen accumulation alters hemodynamic recovery from chronic hypoxia. Journal of biomechanics. 2012;45(5):799-804.

50. Cawston TE, Young DA. Proteinases involved in matrix turnover during cartilage and bone breakdown. Cell and tissue research. 2010;339(1):221-35.

51. Csiszar K. Lysyl oxidases: a novel multifunctional amine oxidase family. Progress in nucleic acid research and molecular biology. 2001;70:1-32.

52. Andrae J, Gallini R, Betsholtz C. Role of platelet-derived growth factors in physiology and medicine. Genes & development. 2008;22(10):1276-312.

53. Hoch RV, Soriano P. Roles of PDGF in animal development. Development. 2003;130(20):4769-84.

54. Heldin CH, Westermark B. Mechanism of action and in vivo role of platelet-derived growth factor. Physiological reviews. 1999;79(4):1283-316.

55. Kazlauskas A, Cooper JA. Autophosphorylation of the PDGF receptor in the kinase insert region regulates interactions with cell proteins. Cell. 1989;58(6):1121-33.

56. Seger R, Krebs EG. The MAPK signaling cascade. FASEB journal : official publication of the Federation of American Societies for Experimental Biology. 1995;9(9):726-35.

57. Burgering BM, Coffer PJ. Protein kinase B (c-Akt) in phosphatidylinositol-3-OH kinase signal transduction. Nature. 1995;376(6541):599-602.

58. Lopez-Ilasaca M, Li W, Uren A, Yu JC, Kazlauskas A, Gutkind JS, et al. Requirement of phosphatidylinositol-3 kinase for activation of JNK/SAPKs by PDGF. Biochemical and biophysical research communications. 1997;232(2):273-7.

59. Berridge MJ. Inositol trisphosphate and calcium signalling. Nature. 1993;361(6410):315-25.

60. Clark EA, Brugge JS. Integrins and signal transduction pathways: the road taken. Science. 1995;268(5208):233-9.

61. Hossain MZ, Ao P, Boynton AL. Platelet-derived growth factor-induced disruption of gap junctional communication and phosphorylation of connexin43 involves protein kinase C and mitogen-activated protein kinase. Journal of cellular physiology. 1998;176(2):332-41.

62. Perros F, Montani D, Dorfmuller P, Durand-Gasselin I, Tcherakian C, Le Pavec J, et al. Platelet-derived growth factor expression and function in idiopathic pulmonary arterial hypertension. American journal of respiratory and critical care medicine. 2008;178(1):81-8.

63. Schermuly RT, Dony E, Ghofrani HA, Pullamsetti S, Savai R, Roth M, et al. Reversal of experimental pulmonary hypertension by PDGF inhibition. The Journal of clinical investigation. 2005;115(10):2811-21.

64. Vane JR, Botting RM. Secretory functions of the vascular endothelium. Journal of physiology and pharmacology : an official journal of the Polish Physiological Society. 1992;43(3):195-207.

65. Denault JB, Claing A, D'Orleans-Juste P, Sawamura T, Kido T, Masaki T, et al. Processing of proendothelin-1 by human furin convertase. FEBS letters. 1995;362(3):276-80.

66. Johnstrom P, Fryer TD, Richards HK, Harris NG, Barret O, Clark JC, et al. Positron emission tomography using 18F-labelled endothelin-1 reveals prevention of binding to cardiac receptors owing to tissue-specific clearance by ET B receptors in vivo. British journal of pharmacology. 2005;144(1):115-22.

67. Sakurai T, Yanagisawa M, Takuwa Y, Miyazaki H, Kimura S, Goto K, et al. Cloning of a cDNA encoding a non-isopeptide-selective subtype of the endothelin receptor. Nature. 1990;348(6303):732-5.

68. Simonson MS, Dunn MJ. Cellular signaling by peptides of the endothelin gene family. FASEB journal : official publication of the Federation of American Societies for Experimental Biology. 1990;4(12):2989-3000.

69. Pernow J, Modin A. Endothelial regulation of coronary vascular tone in vitro: contribution of endothelin receptor subtypes and nitric oxide. European journal of pharmacology. 1993;243(3):281-6.

70. Tsukahara H, Ende H, Magazine HI, Bahou WF, Goligorsky MS. Molecular and functional characterization of the non-isopeptide-selective ETB receptor in endothelial cells. Receptor coupling to nitric oxide synthase. The Journal of biological chemistry. 1994;269(34):21778-85.

71. Clerk A, Kemp TJ, Harrison JG, Mullen AJ, Barton PJ, Sugden PH. Up-regulation of c-jun mRNA in cardiac myocytes requires the extracellular signal-regulated kinase cascade, but c-Jun N-terminal kinases are required for efficient up-regulation of c-Jun protein. The Biochemical journal. 2002;368(Pt 1):101-10.

72. Vignon-Zellweger N, Heiden S, Miyauchi T, Emoto N. Endothelin and endothelin receptors in the renal and cardiovascular systems. Life sciences. 2012;91(13-14):490-500.

73. Nootens M, Kaufmann E, Rector T, Toher C, Judd D, Francis GS, et al. Neurohormonal activation in patients with right ventricular failure from pulmonary hypertension: relation to hemodynamic variables and endothelin levels. Journal of the American College of Cardiology. 1995;26(7):1581-5.

74. Stewart DJ, Levy RD, Cernacek P, Langleben D. Increased plasma endothelin-1 in pulmonary hypertension: marker or mediator of disease? Annals of internal medicine. 1991;114(6):464-9.

75. Chen SJ, Chen YF, Meng QC, Durand J, Dicarlo VS, Oparil S. Endothelin-receptor antagonist bosentan prevents and reverses hypoxic pulmonary hypertension in rats. Journal of applied physiology. 1995;79(6):2122-31.

76. Chen SJ, Chen YF, Opgenorth TJ, Wessale JL, Meng QC, Durand J, et al. The orally active nonpeptide endothelin A-receptor antagonist A-127722 prevents and reverses hypoxia-induced pulmonary hypertension and pulmonary vascular remodeling in Sprague-Dawley rats. Journal of cardiovascular pharmacology. 1997;29(6):713-25.

77. Tilton RG, Munsch CL, Sherwood SJ, Chen SJ, Chen YF, Wu C, et al. Attenuation of pulmonary vascular hypertension and cardiac hypertrophy with sitaxsentan sodium, an orally active ET(A) receptor antagonist. Pulmonary pharmacology & therapeutics. 2000;13(2):87-97.

78. Newman JH, Phillips JA, 3rd, Loyd JE. Narrative review: the enigma of pulmonary arterial hypertension: new insights from genetic studies. Annals of internal medicine. 2008;148(4):278-83.

79. Weiss A, Attisano L. The TGFbeta superfamily signaling pathway. Wiley interdisciplinary reviews Developmental biology. 2013;2(1):47-63.

80. Attisano L, Wrana JL. Signal transduction by the TGF-beta superfamily. Science. 2002;296(5573):1646-7.

81. Itman C, Mendis S, Barakat B, Loveland KL. All in the family: TGF-beta family action in testis development. Reproduction. 2006;132(2):233-46.

82. Blobe GC, Schiemann WP, Lodish HF. Role of transforming growth factor beta in human disease. The New England journal of medicine. 2000;342(18):1350-8.

83. Morrell NW. Pulmonary hypertension due to BMPR2 mutation: a new paradigm for tissue remodeling? Proceedings of the American Thoracic Society. 2006;3(8):680-6.

84. Miyazawa K, Shinozaki M, Hara T, Furuya T, Miyazono K. Two major Smad pathways in TGF-beta superfamily signalling. Genes to cells : devoted to molecular & cellular mechanisms. 2002;7(12):1191-204.

85. Shaulian E, Karin M. AP-1 in cell proliferation and survival. Oncogene. 2001;20(19):2390-400.

86. Silbermann M, Schmidt J, Livne E, von der Mark K, Erfle V. In vitro induction of osteosarcomalike lesion by transformation of differentiating skeletal precursor cells with FBR murine osteosarcoma virus. Calcified tissue international. 1987;41(4):208-17.

87. Nishimura T, Vogt PK. The avian cellular homolog of the oncogene jun. Oncogene. 1988;3(6):659-63.

88. Jochum W, Passegue E, Wagner EF. AP-1 in mouse development and tumorigenesis. Oncogene. 2001;20(19):2401-12.

89. Shaulian E, Karin M. AP-1 as a regulator of cell life and death. Nature cell biology. 2002;4(5):E131-6.

90. Reddy SP, Mossman BT. Role and regulation of activator protein-1 in toxicant-induced responses of the lung. American journal of physiology Lung cellular and molecular physiology. 2002;283(6):L1161-78.

91. Hess J, Angel P, Schorpp-Kistner M. AP-1 subunits: quarrel and harmony among siblings. Journal of cell science. 2004;117(Pt 25):5965-73.

92. Karin M. The regulation of AP-1 activity by mitogen-activated protein kinases. The Journal of biological chemistry. 1995;270(28):16483-6.

93. Karin M, Liu Z, Zandi E. AP-1 function and regulation. Current opinion in cell biology. 1997;9(2):240-6.

94. White K, Loughlin L, Maqbool Z, Nilsen M, McClure J, Dempsie Y, et al. Serotonin transporter, sex, and hypoxia: microarray analysis in the pulmonary arteries of

mice identifies genes with relevance to human PAH. Physiological genomics. 2011;43(8):417-37.

95. Yu Y, Platoshyn O, Zhang J, Krick S, Zhao Y, Rubin LJ, et al. c-Jun decreases voltage-gated K(+) channel activity in pulmonary artery smooth muscle cells. Circulation. 2001;104(13):1557-63.

96. Yoshida T, Suzuki T, Sato H, Nishina H, Iba H. Analysis of fra-2 gene expression. Nucleic acids research. 1993;21(11):2715-21.

97. Nishina H, Sato H, Suzuki T, Sato M, Iba H. Isolation and characterization of fra-2, an additional member of the fos gene family. Proceedings of the National Academy of Sciences of the United States of America. 1990;87(9):3619-23.

98. Sonobe MH, Yoshida T, Murakami M, Kameda T, Iba H. fra-2 promoter can respond to serum-stimulation through AP-1 complexes. Oncogene. 1995;10(4):689-96.

99. Suzuki T, Okuno H, Yoshida T, Endo T, Nishina H, Iba H. Difference in transcriptional regulatory function between c-Fos and Fra-2. Nucleic acids research. 1991;19(20):5537-42.

100. Eferl R, Hasselblatt P, Rath M, Popper H, Zenz R, Komnenovic V, et al. Development of pulmonary fibrosis through a pathway involving the transcription factor Fra-2/AP-1. Proceedings of the National Academy of Sciences of the United States of America. 2008;105(30):10525-30.

101. Maurer B, Busch N, Jungel A, Pileckyte M, Gay RE, Michel BA, et al. Transcription factor fos-related antigen-2 induces progressive peripheral vasculopathy in mice closely resembling human systemic sclerosis. Circulation. 2009;120(23):2367-76.

102. Maurer B, Reich N, Juengel A, Kriegsmann J, Gay RE, Schett G, et al. Fra-2 transgenic mice as a novel model of pulmonary hypertension associated with systemic sclerosis. Annals of the rheumatic diseases. 2012;71(8):1382-7.

103. West J, Harral J, Lane K, Deng Y, Ickes B, Crona D, et al. Mice expressing BMPR2R899X transgene in smooth muscle develop pulmonary vascular lesions. American journal of physiology Lung cellular and molecular physiology. 2008;295(5):L744-55.

104. Taraseviciene-Stewart L, Kasahara Y, Alger L, Hirth P, Mc Mahon G, Waltenberger J, et al. Inhibition of the VEGF receptor 2 combined with chronic hypoxia causes cell death-dependent pulmonary endothelial cell proliferation and severe pulmonary hypertension. FASEB journal : official publication of the Federation of American Societies for Experimental Biology. 2001;15(2):427-38.

105. Greenway S, van Suylen RJ, Du Marchie Sarvaas G, Kwan E, Ambartsumian N, Lukanidin E, et al. S100A4/Mts1 produces murine pulmonary artery changes resembling plexogenic arteriopathy and is increased in human plexogenic arteriopathy. The American journal of pathology. 2004;164(1):253-62.

106. Stenmark KR, Meyrick B, Galie N, Mooi WJ, McMurtry IF. Animal models of pulmonary arterial hypertension: the hope for etiological discovery and pharmacological cure. American journal of physiology Lung cellular and molecular physiology. 2009;297(6):L1013-32.

107. Skjorten I, Hilde JM, Melsom MN, Hansteen V, Steine K, Humerfelt S. Pulmonary artery pressure and PaO2 in chronic obstructive pulmonary disease. Respiratory medicine. 2013;107(8):1271-9.

108. Welsh DJ, Peacock AJ. Cellular responses to hypoxia in the pulmonary circulation. High altitude medicine & biology. 2013;14(2):111-6.

109. Maggiorini M, Leon-Velarde F. High-altitude pulmonary hypertension: a pathophysiological entity to different diseases. The European respiratory journal. 2003;22(6):1019-25.

110. Sommer N, Dietrich A, Schermuly RT, Ghofrani HA, Gudermann T, Schulz R, et al. Regulation of hypoxic pulmonary vasoconstriction: basic mechanisms. The European respiratory journal. 2008;32(6):1639-51.

111. Stenmark KR, Fagan KA, Frid MG. Hypoxia-induced pulmonary vascular remodeling: cellular and molecular mechanisms. Circulation research. 2006;99(7):675-91.

112. Stacher E, Graham BB, Hunt JM, Gandjeva A, Groshong SD, McLaughlin VV, et al. Modern age pathology of pulmonary arterial hypertension. American journal of respiratory and critical care medicine. 2012;186(3):261-72.

113. Voelkel NF, Tuder RM. Hypoxia-induced pulmonary vascular remodeling: a model for what human disease? The Journal of clinical investigation. 2000;106(6):733-8.

114. Jasmin JF, Lucas M, Cernacek P, Dupuis J. Effectiveness of a nonselective ET(A/B) and a selective ET(A) antagonist in rats with monocrotaline-induced pulmonary hypertension. Circulation. 2001;103(2):314-8.

115. Wilson DW, Segall HJ, Pan LC, Dunston SK. Progressive inflammatory and structural changes in the pulmonary vasculature of monocrotaline-treated rats. Microvascular research. 1989;38(1):57-80.

116. White RJ, Meoli DF, Swarthout RF, Kallop DY, Galaria, II, Harvey JL, et al. Plexiform-like lesions and increased tissue factor expression in a rat model of severe

pulmonary arterial hypertension. American journal of physiology Lung cellular and molecular physiology. 2007;293(3):L583-90.

117. Gomez-Arroyo JG, Farkas L, Alhussaini AA, Farkas D, Kraskauskas D, Voelkel NF, et al. The monocrotaline model of pulmonary hypertension in perspective. American journal of physiology Lung cellular and molecular physiology. 2012;302(4):L363-9.

118. Austin ED, Loyd JE. The genetics of pulmonary arterial hypertension. Circulation research. 2014;115(1):189-202.

119. West J, Fagan K, Steudel W, Fouty B, Lane K, Harral J, et al. Pulmonary hypertension in transgenic mice expressing a dominant-negative BMPRII gene in smooth muscle. Circulation research. 2004;94(8):1109-14.

120. Dempsie Y, Nilsen M, White K, Mair KM, Loughlin L, Ambartsumian N, et al. Development of pulmonary arterial hypertension in mice over-expressing S100A4/Mts1 is specific to females. Respiratory research. 2011;12:159.

121. Merklinger SL, Wagner RA, Spiekerkoetter E, Hinek A, Knutsen RH, Kabir MG, et al. Increased fibulin-5 and elastin in S100A4/Mts1 mice with pulmonary hypertension. Circulation research. 2005;97(6):596-604.

122. Veith C, Schmitt S, Veit F, Dahal BK, Wilhelm J, Klepetko W, et al. Cofilin, a hypoxia-regulated protein in murine lungs identified by 2DE: role of the cytoskeletal protein cofilin in pulmonary hypertension. Proteomics. 2013;13(1):75-88.

123. Sawafuji K, Miyakawa Y, Weisberg E, Griffin JD, Ikeda Y, Kizaki M. Aminopeptidase inhibitors inhibit proliferation and induce apoptosis of K562 and STI571-resistant K562 cell lines through the MAPK and GSK-3beta pathways. Leukemia & lymphoma. 2003;44(11):1987-96.

124. Dean CB, Nielsen JD. Generalized linear mixed models: a review and some extensions. Lifetime data analysis. 2007;13(4):497-512.

125. Smyth GK, Speed T. Normalization of cDNA microarray data. Methods. 2003;31(4):265-73.

126. Matters GL, Bond JS. Expression and regulation of the meprin beta gene in human cancer cells. Mol Carcinog. 1999;25(3):169-78.

127. Fantozzi I, Zhang S, Platoshyn O, Remillard CV, Cowling RT, Yuan JX. Hypoxia increases AP-1 binding activity by enhancing capacitative Ca2+ entry in human pulmonary artery endothelial cells. American journal of physiology Lung cellular and molecular physiology. 2003;285(6):L1233-45.

128. Karin M. The regulation of AP-1 activity by mitogen-activated protein kinases. Philosophical transactions of the Royal Society of London Series B, Biological sciences. 1996;351(1336):127-34.

129. Biasin V, Marsh LM, Egemnazarov B, Wilhelm J, Ghanim B, Klepetko W, et al. Meprin beta, a novel mediator of vascular remodelling underlying pulmonary hypertension. The Journal of pathology. 2014;233(1):7-17.

130. Yap LB, Ashrafian H, Mukerjee D, Coghlan JG, Timms PM. The natriuretic peptides and their role in disorders of right heart dysfunction and pulmonary hypertension. Clinical biochemistry. 2004;37(10):847-56.

131. Datta SR, Brunet A, Greenberg ME. Cellular survival: a play in three Akts. Genes & development. 1999;13(22):2905-27.

132. Freitas N, Cunha C. Mechanisms and signals for the nuclear import of proteins. Current genomics. 2009;10(8):550-7.

133. Broder C, Arnold P, Vadon-Le Goff S, Konerding MA, Bahr K, Muller S, et al. Metalloproteases meprin alpha and meprin beta are C- and N-procollagen proteinases important for collagen assembly and tensile strength. Proceedings of the National Academy of Sciences of the United States of America. 2013;110(35):14219-24.

134. Hocevar BA, Brown TL, Howe PH. TGF-beta induces fibronectin synthesis through a c-Jun N-terminal kinase-dependent, Smad4-independent pathway. The EMBO journal. 1999;18(5):1345-56.

135. Galie N, Badesch D, Oudiz R, Simonneau G, McGoon MD, Keogh AM, et al. Ambrisentan therapy for pulmonary arterial hypertension. Journal of the American College of Cardiology. 2005;46(3):529-35.

136. Biasin V, Chwalek K, Wilhelm J, Best J, Marsh LM, Ghanim B, et al. Endothelin-1 driven proliferation of pulmonary arterial smooth muscle cells is c-fos dependent. The international journal of biochemistry & cell biology. 2014;54:137-48.

137. Hall SM, Davie N, Klein N, Haworth SG. Endothelin receptor expression in idiopathic pulmonary arterial hypertension: effect of bosentan and epoprostenol treatment. The European respiratory journal. 2011;38(4):851-60.

138. Chinenov Y, Kerppola TK. Close encounters of many kinds: Fos-Jun interactions that mediate transcription regulatory specificity. Oncogene. 2001;20(19):2438-52.

139. Hibi M, Lin A, Smeal T, Minden A, Karin M. Identification of an oncoprotein- and UV-responsive protein kinase that binds and potentiates the c-Jun activation domain. Genes & development. 1993;7(11):2135-48.

140. Sasaki T, Kojima H, Kishimoto R, Ikeda A, Kunimoto H, Nakajima K. Spatiotemporal regulation of c-Fos by ERK5 and the E3 ubiquitin ligase UBR1, and its biological role. Molecular cell. 2006;24(1):63-75.

141. Angel P, Karin M. The role of Jun, Fos and the AP-1 complex in cell-proliferation and transformation. Biochimica et biophysica acta. 1991;1072(2-3):129-57.

142. Pearson G, Robinson F, Beers Gibson T, Xu BE, Karandikar M, Berman K, et al. Mitogen-activated protein (MAP) kinase pathways: regulation and physiological functions. Endocrine reviews. 2001;22(2):153-83.

143. Kwapiszewska G, Markart P, Dahal BK, Kojonazarov B, Marsh LM, Schermuly RT, et al. PAR-2 inhibition reverses experimental pulmonary hypertension. Circulation research. 2012;110(9):1179-91.

144. Shaulian E, Schreiber M, Piu F, Beeche M, Wagner EF, Karin M. The mammalian UV response: c-Jun induction is required for exit from p53-imposed growth arrest. Cell. 2000;103(6):897-907.

145. Weitzman JB, Fiette L, Matsuo K, Yaniv M. JunD protects cells from p53-dependent senescence and apoptosis. Molecular cell. 2000;6(5):1109-19.

146. Toft DJ, Rosenberg SB, Bergers G, Volpert O, Linzer DI. Reactivation of proliferin gene expression is associated with increased angiogenesis in a cell culture model of fibrosarcoma tumor progression. Proceedings of the National Academy of Sciences of the United States of America. 2001;98(23):13055-9.

147. Lambers C, Roth M, Zhong J, Campregher C, Binder P, Burian B, et al. The interaction of endothelin-1 and TGF-beta1 mediates vascular cell remodeling. PloS one. 2013;8(8):e73399.

148. Kunichika N, Landsberg JW, Yu Y, Kunichika H, Thistlethwaite PA, Rubin LJ, et al. Bosentan inhibits transient receptor potential channel expression in pulmonary vascular myocytes. American journal of respiratory and critical care medicine. 2004;170(10):1101-7.

149. Sterchi EE, Stocker W, Bond JS. Meprins, membrane-bound and secreted astacin metalloproteinases. Molecular aspects of medicine. 2008;29(5):309-28.

150. Sunnerhagen M, Pursglove S, Fladvad M. The new MATH: homology suggests shared binding surfaces in meprin tetramers and TRAF trimers. FEBS letters. 2002;530(1-3):1-3.

151. Jefferson T, Auf dem Keller U, Bellac C, Metz VV, Broder C, Hedrich J, et al. The substrate degradome of meprin metalloproteases reveals an unexpected proteolytic link

between meprin beta and ADAM10. Cellular and molecular life sciences : CMLS. 2013;70(2):309-33.

152. Herzog C, Haun RS, Ludwig A, Shah SV, Kaushal GP. ADAM10 is the major sheddase responsible for the release of membrane-associated meprin A. The Journal of biological chemistry. 2014;289(19):13308-22.

153. Hahn D, Pischitzis A, Roesmann S, Hansen MK, Leuenberger B, Luginbuehl U, et al. Phorbol 12-myristate 13-acetate-induced ectodomain shedding and phosphorylation of the human meprinbeta metalloprotease. The Journal of biological chemistry. 2003;278(44):42829-39.

154. Bertenshaw GP, Norcum MT, Bond JS. Structure of homo- and hetero-oligomeric meprin metalloproteases. Dimers, tetramers, and high molecular mass multimers. The Journal of biological chemistry. 2003;278(4):2522-32.

155. Johnson GD, Bond JS. Activation mechanism of meprins, members of the astacin metalloendopeptidase family. The Journal of biological chemistry. 1997;272(44):28126-32.

156. Ohler A, Debela M, Wagner S, Magdolen V, Becker-Pauly C. Analyzing the protease web in skin: meprin metalloproteases are activated specifically by KLK4, 5 and 8 vice versa leading to processing of proKLK7 thereby triggering its activation. Biological chemistry. 2010;391(4):455-60.

157. Craig SS, Reckelhoff JF, Bond JS. Distribution of meprin in kidneys from mice with high- and low-meprin activity. The American journal of physiology. 1987;253(4 Pt 1):C535-40.

158. Bylander J, Li Q, Ramesh G, Zhang B, Reeves WB, Bond JS. Targeted disruption of the meprin metalloproteinase beta gene protects against renal ischemia-reperfusion injury in mice. American journal of physiology Renal physiology. 2008;294(3):F480-90.

159. Bao J, Yura RE, Matters GL, Bradley SG, Shi P, Tian F, et al. Meprin A impairs epithelial barrier function, enhances monocyte migration, and cleaves the tight junction protein occludin. American journal of physiology Renal physiology. 2013;305(5):F714-26.

160. Trachtman H, Valderrama E, Dietrich JM, Bond JS. The role of meprin A in the pathogenesis of acute renal failure. Biochemical and biophysical research communications. 1995;208(2):498-505.

161. Ambort D, Brellier F, Becker-Pauly C, Stocker W, Andrejevic-Blant S, Chiquet M, et al. Specific processing of tenascin-C by the metalloprotease meprinbeta neutralizes its

inhibition of cell spreading. Matrix biology : journal of the International Society for Matrix Biology. 2010;29(1):31-42.

162. Schutte A, Hedrich J, Stocker W, Becker-Pauly C. Let it flow: Morpholino knockdown in zebrafish embryos reveals a pro-angiogenic effect of the metalloprotease meprin alpha2. PloS one. 2010;5(1):e8835.

163. Bergin DA, Greene CM, Sterchi EE, Kenna C, Geraghty P, Belaaouaj A, et al. Activation of the epidermal growth factor receptor (EGFR) by a novel metalloprotease pathway. The Journal of biological chemistry. 2008;283(46):31736-44.

164. Garcia-Caballero A, Ishmael SS, Dang Y, Gillie D, Bond JS, Milgram SL, et al. Activation of the epithelial sodium channel by the metalloprotease meprin beta subunit. Channels. 2011;5(1):14-22.

165. Minder P, Bayha E, Becker-Pauly C, Sterchi EE. Meprinalpha transactivates the epidermal growth factor receptor (EGFR) via ligand shedding, thereby enhancing colorectal cancer cell proliferation and migration. The Journal of biological chemistry. 2012;287(42):35201-11.

166. Kruse MN, Becker C, Lottaz D, Kohler D, Yiallouros I, Krell HW, et al. Human meprin alpha and beta homo-oligomers: cleavage of basement membrane proteins and sensitivity to metalloprotease inhibitors. The Biochemical journal. 2004;378(Pt 2):383-9.

167. Kronenberg D, Bruns BC, Moali C, Vadon-Le Goff S, Sterchi EE, Traupe H, et al. Processing of procollagen III by meprins: new players in extracellular matrix assembly? The Journal of investigative dermatology. 2010;130(12):2727-35.

168. Intengan HD, Schiffrin EL. Vascular remodeling in hypertension: roles of apoptosis, inflammation, and fibrosis. Hypertension. 2001;38(3 Pt 2):581-7.

169. Nave AH, Mizikova I, Niess G, Steenbock H, Reichenberger F, Talavera ML, et al. Lysyl oxidases play a causal role in vascular remodeling in clinical and experimental pulmonary arterial hypertension. Arteriosclerosis, thrombosis, and vascular biology. 2014;34(7):1446-58.

170. Egeblad M, Rasch MG, Weaver VM. Dynamic interplay between the collagen scaffold and tumor evolution. Current opinion in cell biology. 2010;22(5):697-706.

171. Frisdal E, Gest V, Vieillard-Baron A, Levame M, Lepetit H, Eddahibi S, et al. Gelatinase expression in pulmonary arteries during experimental pulmonary hypertension. The European respiratory journal. 2001;18(5):838-45.

172. Schermuly RT, Kreisselmeier KP, Ghofrani HA, Yilmaz H, Butrous G, Ermert L, et al. Chronic sildenafil treatment inhibits monocrotaline-induced pulmonary hypertension in rats. American journal of respiratory and critical care medicine. 2004;169(1):39-45.

173. Bozec A, Bakiri L, Jimenez M, Schinke T, Amling M, Wagner EF. Fra-2/AP-1 controls bone formation by regulating osteoblast differentiation and collagen production. The Journal of cell biology. 2010;190(6):1093-106.

174. Wang Z, Lakes RS, Eickhoff JC, Chesler NC. Effects of collagen deposition on passive and active mechanical properties of large pulmonary arteries in hypoxic pulmonary hypertension. Biomechanics and modeling in mechanobiology. 2013.

175. Taipale J, Miyazono K, Heldin CH, Keski-Oja J. Latent transforming growth factor-beta 1 associates to fibroblast extracellular matrix via latent TGF-beta binding protein. The Journal of cell biology. 1994;124(1-2):171-81.

176. Megalou AJ, Glava C, Oikonomidis DL, Vilaeti A, Agelaki MG, Baltogiannis GG, et al. Transforming growth factor-beta inhibition attenuates pulmonary arterial hypertension in rats. International journal of clinical and experimental medicine. 2010;3(4):332-40.

177. Sundqvist A, Zieba A, Vasilaki E, Herrera Hidalgo C, Soderberg O, Koinuma D, et al. Specific interactions between Smad proteins and AP-1 components determine TGFbeta-induced breast cancer cell invasion. Oncogene. 2012.

178. Glading A, Uberall F, Keyse SM, Lauffenburger DA, Wells A. Membrane proximal ERK signaling is required for M-calpain activation downstream of epidermal growth factor receptor signaling. The Journal of biological chemistry. 2001;276(26):23341-8.

179. Ma W, Han W, Greer PA, Tuder RM, Toque HA, Wang KK, et al. Calpain mediates pulmonary vascular remodeling in rodent models of pulmonary hypertension, and its inhibition attenuates pathologic features of disease. The Journal of clinical investigation. 2011;121(11):4548-66.

The results of my thesis are published as follows:

- **Endothelin-1 driven proliferation of pulmonary arterial smooth muscle cells is c-fos dependent.**
  Biasin V, Chwalek K, Wilhelm J, Best J, Marsh LM, Ghanim B, Klepetko W, Fink L, Schermuly RT, Weissmann N, Olschewski A, Kwapiszewska G.
  International Journal of Biochemistry and Cell Biology

- **Meprin β, a novel mediator of vascular remodelling underlying pulmonary hypertension.**
  Biasin V, Marsh LM, Egemnazarov B, Wilhelm J, Ghanim B, Klepetko W, Wygrecka M, Olschewski H, Eferl R, Olschewski A, Kwapiszewska G.
  Journal of Pathology

Poster Presentations:

- **Contribution of Fra-2 transcription factor to pulmonary hypertension**

  Valentina Biasin[1], Leigh M. Marsh[1], Bakytbek Egzemanarov[1], Walter Klepetko[2], Robert Eferl[3], Andrea Olschewski[1, 4], Grazyna Kwapiszewska[1,4]

  Poster presented at the American Thoracic Society (ATS), May 2013 Philadelphya, USA

- **Contribution of Fra-2 transcription factor to pulmonary hypertension**

  Valentina Biasin[1], Leigh M. Marsh[1], Bakytbek Egzemanarov[1], Walter Klepetko[2], Robert Eferl[3], Andrea Olschewski[1, 4], Grazyna Kwapiszewska[1,4]

  Poster presented at the Pneumoupdate meeting, June 2013 , Innsbruck, Austria

- **Meprin-β, novel contributor to vascular remodeling**

  Valentina Biasin[1], Leigh M. Marsh[1], Bakytbek Egemnazarov[1], Jochen Wilhelm[2], Bahil Ghanim[1,3], Walter Klepetko[3], Malgorzata Wygrecka[4], Horst Olschewski[5], Robert Eferl[6], Andrea Olschewski[1,7], Grazyna Kwapiszewska[1,7]*

  Poster presented at the Gordon Conference Regulated Proteolysis of Cell Surface Proteins meeting, April 2014 , Ventura, CA,USA

Prize

- **ATS travel grant** offered by Takeda Company and ÖGP (Österreichischen Gesellschaft für Pneumologie).